CHAPERONE MEDIATED PROTECTIVE PROTEIN AGGREGATION AND SPATIAL QUALITY CONTROL

Katie J. Wolfe

A dissertation submitted to the faculty of the University of North Carolina at Chapel Hill in partial fulfillment of the requirements for the degree of Doctor of Philosophy in the Department of Cell Biology and Physiology

Chapel Hill
2013

Approved by:
Douglas Cyr, PhD
Patrick Brennwald, PhD
Mohanish Deshmukh, PhD
Nikolay Dokholyan, PhD
Brian Strahl, PhD

ABSTRACT

Katie Jean Wolfe: Chaperone mediated protective protein aggregation and spatial quality control
(Under the direction of Douglas Cyr, PhD)

The accumulation of amyloid-like aggregates is a characteristic of protein conformational disorders such as Huntington Disease, but whether amyloid-like aggregation is causative or a cytoprotective mechanism remains unclear. Molecular chaperones act as the front line of defense against proteotoxicity, as they protect cells by partitioning misfolded proteins towards refolding, degradation, or assembly into large benign aggregates. Herein, a yeast model of proteotoxicity was utilized to study cellular mechanisms for protective aggregation. Ectopic expression of polyglutamine (polyQ) expanded Huntingtin (Htt103Q) is toxic in yeast, and targeting it to the nucleus enhances toxicity while decreasing SDS-resistant aggregation. I utilized this nuclear Htt103Q as the substrate for a high copy toxicity suppressor screen in yeast which identified Sti1 as a molecule that promotes protective aggregation of Htt103Q. The Hsp70 co-chaperone Sti1 regulates spatial quality control of amyloid-like proteins as it induces formation of perinuclear foci containing SDS-resistant material. Accumulation of distinct perinuclear foci correlates with suppression of toxicity and increased complex formation with the Hsp70/Hsp40 chaperone machinery. Endogenous Sti1 appears to be a crucial player in a chaperone-facilitated protective aggregation pathway, because deletion of Sti1 enhances Htt103Q toxicity while decreasing aggregation. In addition to Sti1, the screen produced a group of polyQ-rich proteins, Nab3, Pop2 and Cbk1, as high-copy suppressors of Htt103Q toxicity. PolyQ proteins play different roles in Htt103Q toxicity, either to a detrimental outcome where a

Q-rich protein is titrated away from its normal function, or beneficially via interactions that promote protective aggregation. Over-expression of Nab3 appears to suppress Htt103Q toxicity by replacing a functional pool of Nab3 that was lost to aberrant polyQ interaction. Over-expression of Pop2 and Cbk1each suppresses toxicity and promotes aggregation of Htt103Q in a slightly different way, but neither can carry out this function in the absence of Sti1. Therefore, Pop2 and Cbk1 act upstream of Sti1 in pathway which promotes protective aggregation of amyloid-like assemblies. These proteins alter the cellular outcome of proteotoxic insult caused by Htt103Q by modulating spatial quality control.

Dedicated to my loving and supportive parents

ACKNOWLEDGEMENTS

My dissertation work would not have been possible without the help and support of numerous individuals which I have had the pleasure of meeting. I would first like to thank my mentor and advisor, Dr. Douglas Cyr. He has provided me with a nurturing lab home and shaped me to be a critical thinking scientist. He has taught me how to persistently and creatively seek out answers to complicated questions. His support and guidance have helped me complete my dissertation in an efficient and timely manner.

My development has also been greatly impacted by past and present members of both the Cyr lab and the Brennwald lab. I would like to thank each one of them for acting as a sounding board and creating a positive work place. I also thank my committee members, Dr. Patrick Brennwald, Dr. Mohanish Deshmukh, Dr. Nikolay Dokholyan, and Dr. Brian Strahl for donating their time and energy to helping me succeed as a graduate student.

Finally, I would like to thank my church, colleagues, friends, and family for providing a network of love, encouragement, and support. I am so grateful to have such amazing parents, John and Linda Mayo. They raised me to believe that I can do anything I set out to accomplish, and have been behind me in every endeavor. I also thank my brother, Dr. Daniel Mayo, for his love and support. Last and most importantly, I thank my wonderful and loving husband, Dr. Derek Wolfe, for literally walking beside me every single step of this journey as we navigated through graduate school together.

PREFACE

Herein is a compilation of my primary author publications. Chapter one is a published review, chapter two is under review, and chapter three will be submitted following revisions. My dissertation work has also included several other projects. One project was carried out in collaboration with the Avrom Caplan lab at the City College of New York which resulted in an authorship on a publication about mechanisms of cytosolic protein turnover. I also contributed to another graduate student's work on chaperone facilitated turnover of short lived cytosolic proteins, and this too resulted in an authorship. Each of these projects and publications combined represent my dissertation work as a whole.

TABLE OF CONTENTS

LIST OF TABLES

LIST OF FIGURES

LIST OF ABBREVIATIONS

CD- conformational disease

CHX- cycloheximide

coIP-co-immuneprecpitation

GF- genomic fragment

GFP- green fluorescent protein

GndHCl- guanidinium hydrochloride

Htt103Q- Huntingtin with 103Q glutamine stretch

IP-immunoprecipitation

IPOD- insoluble protein deposit

JUNQ- juxtanuclear quality control compartment

mRFP- monomeric red fluorescent protein

NLS- nuclear localization signal

NEF- nucleotide exchange factor

ORF- open reading frame

PolyQ- polyglutamine

PQC- protein quality control

StiF- Sti1 inducible foci

TPR- tetratricopeptide repeat

CHAPTER 1

Amyloid in neurodegenerative diseases: Friend or foe?[1]

1.1 Overview

Accumulation of amyloid-like aggregates is a hallmark of numerous neurodegenerative disorders such as Alzheimer's and polyglutamine disease. Yet, whether the amyloid inclusions found in these diseases are toxic or cytoprotective remains unclear. Various studies suggest that the toxic culprit in the amyloid folding pathway is actually a soluble oligomeric species which might interfere with normal cellular function by a multifactorial mechanism including aberrant protein-protein interactions. Molecular chaperones suppress toxicity of amyloidogenic proteins by inhibiting aggregation of non-native disease substrates and targeting them for refolding or degradation. Paradoxically, recent studies also suggest a protective action of chaperones in their promotion of the assembly of large, tightly packed, benign aggregates that sequester toxic protein species.

1.2 Introduction

Protein misfolding and the accumulation of amyloid aggregates are prominent features in a vast array of human diseases including numerous neurodegenerative disorders [1]. An amyloid fibril is an insoluble, highly ordered aggregate and the major component of extracellular plaques found in Alzheimer patient's brains. Amyloid fibrils

[1] Reproduced from *Semin Cell Dev Biol*, 2011. Jul;22(5):476-81.

are defined by a cross-β structure where the β sheets run perpendicular to the fibril axis [2]. Amyloid can be distinguished from other disordered aggregates by several properties including insolubility in ionic detergent, protease resistance, and recognition by diagnostic indicator dyes such as Congo Red [3]. Intracellular inclusions which exhibit similar characteristics are usually termed amyloid-like [2], but for the purposes of this review we will refer to amyloid plaques, fibrils, and amyloid-like aggregates all as amyloid unless otherwise noted. It remains highly controversial whether the amyloid deposits found in patients with amyloid disorders is the root problem as researchers first thought or if, as increasing evidence suggests, the large inclusions serve a protective cellular function [4, 5].

Amyloid diseases are associated with a broader family termed protein conformational diseases, coined by Carrell and Lomas in 1997. They proposed that each disease occurs via a similar mechanism that involves the abnormal folding and aggregation of specific disease associated proteins causing a toxic gain of function [6]. However, the precise reason behind aggregation of a disease protein causing toxicity remains unclear. An equally challenging enigma in neurodegenerative amyloidoses is the cause of selective vulnerability of certain neuronal populations. Each neurodegenerative disorder affects a specific subset of neurons even though the disease associated protein is often present in many cells throughout the brain and the rest of the body [7]. This phenomenon may be a result of interactions between an array of intracellular factors which have both positive and negative influences on the cells ability to buffer accumulation of potentially toxic proteins [8, 9]. It has been suggested that subtle differences in the expression pattern of broad networks of protein homeostatic factors

influence the fate of disease proteins and may account for selective vulnerability [10, 11]. Yet, the components that make up such collectives of protective or harmful interactions remain ambiguous. Herein, we discuss mechanisms for amyloid toxicity and explore how molecular chaperones act to modulate the proteotoxicity associated with formation of intracellular amyloid aggregates.

1.3 Formation of toxic species in amyloid diseases

Although numerous neurodegenerative diseases are associated with the presence of amyloid-like aggregates, the toxic culprit in the aggregation pathway leading to amyloid formation remains elusive. Some researchers suggest that the inclusion bodies found in amyloid diseases (bottom, right in Fig 1) are the toxic species [12], yet there is often a negative correlation between neurotoxicity and existence of large amyloid aggregates[13, 14]. Accumulating literature suggests that a soluble, pre-fibrillar species of the disease protein (Soluble Oligomers in Fig 1) causes cytotoxicity and the fibrillar aggregates may be part of a cytoprotective mechanism whereby toxic species are sequestered [4, 5].

How is a normally folded protein converted to a cytotoxic amyloid-like conformer? The conformation of soluble proteins is dynamic. Native proteins often "breath" and sample partially unfolded non-native states which leads to transient folding intermediates [15]. The equilibrium between native and non-native conformers is shifted toward the non-native state via mutation or upon aging and/or stress [10]. Non-native protein conformers are subject to action of protein quality control (PQC) machines and are partitioned towards refolding, degradation or aggregation (Fig 1). The capacity of a cell to efficiently manage non-native protein conformers can impact cellular life or death

[16]. Although it is clear that directing a natively folded protein towards amyloid formation is linked to disease, the exact conformation of the species causing the primary toxic insult is still unknown. There are many neurodegenerative disorders characterized by amyloid inclusions, but some of the most highly studied are Alzheimer's Disease (AD) and polyglutamine diseases such as Huntington's Disease (HD). Below, we will discuss studies directed towards elucidating what the toxic amyloidogenic species might be in these two diseases.

1.3.1 Oligomeric amyloid assembly

The structural transition from a non-native fold to a pre-fibrillar conformation occurs via nucleated polymerization [15, 17]. The nucleation step of this process begins very slowly, perhaps due to an unfavorable energy barrier. After nucleation, however, polymerization occurs much more rapidly as the folding intermediate is capable of serving as a template or seed for further conformational switching [17]. Interestingly, it appears that all proteins which form amyloid may proceed through the same intermediate steps [18]. In this section, we will review recent advances in amyloid biology which suggest that there are common features in the mechanism for toxicity of structurally distinct proteins; these studies also highlight the toxic nature of soluble intermediates in the amyloid assembly pathway.

1.3.1.1 Polyglutamine diseases: Huntington's Disease

Polyglutamine (polyQ) diseases are a very well studied, yet enigmatic, subset of neurodegenerative disorders. These diseases are characterized by amyloid inclusions where the disease protein contains an expanded polyQ tract [19]. HD occurs when Huntingtin (Htt) has a polyQ tract expanded beyond 33 residues. Disease onset is

associated with cleavage of an N-terminal exon 1 fragment containing the expanded polyQ tract from Htt. This is followed by nuclear accumulation of the cleaved fragment even though the wildtype form of Htt is localized mainly to the cytosol [20, 21].

Although aggregation intermediates have been hard to identify, polyQ length dependent formation of Htt oligomers has indeed been demonstrated both *in vivo* and *in vitro* [22, 23]. Indeed, much evidence supports the hypothesis that there may be an inverse relationship between Htt toxicity and aggregation. For instance, expression of Htt with an expanded glutamine stretch in cultured striatal neurons causes aggregation in a manner that does not correlate with cell death. In fact, suppression of intranuclear Htt inclusion formation is accompanied by increased cell death [14]. While this study analyzed a total population of cells, Arrasate et al designed a series of experiments where they followed individual neurons. During the lifetime of the cells, the group tracked survival, Htt load, and Htt inclusion formation. This inventive experimental setup revealed that neuronal death correlates with increased polyQ expansion length and amount of diffuse Htt within the cell. Additionally, Htt inclusion body formation reduced the amount of soluble Htt thereby increasing neuronal survival [24]. These studies provide fundamental insight which supports the idea that the toxic Htt species is soluble rather than large intranuclear inclusions.

1.3.1.2 Alzheimer's Disease

Like HD, the formation of amyloid containing plaques was long assumed to be the causative agent of neurodegeneration in AD. However, there are accumulating data that suggest that the toxic species is actually a soluble form of the disease causing protein [25, 26]. The disease associated protein in AD is amyloid precursor protein (APP).

Amyloid aggregation in AD occurs with cleavage of APP fragment into Aβ42 which accumulates in extracellular amyloid plaques [27]. Aβ amyloid plaques found in human brains of AD patients have a low correlation with severity of AD [28]. A recent study using a mouse model of AD strongly supports the toxic oligomeric hypothesis [25]. AD symptoms were decreased upon reduction of insulin growth factor signaling which correlated with formation of tightly packed Aβ aggregates. As seems to be the case with Htt, Aβ apparently may undergo oligomerization into a soluble, toxic conformer which can be sequestered by protective cellular pathways into larger benign aggregates.

In AD, the toxic soluble oligomer has been identified in various ways. Injection of medium containing Aβ monomers and oligomers, but lacking amyloid fibrils, was able to inhibit hippocampal long-term potentiation (LTP) in rats [4]. Pretreatment of the sample in order to destroy Aβ monomer followed by injection still resulted in decreased LTP. In another *in vivo* study, rats were injected with an oligomer specific antibody which was able to block inhibition of LTP [26]. Altogether, these *in vivo* results suggest that Aβ oligomers mediate toxicity or nucleate the formation of a toxic protein species. Soluble intermediates in the amyloid assembly pathway for Aβ have a structure in common with other amyloidogenic proteins as evidenced by a structural specific antibody [18]. Importantly, this observation links different amyloid diseases to a common soluble amyloid conformation which seems to correlate with toxicity. Thus, various amyloid associated neurodegenerative disorders are apparently caused by a population of harmful oligomeric conformers which have common toxic properties.

1.3.2 Interaction surfaces of toxic amyloid species

A broad array of protein interaction partners can affect aggregation both positively and negatively, composing a vast protein homeostasis network which needs to be balanced to maintain cell viability [10]. For example, aberrant protein-protein interactions can interfere with the normal function of various transcription factors, such as CREB Binding Protein and TATA Binding Protein, leading to transcriptional dysregulation [29, 30]. Htt and various amyloid disease proteins might also deplete and/or inactivate other necessary cellular factors. These include but are not limited to ubiquitin proteosome machinery [31], ER associated degradation (ERAD) machinery [16], numerous glutamine or glutamine/asparagine (Q/N) rich proteins [32, 33], and large proteins predicted to be highly unstructured which may act as hubs or scaffolds [34]. In addition, coiled-coil (CC) domains were recently suggested to regulate aggregation and toxicity of Q/N rich amyloid proteins [35]. Increased CC propensity in regions of proteins that contain polyQ was found to increase occurrence of aggregation and toxicity. It's possible that the CC structure may be an interaction domain which mediates the nucleation event for pre-fibrillar β-rich amyloid to occur in polyglutamine diseases. Furthermore, there may be distinct chaperone machineries regulating the formation of the CC domain, imparting another level of control over the system. Although we are just beginning to understand mechanism for 'nucleation' of amyloid assembly, it seems that the nature of protein interactions are able to dictate how a non-natively folded protein is handled within the cell.

Yeast prions provide an extremely useful example of interaction surfaces affecting nucleation and toxicity of amyloid forming proteins. Prions are self-

propagating proteinaceous particles [36] which, in yeast, are amyloid-like heritable genetic elements passed from mother to daughter cell [37]. Prion proteins can exist in their natively folded conformation or in their amyloid-like prion conformation. For instance, Rnq1 and Sup35 are the proteins which form [RNQ^+] (also called [PIN^+]) and [PSI^+] prions, respectively. The [RNQ^+] prion serves as a prime example of a protein which affects conformation of another protein. When [RNQ^+] comes into contact with another amyloidogenic protein such as Sup35, the prion allows the interaction partner to assume its amyloid conformation, in this case [PSI^+] [38, 39]. The Rnq1/Sup35 interaction is normally very weak, but nonetheless Rnq1 can serve as a nucleator of amyloid conversion and assembly [40]. In the context of HD, when Htt is expressed in yeast, toxicity only occurs in the presence of [RNQ^+] [41]. Thus, Rnq1 serves as a nucleation factor not only for other yeast prions, but also for other amyloidogenic disease associated proteins. Htt assembly could actually be relocalized to the nucleus by tagging Rnq1 with a nuclear localization signal [42]. Relocalizing Htt assembly to the nucleus hindered amyloid assembly resulting in the accumulation of a soluble Htt species. This correlated with enhanced Htt-induced cell death. Consequently, the specific location of amyloid conversion impacts cytotoxicity perhaps by influencing aberrant protein-protein interactions that might disrupt the essential cellular functions mentioned above. While [RNQ^+] as well as already templated amyloid proteins can serve as nucleators for amyloidogenic proteins, further studies are needed to discover other cellular factors with this capability.

From all of these studies combined, we deduce several things. First, there seems to be a common mechanism of amyloid toxicity even though different disease proteins

misfold and aggregate in specific, disease dependent, neuronal subpopulations. The primary amino acid sequence, which is different for each individual disease protein, may play a role in selective vulnerability. Second, the common amyloid toxicity mechanism seems to stem from soluble oligomeric species which may be the toxic culprit in various neurodegenerative amyloidosis. Finally, though it remains unclear whether the soluble amyloid is a folding intermediate or an off-pathway conformer, the toxic soluble species in various amyloid associated neurodegenerative disorders must adopt a β-rich structure [43, 44]. The toxic β-rich structure may expose surfaces amenable to aberrant intracellular interactions, but when packaged into large benign aggregates, these surfaces may be hidden.

1.4 Suppression of amyloid proteotoxicity by molecular chaperones

Molecular chaperones are a crucial part of PQC and work by maintaining the proper folding status of proteins within a cell. Chaperones recognize misfolded conformers which are then targeted for refolding, aggregation, or triaged towards degradation. They play a vital role in protecting the cell from conformational diseases such as amyloidogenic neurodegenerative disorders. Chaperones do this by either suppressing the initial oligomerization of disease proteins and disassembling disease protein aggregates or stimulating the conversion of toxic amyloid assembly intermediates into benign aggregates [5, 45-47]. In other words, chaperones can either inhibit or promote aggregation but the end goal is to eliminate the toxic soluble species.

1.4.1 Chaperone dependent suppression of aggregation

The Hsp40/Hsp70 system is a well characterized molecular chaperone machine that recognizes non-native disease proteins and prevents aberrant aggregation. Hsp40

functions as a co-chaperone by binding non-natively folded proteins and delivering them to Hsp70 for refolding [48]. The diversity of Hsp40s polypeptide binding domain provides amazing substrate specificity to the Hsp70 [49, 50]. Various Hsp40/Hsp70 machineries act in different ways towards distinct disease protein substrates. This chaperone machinery has been highly studied as a mechanism which inhibits amyloid-like aggregate assembly of disease proteins [51, 52]. In yeast, overexpression of Hsp70, Ssa1, or Hsp40, Ydj1, alters aggregation of mutant Htt by preventing fibrillization [45]. Additionally, elevated expression of Ydj1 reduced aggregation and toxicity of Q/N rich amyloid aggregates [53]. Likewise in cell culture, increasing the amount of Hsp40 and Hsp70 has been shown to decrease formation of polyQ disease protein aggregates as well as alleviate toxicity [54, 55]. Thus it seems that the Hsp40/Hsp70 machinery may act to hold the disease protein in a soluble conformation in order to prevent accumulation of a toxic intermediate or byproduct of the amyloid aggregation pathway.

Molecular chaperones can also antagonize accumulation of amyloid assemblies by acting later in the folding pathway via solubilization of already formed aggregates. Hsp104, an AAA ATPase protein remodeling factor in yeast, is required for propagation of yeast prions via shearing of large amyloid-like aggregates into smaller seeds [38, 56]. Utilizing its solubilization activity, overexpression of Hsp104 in a yeast HD model was able to effectively fragment amyloid-like aggregates of expanded-polyQ Htt [57]. There is no Hsp104 in higher eukaryotes, however, exogenous expression of the chaperone in worm and rat models demonstrates that it retains its functional activity. Expression of Hsp104 in *C. elegans* reduced expanded polyQ protein aggregation and assuaged developmental delay [58]. Presence of Hsp104 in rats was also able to suppress toxicity

and alter distribution of expanded polyQ proteins [59]. Though these are just a few examples, the Hsp40/Hsp70 and Hsp104 machines clearly can protect cells from amyloid disease proteins by suppressing aggregation thereby inhibiting formation of a toxic soluble species.

1.4.2 Chaperone mediated aggregation

Molecular chaperones are also able to reduce the buildup of toxic oligomeric conformers via packaging of these assemblies into larger benign amyloid-like aggregates. Work in yeast provides an excellent basis for understanding chaperone mediated amyloid assembly. In a [RNQ+] yeast background, elevation of Rnq1levels results in toxicity [5]. At normal levels, Rnq1 exists predominately as high molecular weight, SDS insoluble species in these studies. Moderate overexpression of Rnq1 to toxic levels causes accumulation of a lower molecular weight, SDS soluble pool. As in HD and AD, these studies suggest that the toxic Rnq1 species might be a smaller soluble species and the large SDS insoluble aggregates are a benign product. Further substantiating this hypothesis, co-expression of Rnq1 with the Hsp40 co-chaperone, Sis1, suppressed toxicity and promoted Rnq1 assembly into large amyloid-like aggregates [5]. Elevating the levels of Rnq1 in a [RNQ+] cell saturates the [RNQ+] biogenesis pathway and results in the accumulation of toxic aberrant Rnq1 conformers. Co-expression of Sis1 may then alleviate toxicity by increasing [RNQ+] assembly into large SDS insoluble aggregates. Evidence towards this hypothesis also comes from the observation that Sis1 binds directly to [RNQ+] specifically in its prion conformation and is required for prion propagation [60]. Thus Sis1 acts as a PQC factor to promote aggregation in order to prevent accumulation of toxic soluble species of Rnq1 (Letter C in Fig 1).

Chaperone machinery has also been shown to promote aggregation of human amyloidogenic substrates. A human Hsp40, Hdj2, has been shown to increase aggregation of expanded polyQ Htt in Cos-7 cells [61]. In conjunction with Hsp40/Hsp70 machinery, the chaperonin complex, TRiC, also alters amyloid aggregation while suppressing polyQ-mediated toxicity as shown in *C. elegans* [62], yeast [63], and cell culture [64]. These studies demonstrate that depletion of TRiC leads to accumulation of a toxic, soluble, oligomeric Htt species. In fact, Behrends et al. utilized size exclusion chromatography to show that toxic Htt oligomers exhibited a molecular weight of approximately 200 kDa. TRiC, in conjunction with Ssa1 and Ydj1, was able to shift the toxic soluble oligomers into non-toxic 500 kDa aggregates [63]. Thus, promotion of protective aggregation seems to be a mechanism whereby cells eliminate cytotoxic pools of Htt oligomer. Altogether, these studies demonstrate that molecular chaperones protect cells from proteotoxic insult by targeting misfolded proteins away from toxic oligomeric states; chaperones either enhance assembly into fibrillar benign aggregates, or disassemble the oligomers into soluble monomeric forms which can be properly folded [65]. Incredibly, chaperones are able to carry out these opposing activities, both of which lead to promotion of a healthy and functional folding state of non-native proteins in the cellular milieu.

1.4.3 Chaperone assisted protein degradation

Chaperones also mediate clearance of proteotoxic substrates via degradation of non-native proteins. When molecular chaperones cannot repair a misfolded protein, it can be targeted for degradation either via the ubiquitin proteosome system or autophagy. CHIP (carboxy terminus of Hsc70-interactin protein) is an E3 ligase which mediates

transfer of polyubiquitin chains to misfolded substrates, but also has inherent chaperone activity and acts as an Hsp70/Hsc70 co-chaperone [66, 67]. Indeed, CHIP has been shown to play a role in chaperone mediated degradation of expanded polyQ disease proteins. When CHIP was overexpressed, ubiquitination and turnover of polyQ disease substrates such as Htt increased, resulting in suppression of polyQ aggregation and cell death [68, 69]. CHIP's chaperone activity is necessary in order to observe this suppression. Elevated Hsc70 levels increased CHIP's ability to suppress aggregation and cell death, thus CHIP works cooperatively with Hsc70.

Autophagy is another cellular clearance mechanism for neurodegenerative amyloid proteins which is independent of the ubiquitin-proteosome system. Autophagy, literally meaning "self-eating", is a cellular process that involves compartmentalizing bulk cytosol, including cell components and proteins, which is sent to lysosomes to be degraded [70]. When autophagy was suppressed in mice via inhibition of ATG5, even without the presence of disease causing proteins, the mice displayed characteristics of neurodegeneration [71]. As a result, this study suggests that neuronal cells are constantly challenged by the formation of misfolded proteins and autophagy is required for the removal of these proteins. In the absence of this pathway, misfolded proteins accumulate and disrupt normal cellular function. In the context of neurodegenerative diseases, expanded polyQ disease proteins have indeed been shown to be degraded via autophagy [72]. Furthermore, recent evidence suggests that mutant Htt can specifically be targeted to autophagosomes by acetylation [73]. Altogether, these studies establish that degradation, which can also be chaperone mediated, is a crucial mechanism by which neurodegenerative disease associated proteins are cleared from the cell.

1.5 Concluding Remarks

Normal PQC is crucial to cell viability because it maintains the balance of non-native proteins targeted towards refolding or degradation. A shift in this equilibrium can be highly detrimental to the cell, leading to death. Specific mechanisms of proteotoxicity caused by misfolded protein accumulation remain unclear, but many cellular processes have been implicated. Neurodegenerative disorders characterized by amyloid inclusions seem to be caused by a multifactorial mechanism which may be centered around titration and inactivation of essential cellular components in processes such as transcription [74], degradation via the ubiquitin proteosome [31], and ER associated degradation (ERAD) [16] among others. Aberrant interactions arising from exposed hydrophobic surfaces within the amyloidogenic disease protein [33, 75] and/or mislocalization [42] can lead to cell death.

Not all cell types are equally affected by a single amyloidogenic protein, however. The equilibrium between a native and non-native conformation is cell type specific, and not all cell types equally respond to the same protein misfolding event. Some cell types may be less equipped than others and therefore unable to clear toxic amyloid species. Cellular mechanisms for clearance of these toxic amyloid species include chaperone dependent suppression or promotion of aggregation, chaperone dependent turnover, and clearance via autophagy.

Although chaperone machinery can partition misfolded proteins between these various pathways, some proteins are able to escape normal PQC mechanisms and cause havoc within the cell. By gaining a better understanding of the affinities of non-native proteins for chaperones versus their propensity to aggregate, we may shed light upon

exactly how those proteins can escape PQC machinery. Cellular environment seems to play a major role here. Upon cellular stress, it has been well documented that the environment within the cell shifts in order to avoid accumulation of misfolded protein species. Over time, these PQC pathways become less efficient. If the balance between refolding, degradation, and protective aggregation pathways is jeopardized then cytotoxic protein conformers are able to accumulate. Specific cell types may or may not be unable to respond accordingly by upregulating an alternative pathway to compensate for the stress. Thus, future research in the realm of amyloid diseases should focus on defining the protein networks within cells that help protect against that fate. In the long term, identification of protective cellular factors and how these networks are integrated and regulated will help us better understand exactly how amyloid causes disease.

1.6 Figures

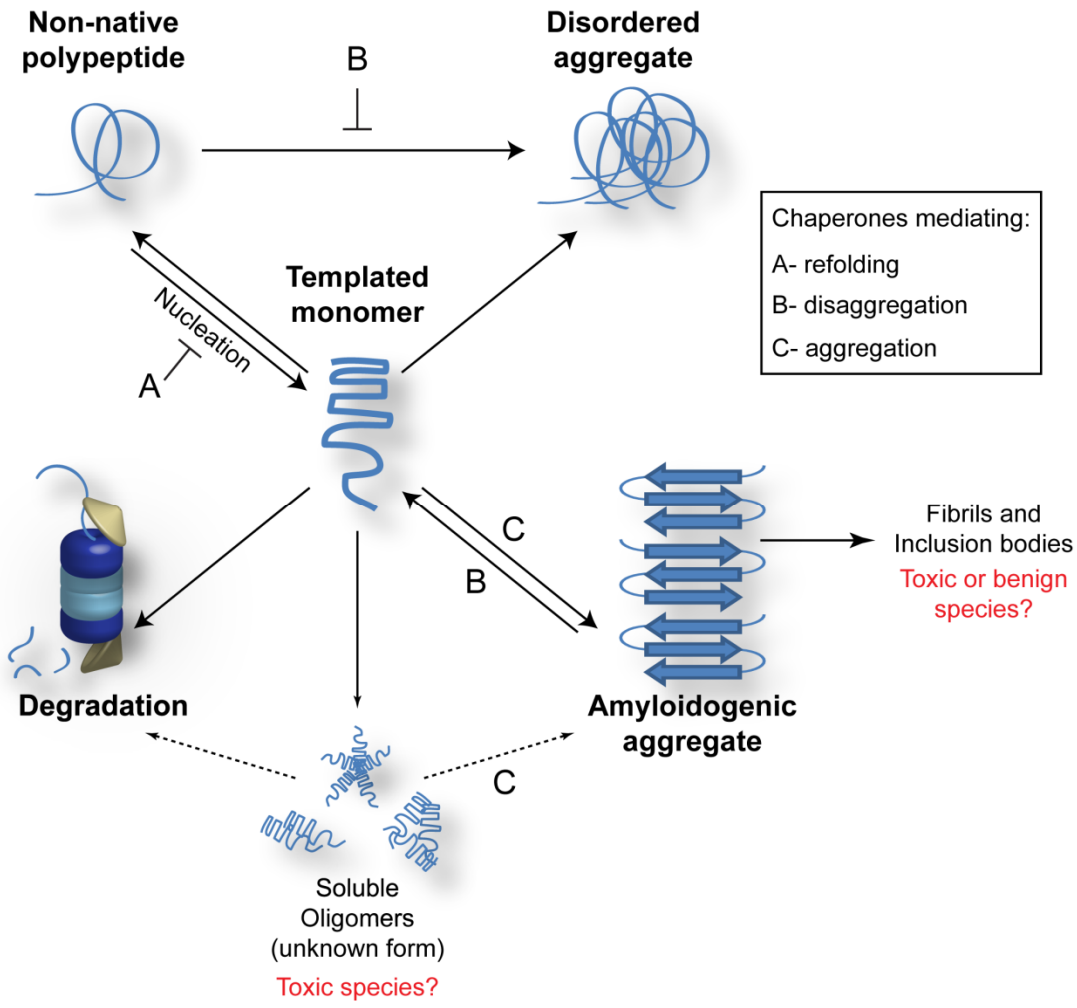

Figure 1.1 Protein folding and amyloid formation.
Non-native proteins can be partitioned into several conformational fates including refolding, ordered or disordered aggregate formation, and degradation. Amyloid is a type of very structured (or ordered) aggregate and forms through a poorly understood pathway. Sometimes a protein comes into contact with another surface that influences how it folds, but exactly how this occurs remains unclear. This interaction could be called nucleation since the newly "templated" monomer can now influence other monomers to adopt the same conformation. Following nucleation, possible small oligomeric species or amyloidogenic aggregates can assemble although the structure of this species is unknown. Molecular chaperones act at various points in the amyloid formation pathway to influence how the non-native protein is handled, as designated with letters A-C.

REFERENCES

1. Chiti, F. and C.M. Dobson, *Protein misfolding, functional amyloid, and human disease.* Annu Rev Biochem, 2006. **75**: p. 333-66.

2. Sipe, J.D., et al., *Amyloid fibril protein nomenclature: 2010 recommendations from the nomenclature committee of the International Society of Amyloidosis.* Amyloid, 2010. **17**(3-4): p. 101-4.

3. Ross, C.A. and M.A. Poirier, *Opinion: What is the role of protein aggregation in neurodegeneration?* Nat Rev Mol Cell Biol, 2005. **6**(11): p. 891-8.

4. Walsh, D.M., et al., *Naturally secreted oligomers of amyloid beta protein potently inhibit hippocampal long-term potentiation in vivo.* Nature, 2002. **416**(6880): p. 535-9.

5. Douglas, P.M., et al., *Chaperone-dependent amyloid assembly protects cells from prion toxicity.* Proc Natl Acad Sci U S A, 2008. **105**(20): p. 7206-11.

6. Carrell, R.W. and D.A. Lomas, *Conformational disease.* Lancet, 1997. **350**(9071): p. 134-8.

7. Mazarei, G., et al., *Expression analysis of novel striatal-enriched genes in Huntington disease.* Hum Mol Genet, 2010. **19**(4): p. 609-22.

8. Giorgini, F., et al., *A genomic screen in yeast implicates kynurenine 3-monooxygenase as a therapeutic target for Huntington disease.* Nat Genet, 2005. **37**(5): p. 526-31.

9. Willingham, S., et al., *Yeast genes that enhance the toxicity of a mutant huntingtin fragment or alpha-synuclein.* Science, 2003. **302**(5651): p. 1769-72.

10. Balch, W.E., et al., *Adapting proteostasis for disease intervention.* Science, 2008. **319**(5865): p. 916-9.

11. Gidalevitz, T., et al., *Progressive disruption of cellular protein folding in models of polyglutamine diseases.* Science, 2006. **311**(5766): p. 1471-4.

12. Yang, W., et al., *Aggregated polyglutamine peptides delivered to nuclei are toxic to mammalian cells.* Hum Mol Genet, 2002. **11**(23): p. 2905-17.

13. Kuemmerle, S., et al., *Huntington aggregates may not predict neuronal death in Huntington's disease.* Ann Neurol, 1999. **46**(6): p. 842-9.

14. Saudou, F., et al., *Huntingtin acts in the nucleus to induce apoptosis but death does not correlate with the formation of intranuclear inclusions.* Cell, 1998. **95**(1): p. 55-66.

15. Jahn, T.R., et al., *Amyloid formation under physiological conditions proceeds via a native-like folding intermediate.* Nat Struct Mol Biol, 2006. **13**(3): p. 195-201.

16. Duennwald, M.L. and S. Lindquist, *Impaired ERAD and ER stress are early and specific events in polyglutamine toxicity.* Genes Dev, 2008. **22**(23): p. 3308-19.

17. Jarrett, J.T. and P.T. Lansbury, Jr., *Seeding "one-dimensional crystallization" of amyloid: a pathogenic mechanism in Alzheimer's disease and scrapie?* Cell, 1993. **73**(6): p. 1055-8.

18. Kayed, R., et al., *Common structure of soluble amyloid oligomers implies common mechanism of pathogenesis.* Science, 2003. **300**(5618): p. 486-9.

19. Zoghbi, H.Y. and H.T. Orr, *Glutamine repeats and neurodegeneration.* Annu Rev Neurosci, 2000. **23**: p. 217-47.

20. Davies, S.W., et al., *Formation of neuronal intranuclear inclusions underlies the neurological dysfunction in mice transgenic for the HD mutation.* Cell, 1997. **90**(3): p. 537-48.

21. DiFiglia, M., et al., *Aggregation of huntingtin in neuronal intranuclear inclusions and dystrophic neurites in brain.* Science, 1997. **277**(5334): p. 1990-3.

22. Legleiter, J., et al., *Mutant huntingtin fragments form oligomers in a polyglutamine length-dependent manner in vitro and in vivo.* J Biol Chem, 2010. **285**(19): p. 14777-90.

23. Takahashi, T., et al., *Soluble polyglutamine oligomers formed prior to inclusion body formation are cytotoxic.* Hum Mol Genet, 2008. **17**(3): p. 345-56.

24. Arrasate, M., et al., *Inclusion body formation reduces levels of mutant huntingtin and the risk of neuronal death.* Nature, 2004. **431**(7010): p. 805-10.

25. Cohen, E., et al., *Reduced IGF-1 signaling delays age-associated proteotoxicity in mice.* Cell, 2009. **139**(6): p. 1157-69.

26. Klyubin, I., et al., *Amyloid beta protein immunotherapy neutralizes Abeta oligomers that disrupt synaptic plasticity in vivo.* Nat Med, 2005. **11**(5): p. 556-61.

27. Haass, C. and D.J. Selkoe, *Soluble protein oligomers in neurodegeneration: lessons from the Alzheimer's amyloid beta-peptide.* Nat Rev Mol Cell Biol, 2007. **8**(2): p. 101-12.

28. Terry, R.D., et al., *Physical basis of cognitive alterations in Alzheimer's disease: synapse loss is the major correlate of cognitive impairment.* Ann Neurol, 1991. **30**(4): p. 572-80.

29. Riley, B.E. and H.T. Orr, *Polyglutamine neurodegenerative diseases and regulation of transcription: assembling the puzzle.* Genes Dev, 2006. **20**(16): p. 2183-92.

30. Nucifora, F.C., Jr., et al., *Interference by huntingtin and atrophin-1 with cbp-mediated transcription leading to cellular toxicity.* Science, 2001. **291**(5512): p. 2423-8.

31. Bence, N.F., R.M. Sampat, and R.R. Kopito, *Impairment of the ubiquitin-proteasome system by protein aggregation.* Science, 2001. **292**(5521): p. 1552-5.

32. Furukawa, Y., et al., *Cross-seeding fibrillation of Q/N-rich proteins offers new pathomechanism of polyglutamine diseases.* J Neurosci, 2009. **29**(16): p. 5153-62.

33. Duennwald, M.L., et al., *A network of protein interactions determines polyglutamine toxicity.* Proc Natl Acad Sci U S A, 2006. **103**(29): p. 11051-6.

34. Olzscha, H., et al., *Amyloid-like aggregates sequester numerous metastable proteins with essential cellular functions.* Cell, 2011. **144**(1): p. 67-78.

35. Fiumara, F., et al., *Essential role of coiled coils for aggregation and activity of Q/N-rich prions and PolyQ proteins.* Cell, 2010. **143**(7): p. 1121-35.

36. Prusiner, S.B., *Novel proteinaceous infectious particles cause scrapie.* Science, 1982. **216**(4542): p. 136-44.

37. Shorter, J. and S. Lindquist, *Prions as adaptive conduits of memory and inheritance.* Nat Rev Genet, 2005. **6**(6): p. 435-50.

38. Sondheimer, N. and S. Lindquist, *Rnq1: an epigenetic modifier of protein function in yeast.* Mol Cell, 2000. **5**(1): p. 163-72.

39. Derkatch, I.L., et al., *Prions affect the appearance of other prions: the story of [PIN(+)].* Cell, 2001. **106**(2): p. 171-82.

40. Vitrenko, Y.A., et al., *Propagation of the [PIN+] prion by fragments of Rnq1 fused to GFP.* Curr Genet, 2007. **51**(5): p. 309-19.

41. Meriin, A.B., et al., *Huntington toxicity in yeast model depends on polyglutamine aggregation mediated by a prion-like protein Rnq1.* J Cell Biol, 2002. **157**(6): p. 997-1004.

42. Douglas, P.M., et al., *Reciprocal Efficiency of RNQ1 and Polyglutamine Detoxification in the Cytosol and Nucleus.* Mol Biol Cell, 2009.

43. Nekooki-Machida, Y., et al., *Distinct conformations of in vitro and in vivo amyloids of huntingtin-exon1 show different cytotoxicity.* Proc Natl Acad Sci U S A, 2009. **106**(24): p. 9679-84.

44. Zhang, Q.C., et al., *A compact {beta} model of huntingtin toxicity.* J Biol Chem, 2011.

45. Muchowski, P.J., et al., *Hsp70 and hsp40 chaperones can inhibit self-assembly of polyglutamine proteins into amyloid-like fibrils.* Proc Natl Acad Sci U S A, 2000. **97**(14): p. 7841-6.

46. Gokhale, K.C., et al., *Modulation of prion-dependent polyglutamine aggregation and toxicity by chaperone proteins in the yeast model.* J Biol Chem, 2005. **280**(24): p. 22809-18.

47. Douglas, P.M., D.W. Summers, and D.M. Cyr, *Molecular chaperones antagonize proteotoxicity by differentially modulating protein aggregation pathways.* Prion, 2009. **3**(2): p. 51-8.

48. Cyr, D.M., T. Langer, and M.G. Douglas, *DnaJ-like proteins: molecular chaperones and specific regulators of Hsp70.* Trends Biochem Sci, 1994. **19**(4): p. 176-81.

49. Fan, C.Y., et al., *Exchangeable chaperone modules contribute to specification of type I and type II Hsp40 cellular function.* Mol Biol Cell, 2004. **15**(2): p. 761-73.

50. Kota, P., et al., *Identification of a consensus motif in substrates bound by a Type I Hsp40.* Proc Natl Acad Sci U S A, 2009. **106**(27): p. 11073-8.

51. Lotz, G.P., et al., *Hsp70 and Hsp40 functionally interact with soluble mutant huntingtin oligomers in a classic ATP-dependent reaction cycle.* J Biol Chem, 2010. **285**(49): p. 38183-93.

52. Warrick, J.M., et al., *Suppression of polyglutamine-mediated neurodegeneration in Drosophila by the molecular chaperone HSP70.* Nat Genet, 1999. **23**(4): p. 425-8.

53. Summers, D.W., et al., *The type I Hsp40 Ydj1 utilizes a farnesyl moiety and zinc finger-like region to suppress prion toxicity.* J Biol Chem, 2009. **284**(6): p. 3628-39.

54. Jana, N.R., et al., *Polyglutamine length-dependent interaction of Hsp40 and Hsp70 family chaperones with truncated N-terminal huntingtin: their role in suppression of aggregation and cellular toxicity.* Hum Mol Genet, 2000. **9**(13): p. 2009-18.

55. Chai, Y., et al., *Analysis of the role of heat shock protein (Hsp) molecular chaperones in polyglutamine disease.* J Neurosci, 1999. **19**(23): p. 10338-47.

56. Chernoff, Y.O., et al., *Role of the chaperone protein Hsp104 in propagation of the yeast prion-like factor [psi+].* Science, 1995. **268**(5212): p. 880-4.

57. Cashikar, A.G., M. Duennwald, and S.L. Lindquist, *A chaperone pathway in protein disaggregation. Hsp26 alters the nature of protein aggregates to facilitate reactivation by Hsp104.* J Biol Chem, 2005. **280**(25): p. 23869-75.

58. Satyal, S.H., et al., *Polyglutamine aggregates alter protein folding homeostasis in Caenorhabditis elegans.* Proc Natl Acad Sci U S A, 2000. **97**(11): p. 5750-5.

59. Perrin, V., et al., *Neuroprotection by Hsp104 and Hsp27 in lentiviral-based rat models of Huntington's disease.* Mol Ther, 2007. **15**(5): p. 903-11.

60. Lopez, N., R. Aron, and E.A. Craig, *Specificity of class II Hsp40 Sis1 in maintenance of yeast prion [RNQ+].* Mol Biol Cell, 2003. **14**(3): p. 1172-81.

61. Wyttenbach, A., et al., *Effects of heat shock, heat shock protein 40 (HDJ-2), and proteasome inhibition on protein aggregation in cellular models of Huntington's disease.* Proc Natl Acad Sci U S A, 2000. **97**(6): p. 2898-903.

62. Nollen, E.A., et al., *Genome-wide RNA interference screen identifies previously undescribed regulators of polyglutamine aggregation.* Proc Natl Acad Sci U S A, 2004. **101**(17): p. 6403-8.

63. Behrends, C., et al., *Chaperonin TRiC promotes the assembly of polyQ expansion proteins into nontoxic oligomers.* Mol Cell, 2006. **23**(6): p. 887-97.

64. Tam, S., et al., *The chaperonin TRiC blocks a huntingtin sequence element that promotes the conformational switch to aggregation.* Nat Struct Mol Biol, 2009. **16**(12): p. 1279-85.

65. Sakahira, H., et al., *Molecular chaperones as modulators of polyglutamine protein aggregation and toxicity.* Proc Natl Acad Sci U S A, 2002. **99 Suppl 4**: p. 16412-8.

66. Jiang, J., et al., *CHIP is a U-box-dependent E3 ubiquitin ligase: identification of Hsc70 as a target for ubiquitylation.* J Biol Chem, 2001. **276**(46): p. 42938-44.

67. Rosser, M.F., et al., *Chaperone functions of the E3 ubiquitin ligase CHIP.* J Biol Chem, 2007. **282**(31): p. 22267-77.

68. Jana, N.R., et al., *Co-chaperone CHIP associates with expanded polyglutamine protein and promotes their degradation by proteasomes.* J Biol Chem, 2005. **280**(12): p. 11635-40.

69. Miller, V.M., et al., *CHIP suppresses polyglutamine aggregation and toxicity in vitro and in vivo.* J Neurosci, 2005. **25**(40): p. 9152-61.

70. Levine, B. and D.J. Klionsky, *Development by self-digestion: molecular mechanisms and biological functions of autophagy.* Dev Cell, 2004. **6**(4): p. 463-77.

71. Hara, T., et al., *Suppression of basal autophagy in neural cells causes neurodegenerative disease in mice.* Nature, 2006. **441**(7095): p. 885-9.

72. Ravikumar, B., R. Duden, and D.C. Rubinsztein, *Aggregate-prone proteins with polyglutamine and polyalanine expansions are degraded by autophagy.* Hum Mol Genet, 2002. **11**(9): p. 1107-17.

73. Jeong, H., et al., *Acetylation targets mutant huntingtin to autophagosomes for degradation.* Cell, 2009. **137**(1): p. 60-72.

74. McCampbell, A., et al., *CREB-binding protein sequestration by expanded polyglutamine.* Hum Mol Genet, 2000. **9**(14): p. 2197-202.

75. Campioni, S., et al., *A causative link between the structure of aberrant protein oligomers and their toxicity.* Nat Chem Biol, 2010. **6**(2): p. 140-7.

CHAPTER 2

The Hsp70/90 co-chaperone, Sti1, suppresses proteotoxicity by regulating spatial quality control of amyloid-like proteins[2]

2.1 Overview

Conformational diseases are associated with the conversion of normal proteins into aggregation prone toxic conformers with structures similar to β-amyloid. Spatial distribution of amyloid-like proteins into intracellular quality control centers can be beneficial, but cellular mechanisms for protective aggregation remain unclear. A high-copy suppressor screen in yeast was utilized to identify roles for the Hsp70 system in organization of toxic polyglutamine expanded Huntingtin (Htt103Q) into benign assemblies. The TPR-repeat co-chaperone Sti1 is reported to mediate the spatial organization of Htt103Q-GFP into benign foci. Under toxic conditions, Htt103Q accumulates in unassembled states and speckled cytosolic foci. Subtle modulation of Sti1 activity reciprocally impacts Htt toxicity and the packaging of Htt103Q into foci. Loss of Sti1 exacerbates Htt toxicity and hinders foci formation, whereas elevation of Sti1 suppresses Htt toxicity while organizing small Htt103Q foci into larger assemblies. Sti1 also suppresses cytotoxicity of the glutamine-rich yeast prion [RNQ+] while reorganizing speckled Rnq1-mRFP into distinct foci. Htt103Q and Rnq1 are normally detected in peripheral IPOD compartments, and Sti1 inducible foci (StiF) are unique because they are perinuclear and do not colocalize with the aggresome. Sti1 aids in

[2] A revised version of this chapter has been accepted for publication at Molecular Biology of the Cell

suppression of proteotoxicity by redirecting amyloid-like proteins to accumulate in the StiF.

2.2 Introduction

Protein conformational diseases represent a collection of disorders in which structurally diverse proteins are converted to a common cytotoxic conformational state that has features of β-amyloid [1]. A large number of normal proteins are converted to an amyloid-like state that is rich in β-structure, detergent insoluble, and binds indicator dyes such as thioflavin-T [2]. β-amyloid is deposited in extracellular plaques in the brains of Alzheimer's patients [2-4], and there are also numerous instances where protein conformational disease is associated with intracellular accumulation of amyloid-like assemblies [1]. Flux of proteins through the amyloid assembly pathway is associated with disease, but whether the amyloid-like aggregates themselves or small oligomers of converted proteins are toxic is debatable [5-7]. There is mounting evidence that molecular chaperones facilitate the packaging of toxic protein species into protein handling depots to suppress proteotoxicity [8, 9]. Yet, the cellular mechanisms for molecular chaperone function in protective protein aggregation remain unclear.

Hsp70 functions with specialized co-chaperones to suppress protein aggregation, refold clients, and promote protein degradation [10-13]. Hsp70 binds extended regions of polypeptide chains in an ATP-dependent reaction cycle that is regulated by Hsp40 [14-16]. Hsp40 serves as a substrate selector and helps stabilize Hsp70:polypeptide complexes by converting Hsp70-ATP to Hsp70-ADP. Substrate release from Hsp70 is regulated by nucleotide exchange factors and tetratricopeptide repeat (TPR) co-chaperones [17-19]. TPR co-chaperones contain a TPR repeat which serves as an

Hsp70/Hsp90 interaction domain that recognizes a conserved C-terminal EEVD motif [17], and specialized functional domains that dictate the fate of chaperone bound clients. Several examples of this are as follows: Sti1, whose mammalian homologue is HOP, contains 3 separate TPR domains which organize Hsp70 and Hsp90 into complexes and permit sequential action of these chaperones upon clients such as kinases and hormone receptors [20]; Sti1 also functions with Hsp70 and Hsp40 to modulate the biogenesis and function of prions in yeast and humans [21-23] ; CyP40 contains a cis-trans-prolyl-isomerase domain that facilitates conformational maturation of late stage protein folding intermediates [24]; CHIP is an ubiquitin ligase that regulates the heat stress response [25, 26] and targets misfolded proteins for proteasomal degradation [13, 27]. Thus, TPR-repeat co-chaperones of Hsp70/Hsp90 act downstream of Hsp40s and participate in multiple aspects of protein homeostasis.

In protein aggregates, hydrophobic surfaces that would be recognized by components of the Hsp70 system are buried, so they escape recognition by protein quality control machines. Thus, aggregates are inefficiently cleared from cells and cause cytotoxicity by damaging cell membranes, altering the conformation of other proteins and sequestering essential cellular proteins [4, 28, 29]. Aberrant proteins that are not initially cleared from the cytosol can be segregated into distinct cytosolic foci, observed in both yeast and mammalian systems, that appear to store oligomers and aggregates until conditions favor refolding or degradation [30-38]. Remarkably, detergent soluble and amyloid-like protein conformers are segregated into different protein handling depots, and this process is influenced by components in the Hsp70 system [8, 34, 36, 39]. Amyloid-like and detergent insoluble protein assemblies accumulate in perinuclear

aggresomes [31, 38], and insoluble protein deposits (IPOD), which are located in the cell periphery [30, 37]. Protein oligomers and aggregates that are soluble in detergents accumulate in the spatially distinct juxtanuclear quality control (JUNQ) [30, 33] and peripheral compartments [32]. Ubiquitinated proteins that evade the proteasome and terminally misfolded proteins that escape recognition by protein quality control (PQC) E3 ligases are swept into the JUNQ [30]. Proteins in the JUNQ can be solubilized and degraded by the proteasome in a pathway that involves the PQC E3 ligase Ubr1 [34]. The peripheral compartment contains Hsp42, and holds proteins in a folding competent state [32]. The IPOD may function in protein disaggregation of detergent insoluble aggregates [37] whereas the peripherial compartment and JUNQ aid in refolding [32] and degradation [30] of detergent soluble protein assemblies, respectively. The aggresome resembles an inclusion body and may represent a long-term storage site for aberrant proteins [31, 38]. Thus, cells have the capacity to sequester potentially toxic protein species, but the mechanism for spatial segregation of protein handling centers is a mystery.

Although flux through protein aggregation pathways is associated with cell death, chaperone dependent sequestration of amyloid-like proteins into protein handling centers correlates with suppression of proteotoxicity [3, 6, 8, 40]. In yeast models, overexpression of the yeast prion protein Rnq1 is toxic, but only if preexisting [RNQ+] prions are present to seed its conversion to an amyloid-like conformation [8, 41, 42]. The Hsp70, Ssa1, cooperates with the Hsp40, Sis1, to increase the efficiency by which seeded forms of Rnq1 assemble into amyloid-like [RNQ+] prions and thereby suppress proteotoxicity [8]. Interestingly, a fragment of Huntingtin (Htt) similar to those found in

inclusions from Huntington's Disease brains (Htt103Q), is toxic when expressed ectopically in yeast, but only if [RNQ+] prions are present [43]. In yeast, the aggregation state of Htt103Q and its toxicity are inversely correlated with very tight, detergent insoluble aggregates being benign and loose, detergent soluble aggregates being toxic [44]. Aggregation and toxicity of Htt103Q is influenced by its subcellular environment and also by the sequences of amino acids that flank its polyQ stretch [39, 44, 45]. Forms of Htt103Q that contain the polyproline region which follows the polyQ domain in full length Htt are benign due to their sequestration into the aggresome in a process that requires the ringed molecular chaperone p97 [38]. Forms of Htt103Q which lack the polyproline region are toxic as they accumulate in loose aggregates that are distributed throughout the cytosol in speckled foci, and tight aggregates that accumulate in the IPOD [30, 39]. Thus, studies of proteotoxicity of Htt103Q and Rnq1 in yeast provide an excellent model system to uncover mechanisms for Hsp70 function in protein detoxification through protective protein aggregation.

Herein we uncovered a role for the co-chaperone Sti1 in orchestrating spatial organization of Htt103Q and Rnq1 into benign amyloid-like assemblies. We employed the toxic form of Htt103Q lacking the proline-rich region and screened for proteins that suppressed proteotoxicity by facilitating its aggregation. Sti1 cooperates with the Hsp70 system to control the spatial organization of amyloid-like protein assemblies, thereby suppressing proteotoxicity. Sti1 interacts with Hsp70 to redirect Htt103Q away from the IPOD and other cytosolic protein deposition sites and induce accumulation of amyloid-like protein species into protective perinuclear foci. Sti1 functions as a central

coordinator of spatial PQC to organize molecular chaperone assemblies with their substrates as to drive protective aggregation of amyloidogenic proteins.

2.3 Results

2.3.1 The Hsp70/Hsp90 co-chaperone Sti1 suppresses Htt103Q toxicity

In order to identify cellular factors that defend against proteotoxicity, we carried out a high copy screen in *Saccharomyces cerevisiae* to discover proteins that suppressed Htt103Q toxicity. A construct encoding the first 17 amino acids of the Htt gene followed by 103 glutamines and a GFP moiety (Htt103Q) was integrated into a W303α strain under control of the galactose promoter. Htt103Q expression caused a growth defect in a glutamine length dependent manner [43] [44], and differential sensitivity to Htt103Q was exhibited by individual strains (Figure 2.1A). The yeast Hsp70/Hsp90 co-chaperone Sti1 [46] was identified as a high copy suppressor of the severe Htt103Q dependent growth defect. Expression of another TPR family co-chaperone, Sgt2, did not suppress Htt103Q toxicity (Figure 2.2A) indicating this activity is not a characteristic of TPR proteins in general. Additionally, deletion of Sti1 caused Htt103Q to be toxic in a strain where it was normally benign (Figure 2.1A right panels). Parallel growth assays using wildtype and ΔSti1 Htt25Q strains demonstrate that this phenotype was not due to reduced growth on galactose (Figure 2.1A left panels).

Elevation of Sti1 caused the subcellular localization of Htt103Q to become redistributed from a mixture of diffuse material and foci that are dispersed throughout the cytosol to several distinct large foci that were often found in close proximity to the nucleus (Figure 2.1B). Conversely, deletion of Sti1 greatly reduced Htt103Q punctae formation, with the majority of Htt dispersed in a diffuse cytosolic pattern (Figure 2.1B).

Sti1 overexpression had no effect upon Htt103Q levels, yet deletion reduced expression (Figure 2.1C), likely due to delayed induction from the galactose promoter [47]. Deletion of Sti1 clearly sensitizes the cell to Htt103Q because even though there was reduced Htt103Q expression, the growth defect was exacerbated.

Sti1 may suppress Htt103Q toxicity by organizing it into foci, however, fewer foci may be observed in the ΔSti1 strain since there is less Htt103Q being expressed. To rule out this possibility, Htt103Q-GFP localization was examined when expressed to equivalent levels via copper inducible promoter in wildtype and ΔSti1 strains (Figure 2.1D). Again Sti1 was required for efficient organization of Htt103Q into foci. We also examined the influence of Sti1 expression upon temporal aspects of Htt103Q foci accumulation. Over a 4 hour time course, Sti1 accelerated Htt103Q foci formation while reducing number of foci per cell (Figure 2.2B). Cycloheximide chase experiments demonstrate that once formed, the Sti1 dependent foci containing Htt103Q were stable for at least 5 hours (Figure 2.2C). These data provide a correlation between Sti1 action in suppression of Htt toxicity and the packaging of Htt103Q into perinuclear foci.

Does Sti1 act only on Htt103Q, or can it also modulate the organization of other cytosolic protein aggregates? To answer this question, we utilized mCitrine tagged luciferase, an Hsp70 client which aggregates during heat stress [32]. At 30°C, mCitrine-luciferase is diffuse throughout the cytosol and was not impacted by Sti1 overexpression (Figure 2.1E, top panels). During thermal stress at 42°C for 20 minutes, luciferase accumulated in numerous aggregates throughout the cytosol. Neither elevation nor deletion of Sti1 changed the appearance of the luciferase aggregates (Figure 2.1E, bottom panels). Thus, since Sti1 does not suppress aggregation of heat-damaged luciferase or

organize aggregated luciferase into foci, it appears to act specifically on aggregated forms of Htt103Q.

The TPR co-chaperone CHIP inhibits Hsp70 function in protein folding [27], so it is possible that Sti1 impacts Htt103Q assembly into foci by similarly interfering with Hsp70. This is unlikely, because Sti1 overexpression does not cause mCitrine-luciferase to aggregate (Figure 2.1E). Nevertheless, we examined in the impact of purified Sti1 on the ability of Ssa1 and Sis1 to refold denatured luciferase and found that Sti1 has no effect (Figure 2.2, D and E). Elevation of Sti1 does not appear to cause a change in Htt103Q aggregation by inhibition of normal Hsp70 folding activity.

If Sti1 has a direct effect upon Htt103Q, it should be present with Htt103Q foci. When expressed alone, Sti1 tagged with a monomeric RFP (mRFP) exhibited a diffuse localization pattern in the cytosol (Figure 2.1F). When co-expressed with Htt103Q, it redistributed the polyQ protein into distinct punctae, and Sti1-mRFP was indeed concentrated in foci with Htt103Q (Figure 2.1F, arrows). These data demonstrate that Sti1 promotes Htt103Q foci formation and this is beneficial to the cell, so there is an inverse relationship between Htt103Q aggregation and toxicity that is modulated by Sti1.

2.3.2 Sti1 interacts with high molecular weight forms of Htt103Q

To understand the mechanism for Sti1 action, we asked if it interacted with unassembled low molecular weight Htt103Q monomers or high molecular weight oligomeric assemblies. Therefore, we analyzed the elution patterns of Sti1 and Htt103Q on a Sephacryl S200 gel filtration column. Cell lysates prepared by homogenizing spheroplasts in the absence of detergent were immediately applied to the gel filtration column. Every third fraction collected was run on an SDS-PAGE gel and probed by

Western blot for levels of Htt103Q and Sti1 (Figure 2.3A-C). A portion of high molecular weight SDS-resistant Htt103Q is retained at the stacking front of the gel [39], so both the stacking and running gel sections are shown. Htt expression was similar in the presence of endogenous and overexpressed Sti1 (Figure 2.1C) and under all conditions, a pool of Sti1 (molecular weight of 67.6 KDa) migrated as a dimer [48] (Figure 2.3A). In addition to the dimeric form, endogenous Sti1 co-migrated with high molecular weight forms of Htt103Q. Yet, Htt103Q did not co-migrate in the fractions where the dimeric form of Sti1 was present (Figure 2.3A top panel/control). Importantly, endogenous Sti1 did not migrate in a high molecular weight fraction when non-aggregation prone Htt25Q was expressed (Figure 2.3A bottom panel). Upon overexpression of Sti1, the high molecular weight pools of Sti1 and Htt103Q both increased proportionally (Figure 2.3A top panel/+Sti1, and 2.3C), yet this was not observed when Sti1 levels were elevated in the presence of Htt25Q (Figure 2.3A bottom panel/+Sti1). Sti1 was also present in immune complexes when high molecular weight Htt103Q was precipitated from column fraction 12, (Figure 2.3B). This interaction was specific because there was no Sti1 signal detected in the absence of Htt103Q (Figure 2.3B). While reorganizing foci and suppressing toxicity, Sti1 appears to interact with high molecular weight forms of Htt103Q.

2.3.3 Sti1 modulates assembly of amyloidogenic substrates at a perinuclear location

Htt103Q is toxic to yeast upon undergoing a conformational change driven by interaction with the [RNQ+] prion [42, 43]. [RNQ+] prion biogenesis and toxicity is modulated by Hsp70 and Hsp40 [8, 49-51] and weak variants of the prion [*PSI*+] are eliminated from yeast by elevation of Sti1 activity [52]. Thus, the impact of Sti1 on

[RNQ+] prion toxicity and subcellular organization was evaluated. Just as with Htt103Q, an increase in Sti1 suppressed the toxicity associated with Rnq1 overexpression (Figure 2.4A). Under conditions utilized, Rnq1 expression is highly toxic, so deletion of Sti1 only led to a modest increase in growth defects caused by Rnq1 overexpression (Figure 2.4B). At endogenous levels of Sti1, Rnq1-mRFP foci were speckled throughout the cytosol, but upon overexpression of Sti1, Rnq1-mRFP became localized to one or two distinct juxtanuclear foci (Figure 2.4C). In contrast to what is observed with Htt103Q-GFP, speckled Rnq1-mRFP foci were still detected in a ΔSti1 strain indicating that this strain remains in the [RNQ+] prion state (Figure 2.4C, ΔSti1). Sti1 is not required for maintenance of [RNQ+] prions and Sti1 overexpression does not eliminate [RNQ+] prions. Instead, suppression of Rnq1 and Htt103Q toxicity by Sti1 is associated with reorganization of multiple punctae containing these proteins into one or two distinct perinuclear foci.

We next sought to determine what conformational state of Rnq1 and Htt103Q is favored under conditions where Sti1 suppresses their proteotoxicty. Sti1 increased accumulation of oliogmeric SDS-resistant forms of Rnq1 and Htt103Q by more than two-fold (Figure 2.5A). Deletion of Sti1 reduced Htt103Q SDS-resistant material by over 50% while there was little effect upon Rnq1 (Figure 2.5A). Sti1 appears to act on the oligomeric assemblies of Htt and Rnq1 that only form in [RNQ+] prion strains because its overexpression has no effect upon localization of Htt103Q or Rnq1 in [rnq-] strains (Figure 2.5B).

Conversion to an SDS-resistant oligomer is a characteristic of amyloid, so Sti1 appears to target amyloid-like forms of proteins to perinuclear foci. To gain experimental

support for this conclusion, we asked if Sti1 inducible foci stain positive for the amyloid specific dye thioflavin-T [2]. Rnq1-mRFP was used as a tool instead of Htt103Q-GFP because, upon binding amyloid, thioflavin-T emission is enhanced to a wavelength in the excitation range of GFP [53]. [RNQ+] prions have features of amyloid-like protein species as they bind thioflavin-T, whereas the dye does not bind to amorphous aggregates of Rnq1 that accumulate in a [rnq-] strain [8]. Speckled Rnq1-mRFP foci in both the cell periphery and in a perinuclear location were positive for thioflavin-T staining, as were the perinuclear Sti1 induced Rnq1-mRFP foci (Figure 2.5C).

To ascertain whether Htt103Q is also present in foci with amyloid-like [RNQ+] prions, we asked if they co-localize with each other in the presence and absence of Sti1 overexpression (Figure 2.5D). When Htt103Q-GFP and Rnq1-mRFP were co-expressed, a mixed population of speckled foci was detected with approximately 20% of foci containing both proteins (Figure 2.5D, inset and arrows). Sti1 elevation resulted in redistribution of most of the Htt103Q and Rnq1 to one or two larger perinuclear foci that contain both proteins (Figure 2.5D).

Due to the co-localization of Htt103Q and Rnq1 in foci that contain amyloid-like proteins, we asked if Sti1 is necessary for these proteins to interact. In order to answer this question, we took advantage of the fact that addition of a nuclear localization signal (NLS) to Rnq1 directs [RNQ+] prions to the nucleus and Htt103Q follows [39]. Thus, if Sti1 is required for interaction between Htt103Q and Rnq1, deletion of Sti1 would prevent this relocalization. However, Rnq1-NLS still redistributed Htt103Q to the nucleus in both the presence and absence of Sti1 (Figure 2.6A). Thus, Sti1 promotes accumulation of Htt103Q and foci that contain amyloid-like species of Rnq1, but does

not appear to be necessary for Rnq1 and Htt to interact. Instead, Sti1 may control the spatial organization of amyloid-like proteins into different protein handling centers.

2.3.4 Sti1 inducible foci are distinct protein quality control depots

Sti1 inducible foci (StiF) are perinuclear and contain amyloid-like material, thus are distinct from the IPOD and JUNQ. To characterize the StiF in more detail, we determined whether these foci contain PQC machinery which would help protect cells from proteotoxic stress. At endogenous levels of Sti1, Hsp104 and Hsp42 were not detected in foci which contained Htt103Q-GFP (Figure 2.7, A and B). Yet, while Htt103Q-GFP and Hsp104 co-localized in the StiF (Figure 2.7A), Hsp42 was not typically present (Figure 2.7B).

Since the StiF is an Hsp104 positive inclusion, we next determined if StiF formation is impacted by modulation of Hsp104 activity. Here, we treated cells containing endogenous or overexpressed Sti1 with guanidinium hydrochloride (GndHCl) for 4 hrs to inhibit Hsp104 activity [54, 55], and the effect this had on organization of Rnq1-mRFP into foci was monitored. To determine the nature of the foci observed, we employed strains containing a GFP tagged version of Hsp42 or Spc42, a spindle pole body component which marks the aggresome [31], which were under control of their endogenous promoter. Hsp104 inhibition condensed most of the Rnq1-mRFP material to one peripherally localized puncta, which co-localized with Hsp42, but not with Spc42 (Figure 2.7, C and D). Foci formed during Sti1 overexpression in the untreated samples did not co-localize with Spc42 revealing that the StiF is not the aggresome (Figure 2.7C). Furthermore, Htt103Q-GFP containing the proline-rich region is targeted in a p97 dependent manner to aggresomes [38] and deletion of Sti1 has no effect on aggregation

of Htt103Q-Pro (Figure 2.6B). Therefore, Sti1 is not promoting the accumulation of Htt103Q in the yeast aggresome.

Strikingly, Sti1 appears to divert proteins from the IPOD and promote their accumulation in the StiF, a previously unidentified protein handling depot. Rnq1 is considered to be an IPOD marker [30, 37] and the single Hsp42-GFP containing peripheral foci detected when Hsp104 is inhibited for 2 hrs appears to be the IPOD (Figure 2.7, C and D). Elevation of Sti1 in the presence of GndHCl prevents Rnq1-mRFP from accumulating in a peripheral foci and instead promotes its accumulation in the StiF.

These data demonstrate that organization of Rnq1 in speckled foci is highly sensitive to activity of Hsp104 and the Hsp70 system. Impairment of Hsp104 leads Rnq1-mRFP to accumulate in cytosolic foci. The effects of Sti1 on Rnq1-mRFP foci resemble those of Hsp104, except Sti1 promotes accumulation of amyloid-like proteins in StiF rather than a peripheral puncta. The StiF is a novel perinuclear quality control depot that contains Sti1, Hsp104, and amyloid-like proteins. It appears to be distinct from the aggresome as it does not form at the spindle pole body [38] and may serve as a detoxification center for amyloid-like proteins.

2.3.5 Sti1 reorganizes complexes that contain Htt103Q and Hsp70

Sti1 associates with oligomeric forms of Htt103Q (Figure 2.3) and co-localizes with amyloid-like proteins in the StiF (Figure 2.5), which might enable it to suppress Htt toxicity by acting alone or in concert with Hsp70/Hsp90. The co-chaperone function of Sti1 is conferred by three TPR repeats which are important for interaction with Hsp70 and Hsp90 (Figure 2.8A). TPR1 is implicated in interaction with Hsp70, and TPR2a with Hsp90, while both chaperones bind with lower affinity to the TPR2b region [20, 56, 57].

Hence, point mutations in respective TPR domains were constructed and the ability of different TPR mutants to suppress Htt103Q toxicity and promote StiF formation was evaluated (Figure 2.8B). While mutations in TPR2a and TPR2b had no effect (Figure 2.8, B-D), mutations in TPR1 hindered the ability of Sti1 to redistribute Htt103Q to the StiF (Figure 2.8D). TPR1 mutants also lost their ability to suppress the Htt103Q growth defect (Figure 2.8B). Thus, StiF formation and suppression of Htt103Q toxicity requires functional domains of Sti1 that enable it to interact with the Hsp70/Hsp90 system.

To determine the impact Sti1 has upon interactions between Hsp70 and Hsp90 with Htt103Q, complex formation between these proteins was evaluated by co-immuneprecipation (coIP) (Figure 2.8, E and F). Htt103Q was immuneprecipitated from yeast lysates prepared under non-denaturing conditions, and the presence of Ssa1, Hsp90, Ydj1, Sis1, and Sse1 in precipitates was determined by western blot. Entrance of Sti1 into complexes altered relative quantities of different molecular chaperones that associated with Htt103Q (Figure 2.8, E and F). The influence of Sti1 on Hsp70/Hsp90 interactions with Htt103Q was sensitive to changes in nucleotide level and appeared to result from ATP dependent chaperone:substrate interactions (Figure 2.8E). Interestingly, Sti1 increased levels of Ssa1's cognate Hsp40, Sis1, by around 4-fold and Ssa1 by over 2-fold (Figure 2.8, E and F). In contrast, little of an alternative Hsp40, Ydj1, was present and Sti1 reduced the amount of co-precipitated Hsp90 and Sse1. These collective data indicate that spatial quality control of amyloid-like assemblies involves Sti1 dependent reorganization of complexes containing Hsp70 and Htt103Q with the greatest effect being a dramatic increase in the presence of Sis1.

2.3.6 Sti1 and Sis1 cooperate to modulate amyloid toxicity

Sis1 interacts with oligomeric forms of Rnq1 to facilitate the propagation and impact the spatial organization of [RNQ+] prions [39, 49, 50]. Thus, Sti1 and Sis1 may cooperate to suppress growth defects caused by the presence of amyloid-like protein in the cytosol. We therefore investigated whether or not Sti1 is required for Sis1 to suppress Rnq1 and Htt103Q toxicity (Figure 2.9, A and B). Elevation of Sis1 diminished Rnq1 toxicity in a wild type strain, but its protective effect was severely diminished in a ΔSti1 strain, even though deletion of Sti1 had no effect on Sis1 expression. Similarly, elevated Sis1 also suppressed the growth defect caused by Htt103Q, and this protective effect was reduced in a ΔSti1 strain (Figure 2.9B).

Further support for functional interaction between Sti1 and Sis1 in buffering the toxicity of amyloid-like proteins comes from the demonstration that Sti1 drives the redistribution of Sis1 to the StiF (Figure 2.9C). Under normal conditions, Rnq1-mRFP was found in speckled foci and Sis1-GFP was distributed between the cytosol and nucleus (Figure 2.9C and [39]). Upon elevation of Sti1, the localization pattern of Sis1 changed dramatically and a large pool of it was concentrated in the StiF with Rnq1-mRFP (Figure 2.9B). Data presented in Figure 2.7-2.9 suggests that Sti1 helps suppress proteotoxicity via stabilization of complexes between Hsp70, Sis1, and amyloid-like protein assemblies to promote their accumulation in the perinuclear StiF.

2.4 Discussion

The Hsp70/90 co-chaperone, Sti1, suppresses proteotoxicity by reorganizing amyloid-like assemblies into the StiF, a novel protein handling depot. The StiF is a juxtanuclear compartment containing thioflavin-T positive assemblies of Rnq1 and

templated Htt103Q. Amyloid-like protein accumulation in the StiF correlates with suppression of proteotoxicity caused by Rnq1 and Htt103Q. Partitioning of aberrant proteins between the StiF and other protein handling centers is controlled by interactions between Sti1 and the Hsp70 chaperone system. Loss of Sti1 exacerbates Htt proteotoxicity while increases in Sti1 levels suppress it by increasing protein accumulation in the StiF. Sti1 is identified as an important component of the Hsp70/Hsp90 system that acts in spatial PQC to promote protective protein aggregation.

Sti1 serves to reorganize speckled foci containing amyloid-like forms of Rnq1 and Htt103Q into the StiF (Figure 2.10). The StiF appears to be distinct from other misfolded protein deposition sites because it contains amyloid-like protein species, is perinuclear, and does not co-localize with an aggresome marker. The StiF is one of five cytosolic protein handling centers, most of which have been characterized in both yeast and humans to function in protein homeostasis [30, 31, 33, 38]**.** The aggresome and the IPOD are responsible for storage of detergent insoluble and amyloid-like protein species [30, 38], whereas the peripheral compartment and JUNQ handle detergent soluble protein aggregates [30, 32]. The detection of substrate accumulation in these sites often requires gross protein overexpression and/or inhibition of the proteasome. Importantly, amyloid-like proteins are present in the StiF under conditions of modest protein expression and normal flux through the proteasome. Thus, amyloid-like proteins appear to transit through the StiF under normal growth conditions.

Why is accumulation of Htt103Q or [RNQ+] prions in the StiF versus other PQC centers cytoprotective? Onset of [RNQ+] prion or Htt103Q toxicity is detected within 4 hours of expression [8, 39], and at this time they appear in the cytosol as speckled

punctae and diffuse assemblies. Elevation of Sti1 accelerates the sequestration of amyloid-like proteins into the StiF and increases detergent insoluble oligomers of [RNQ+] and Htt103Q over 2 fold. This may occur by diversion of amyloidogenic proteins away from the IPOD where they could be sheared by Hsp104, possibly generating toxic oligomers [37, 58]. Shunting amyloid-like proteins away from the aggresome to the StiF is protective because this prevents sequestration of essential proteins into aggregates. For example, [RNQ+] prions sequester Spc42 away from its normal function in the spindle pole body leading to cell death [59], so increasing flux of [RNQ+] prions to the StiF would be protective. Accumulation of amyloid-like protein species in the JUNQ is cytotoxic as it inhibits normal PQC function [30, 33-35], so diverting these proteins to the StiF would assure normal function of the ubiquitin proteasome system. The fate of proteins that enter the StiF is not entirely clear, yet these foci are highly stable, so they may serve as a long-term storage vault for otherwise toxic proteins.

How does modulation of Sti1 alter spatial partitioning of amyloid-like aggregates? Sti1 promotes association of Ssa1 and Sis1 with Htt103Q while reducing the presence of Hsp90, thus stabilizing the Hsp70:substrate bound complex. Sti1 interaction with the Hsp70 system seems to allow the co-chaperone to directly affect the substrate's fate. In support of this concept, Sti1 was found in complex with a high molecular weight assembly of Htt103Q, can be precipitated from this complex, and co-localizes in the StiF. Although Sti1 is involved in kinase maturation and folding [60], the physical association of Sti1 with amyloid-like protein species support a direct role for Sti1 in Hsp70 client handling rather than an indirect role via altering kinase signaling pathways.

Sti1's cooperation with Sis1 in spatial distribution of amyloid-like proteins is consistent with observations that Sis1 impacts the subcellular localization of prions and misfolded proteins [36, 39]. During heat stress, Sis1 is proposed to interact with the aggregate sorting factor Btn2, targeting misfolded proteins to a juxtanuclear location [36]. Sis1 function is also implicated in targeting of [RNQ+] prions to the nucleus [8, 39] in a process that may involve Cur1 [36]. Levels of Btn2 and Cur1 during heat stress are thought to regulate the relative cytosolic concentrations of Sis1, thereby dictating whether misfolded protein accumulates with Sis1 at a juxtanuclear site or with Hsp42 at a peripheral cytosolic site [36]. Thus, there are protein sorting factors that interact with Sis1 and impact targeting of protein aggregates to different protein handling centers. Cur1, Btn2, and Hsp42 were deleted from strains expressing Htt103Q, but were dispensable for Sti1 dependent accumulation of Htt103Q in the StiF and suppression Htt toxicity (Figure 2.11). Nevertheless, the existence of such spatial PQC factors suggests the possibility that Sti1 plays a similar role in an alternate pathway that may be specific for amyloid-like proteins.

How might Sti1 reorganize the subcellular foci that contain the amyloid-like oligomers with which it interacts? Hsp104 functionally interacts with Ssa1, Sis1, and Sti1 in maintenance of the yeast prion [PSI+] [21, 52], as evidenced by the observation that deletion of Sti1 inhibits the ability of overexpressed Hsp104 to eliminate [PSI+] [21]. Interestingly, both the elevation of Sti1 and inhibition of Hsp104 for a short period with GndHCl prevent speckled Rnq1-mRFP foci accumulation. Yet, GndHCl promotes foci formation in a peripheral location and Sti1 in a perinuclear location, with Sti1 being dominant over GndHCl. Inhibition of Hsp104 eliminates [RNQ+] prions from cells [41],

but Sti1 overexpression does not cure yeast of [RNQ+] prions (Figure 2.12A, left panel). However, when Hsp104 is inhibited, Sti1 elevation accelerates the rate of [RNQ+] prion curing caused by inhibition of Hsp104 (Figure 2.12). Thus, Sti1 is not an inhibitor or Hsp104. Instead, it appears to interact with Sis1 and possibly other spatial PQC factors to direct amyloid-like proteins to the StiF, and this sequesters pools Rnq1 and Htt103Q away from the machinery that would normally break them into smaller foci.

The co-chaperones CHIP and BAG3 target Hsp70 clients for degradation via the ubiquitin proteasome or autophagy, respectively [10, 13, 61]. Sti1 is now reported to enable Hsp70 to function in spatial PQC by targeting amyloid-like proteins to the StiF. Sti1 is stress inducible, and, in humans, CHIP and Sti1 differentially bind to Hsp70 and Hsp90 based on changes in phosphorylation [62]. Thus, under normal and stress conditions, subtle changes in Sti1 levels or phosphorylation status could impact targeting of Hsp70 clients to an alternate fate. Sti1 is differentially expressed in various brain regions of both healthy humans and neurodegenerative disease patients [63, 64]. Thus, differences in Sti1 activity in different tissues or cell types could impact the efficiency of mammalian spatial PQC, influencing the onset of protein conformational disorders. In the future, it will be interesting to determine if differences in the cellular set-point of spatial quality control factors in healthy and diseased tissues correlate with neuronal subpopulations where neurodegenerative diseases originate.

2.5 Methods

Strains and plasmids

Yeast strains and plasmids are listed in Tables S1 and S2. All strains harbored Rnq1 in its [RNQ^{+}] prion form unless otherwise indicated. The generation of isogenic [*rnq*-] strains was accomplished via sequential passage of cells on plates containing 3mM guanidinium-HCl. Strains were transformed with plasmids and cultured in synthetic media as described previously [8]. Constructs containing a copper inducible promoter (CUP1) were induced at a low constitutive level from basal levels of copper in media unless specified that media was supplemented with additional $CuSO_4$. This is the case for all Rnq1-mRFP microscopy unless otherwise indicated. For Sti1 overexpression experiments, Sti1 was always expressed from its endogenous promoter on a high copy plasmid.

Expression of Htt103Q

Htt25Q and Htt103Q integration strains were generated using the pRS305 plasmid backbone. This vector carried a construct containing an amino terminal FLAG tag, the first 17 amino acids of Htt, a 25 or 103 polyQ stretch, and a carboxy terminal GFP tag. The Htt constructs were integrated under control of a galactose inducible promoter (GAL1). Htt cultures were grown in synthetic media containing 2% glucose until cultures reached a density of 4 OD_{600} or greater. They were then diluted back in 2% raffinose, allowed to recover to mid-log phase growth, and finally induced for indicated times with 2% galactose. Except during time courses, Htt25Q and Htt103Q were induced for 4 hours. The only exception to these expression conditions was when we utilized the Htt103Q-Pro construct. This construct lacked the N terminal FLAG tag and contained a

Proline rich region following the polyQ stretch. Expression of Htt103Q-Pro was induced with 2% galactose for 24 h from a low copy plasmid and galactose inducible promoter.

Toxicity assays

Yeast samples were normalized to the same OD_{600}, then 5 fold serial diluted in a sterile 96-well plate. Each dilution was plated in 10uL spots on appropriate synthetic dropout media. Most images of yeast grown on glucose were scanned at 48h and galactose at 72h. Lysates for Western blots from toxicity assays were prepared using cultures picked from control growth plates after they were scanned. Rnq1 toxicity was assessed on plates containing 2% glucose with 500uM $CuSO_4$ and Htt toxicity plates contained 2% galactose.

SDS-PAGE and Western Blotting

Lysates were prepared from pellets of yeast by either mechanical disruption via glass bead breaking (for SDD-AGE and co-IP) as described previously [8, 39] or an alkali lysis method as described previously [34] (for samples which were directly run on SDS-PAGE gels). When using mechanical disruption, the lysis buffer used was 0.1% Triton X-100, 75mM Tris pH7.4, 150mM NaCl, 1mM EDTA, 1mM PMSF, and Sigma protease inhibitor cocktail. Standard separation techniques were used to analyze lysates via SDS-PAGE. Protein was transferred to nitrocellulose for 75-90 min at 110V, and probed using the indicated antibodies. Antibodies used in this study are listed in Table S3.

Fluorescence microscopy

Fluorescence microscopy was carried out as described previously [39]. Briefly, cultures were fixed with 4% formaldehyde and 0.1M KPO_4 pH 7.4, and stored in 0.1M

KPO_4 pH 7.4 with 1.2M sorbitol. When dapi stained, cells were permeabilized with 0.1% Triton in PBS, washed twice with PBS, incubated with 0.5ug/mL dapi for 10min, washed twice again with PBS, and resuspended in the sorbitol solution. An Olympus IX81 motorized inverted fluorescence microscope paired with Metamorph software was used to collect images. Micrographs were merged and processed using ImageJ.

Immunofluorescence and thioflavin-T staining

Cells were collected and fixed as described above. Following fixation, spheroplasts were generated using 5 mg/mL zymolyase as described for size exclusion chromatography below. For thioflavin-T staining, spheroplasts were treated with 0.1% Triton in PBS for 10 min, then washed with sorbitol solution. Following this permeabilization, cells were incubated with 0.001% thioflavin-T for 10 min, washed, and resuspended in sorbitol solution. For immunofluorescence, spheroplasts were applied to teflon coated glass slides (Electron Microscopy Sciences) with poly-L-lysine coated wells. Then wellsh were then blocked using buffer containing 0.1M KPO4 pH 7.5, 0.5% BSA, 0.02% Tween-20. Primary and secondary antibodies were applied with washes after each. Antibody incubation and washes all were carried out with the same blocking buffer.

SDD-AGE

Semi-denaturing detergent agarose gel electrophoresis (SDD-AGE) was carried out as described previously [8]. Briefly, samples were prepared via bead breaking as described above and normalized by a protein determination assay (DC protein assay kit; Bio-Rad). Equivalent amounts of total protein were loaded on a 1.4% agarose gel

containing 0.1% SDS, run at 90-100V for approximately 2h, then transferred to PVDF at 12V for 15h.

Size exclusion chromatography

Non-denaturing extracts from the Htt103Q strain were prepared via spheroplasting as follows. Approximately 150 ODs of mid-log phase cells were resuspended in 2mL Z buffer containing 50mM TrisCl pH 7.5, 10 mM $MgCl_2$, 1M sorbitol and 30mM DTT, then incubated at room temperature for 15min. Sample was then centrifuged and resuspended in 1mL Z buffer with 5mg zymolyase added (30mM DTT), and incubated at 30°C in shaker at 50 rpm for 45min. Following zymolyase treatment, spheroplasts were centrifuged and carefully washed twice with 1mL cold Z buffer (1mM DTT), then thoroughly resuspend with 800uL of lysis buffer (listed above, without Triton) using a cold glass disposable pipet. Samples were pre-cleared to remove cell debris and normalized so that the same amount of protein was loaded to the column each time. A 500uL loop was loaded into a Sephacryl S200 column, and 500uL fractions were collected. Western blots show every third fraction starting slightly before the void volume as determined by Thyroglobulin.

Co-immunoprecipitation

The Htt103Q strain carried either an empty vector or the YepLac-Sti1 construct, and were induced and lysed via bead breaking as described above. For experiments where ATP was present the lysis buffer contained 75mM Tris pH7.4, 150mM NaCl, 0.1% Triton, 10mM MgCl, and 4mM ATP. Lysates were incubated with anti-FLAG M2 affinity gel (Sigma). Htt103Q which was captured was then eluted by addition of 0.2mg/mL FLAG peptide (Sigma) and incubation at 37°C for 20min. Following

incubation, samples were spun at 4000rpm for 5min, and supernatant was harvested, combined with sample buffer, and loaded on an SDS-PAGE gel along with an input sample. In the case of co-IP from column fractions, two 500uL fractions were combined, a small amount reserved for an input sample, and the remaining sample was used for the IP.

Luciferase refolding assay

Refolding of denatured luciferase by Ssa1 and Sis1 was performed as described previously [65]. Briefly, firefly luciferase (13.3 mg/ml; Promega) was diluted 42-fold into 25 mM HEPES, pH 7.4, 50 M KCl, 5 mM $MgCl_2$, 6 M GndHCl, 5 mM DTT and denatured by incubation at 25°C for 1 h. Aliquots (1 µl) were removed and added to 124 µl of refolding buffer that was composed of 25 mM HEPES, pH 7.4, 50 mM KCl, 5 mM MgCl2, 1 mM ATP and contained the indicated concentration of Ssa1, Sis1, Sti1, and/or CHIP. Reaction mixtures were incubated at 30°C, and 1-µl aliquots were removed and mixed with 60 µl of luciferase assay buffer (Promega) at the indicated timepoints and luminescence was collected for 10 sec with a TD20/20 luminometer (Turner Designs).

Analysis of Rnq1 to determine Hsp104 shearing activity

The W303α yeast strain harbored either an empty vector (control) or Sti1 construct expressed from its endogenous promoter and p315-Cup1-Rnq1-GFP. Cultures were maintained at log phase in synthetic media containing glucose. Following addition of 3mM guanidinium-HCl, cultures were monitored at OD_{600} for doubling time. At the indicated generations, a portion of the culture was pelleted and frozen. After all time points were collected, pellets were thawed on ice, lysed via bead breaking, and

normalized. An aliquot was separated to use as the total fraction, then the remaining lysate was subjected to 100,000xg spin in an ultracentrifuge at 4°C. An aliquot of the supernatant was collected, then the pellet resuspended in the beginning volume with the same lysis buffer. A 20uL portion of each sample (total, supernatant, and pellet) was run on a 9% SDS-PAGE gel and transferred to nitrocellulose, then probed using anti-GFP antibody to monitor Rnq1 solubility. A control culture was grown for the same amount of time without GndHCl and analyzed in the same way.

2.7 Tables and Figures

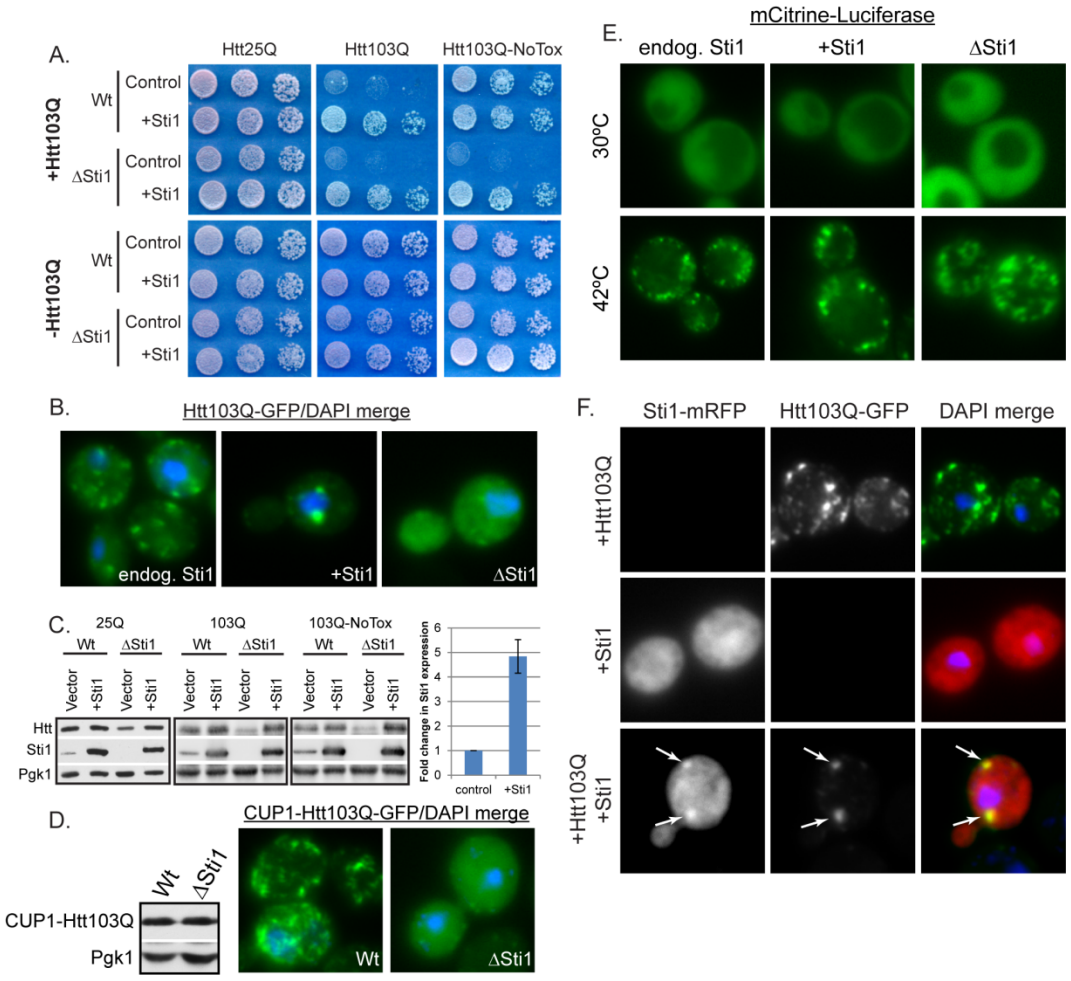

Figure 2.1 Sti1 suppresses Htt103Q toxicity and reorganizes Htt103Q-GFP foci
(A) Impact of Sti1 upon Htt103Q growth defect as monitored by cell growth assay plated in fivefold dilutions. Htt103Q and Htt103Q-NoTox are two integration strains with similar Htt expression that differ in severity of the growth defect. (B) Impact of Sti1 on organization of Htt103Q-GFP foci. (C) Expression levels of Htt as detected by Western blot analysis of lysates taken from cultures grown from strains in A. Graph depicts quantitation of Sti1 overexpression compared to endogenous Sti1 (n=6). (D) Expression level and localization of Htt103Q-GFP as in (B and C). Here Htt103Q was expressed from a CUP1 promoter induced with 500uM CuSO4 for 4 h. (E) Influence of Sti1 upon organization of mCitrine-Luciferase during heat shock. Cells were imaged live during growth at 30°C and then again after a shift to 42°C for 20 min. (F) Co-localization of Htt103Q-GFP and Sti1-mRFP. White arrows indicate co-localization. Nuclei were visualized using DAPI staining. Lysates for Western blot analysis came from cells grown under the same conditions used for fluorescence microscopy.

A.

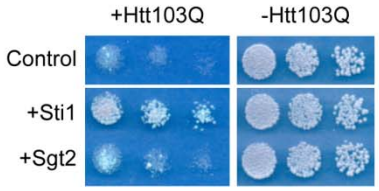
+Htt103Q
-Htt103Q
Control
+Sti1
+Sgt2

B.

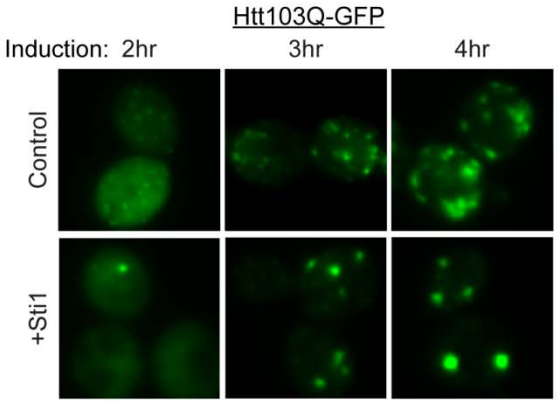
Htt103Q-GFP
Induction: 2hr
3hr
4hr
Control
+Sti1

C.

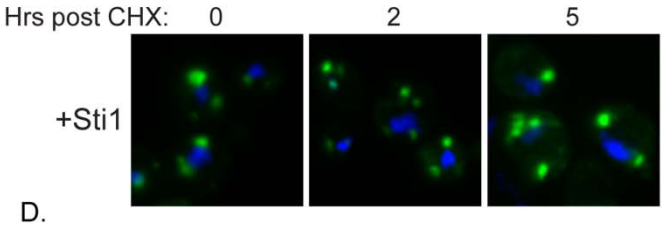
Hrs post CHX:
0
2
5
+Sti1

D.

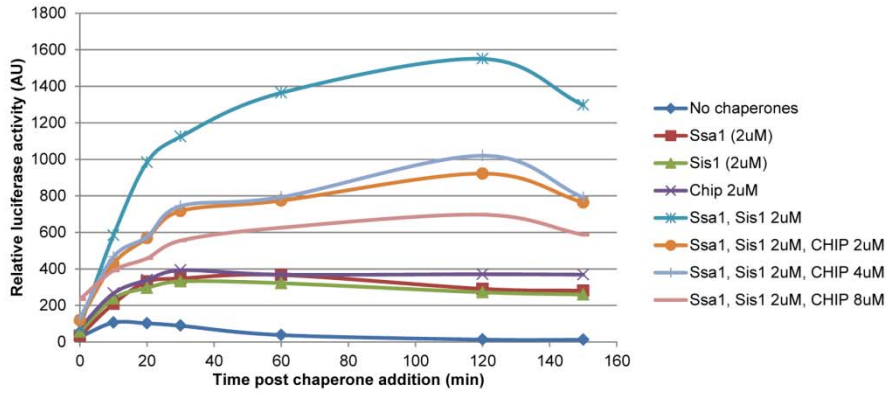
Relative luciferase activity (AU)
Time post chaperone addition (min)
No chaperones
Ssa1 (2uM)
Sis1 (2uM)
Chip 2uM
Ssa1, Sis1 2uM
Ssa1, Sis1 2uM, CHIP 2uM
Ssa1, Sis1 2uM, CHIP 4uM
Ssa1, Sis1 2uM, CHIP 8uM

E.

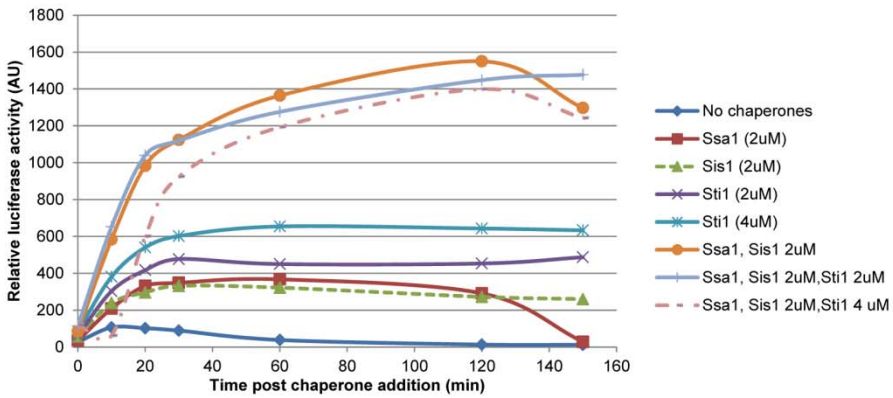
Relative luciferase activity (AU)
Time post chaperone addition (min)
No chaperones
Ssa1 (2uM)
Sis1 (2uM)
Sti1 (2uM)
Sti1 (4uM)
Ssa1, Sis1 2uM
Ssa1, Sis1 2uM,Sti1 2uM
Ssa1, Sis1 2uM,Sti1 4 uM

Figure 2.2 Sti1 specifically alters Htt103Q-GFP spatial and temporal foci formation (A) Sgt2 does not suppress the Htt103Q growth defect as monitored by cell growth assay plated in fivefold dilutions. The toxicity assay was plated on synthetic media containing 500uM CuSO4 to induce Sgt2 expression. (B) Impact of Sti1 upon Htt103Q-GFP foci formation over time. Live images were captured at the indicated times after galactose induction of Htt103Q-GFP. (C) Stability of Htt103Q-GFP foci during Sti1 overexpression as monitored by cycloheximide decay. After 4 h of Htt103Q-GFP induction, cells were treated with cycloheximide, then fixed and imaged at the indicated times. Nuclei were visualized using DAPI staining. (D and E) Influence of (D) CHIP or (E) Sti1 upon Ssa1 and Sis1 chaperone activity as measured by in vitro luciferase activity assay. Chaperones were added at the indicated concentrations to GndHCl treated luciferase and luminescence was measured as a readout for chaperone mediated refolding.

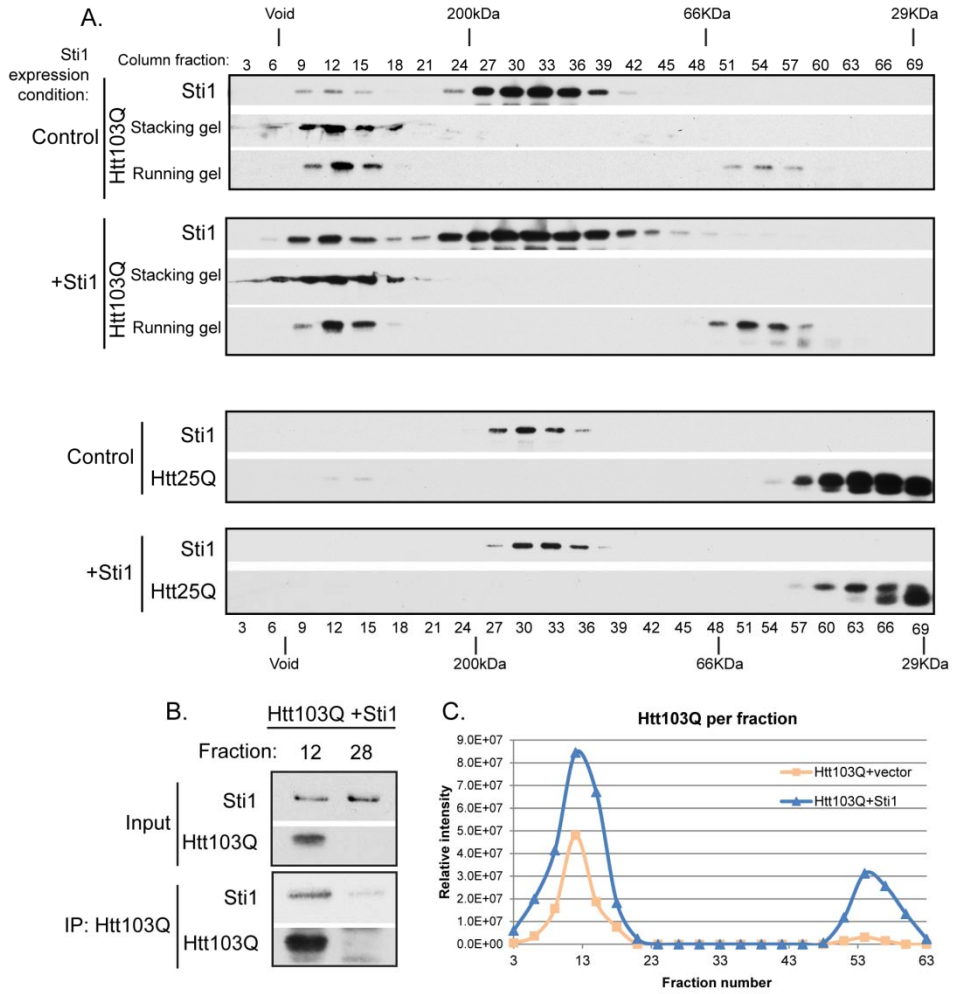

Figure 2.3 Sti1 co-fractionates with high molecular weight forms of Htt103Q
(A) Migration of indicated forms of Htt with Sti1 on Sephacryl S200 gel filtration column at endogenous (control) or overexpressed Sti1 levels as detected by Western blot. (B) Detection of Sti1 in immune precipitates with FLAG-Htt103Q-GFP. Immunoprecipitation was performed with anti-FLAG conjugated beads from aliquots of fraction 12 containing both Htt103Q and Sti1 or from fraction 28 containing only Sti1 as a background control. The IP was carried out using the column sample with elevated levels of Sti1 and precipitates were analyzed by Western blot. (C) Quantitation of Htt103Q in column fractions. Non-denaturing lysates were prepared as described in the methods, and equivalent amounts of total protein per sample were applied to the S200 column.

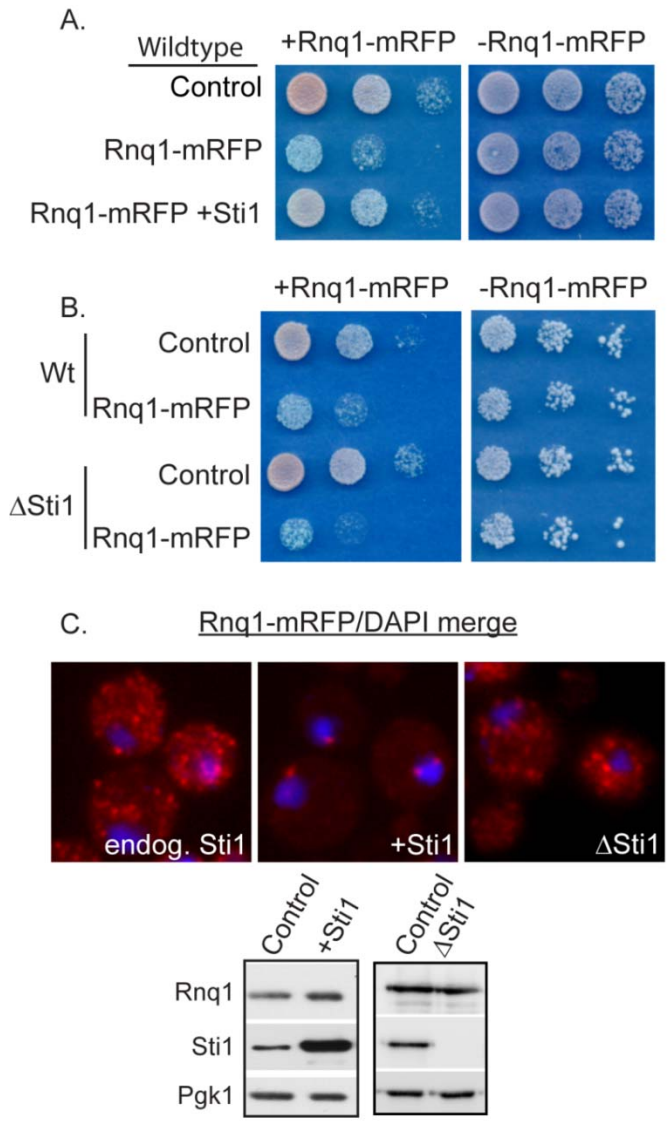

Figure 2.4 Sti1 suppresses Rnq1 toxicity and reorganizes Rnq1-mRFP foci
(A and B) Impact of Sti1 upon the growth defect caused by Rnq1-mRFP overexpression as monitored by cell growth assay plated in fivefold dilutions. Toxicity assay was plated on synthetic media containing 2% glucose and 500uM CuSO4. (C) Impact of Sti1 upon organization of Rnq1-mRFP foci. Expression levels of Rnq1-mRFP were detected by Western blot analysis under conditions identical to those used for fluorescence microscopy and described in the methods section.

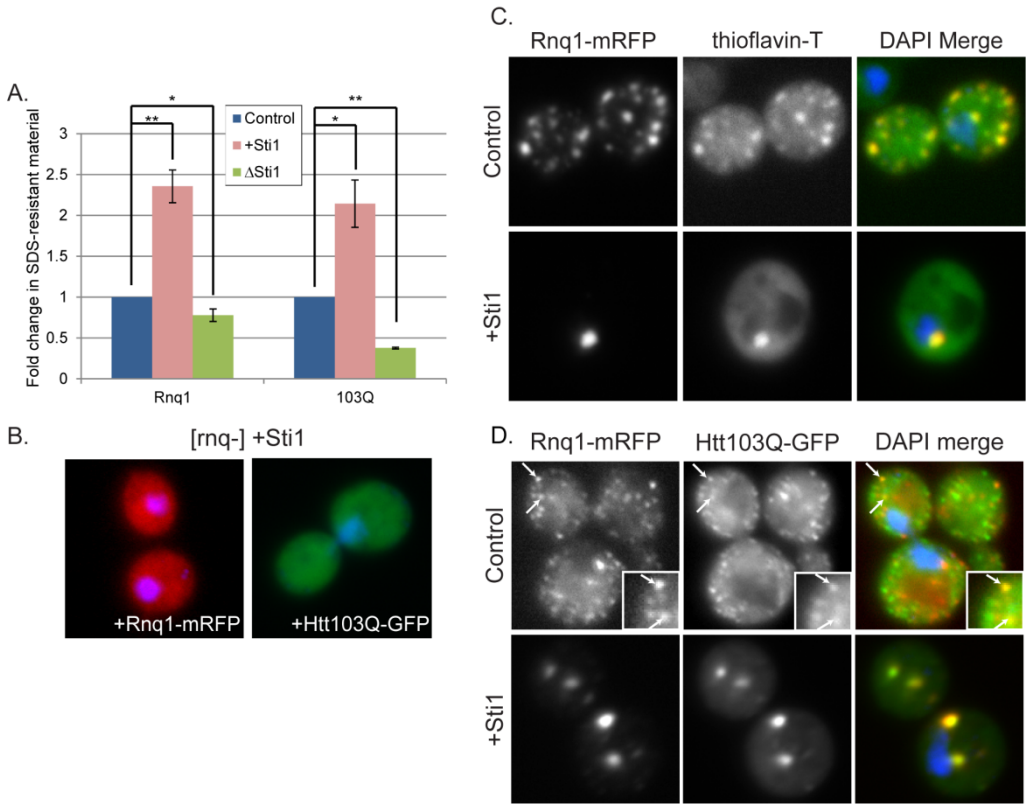

Figure 2.5 Sti1 modulates assembly of amyloidogenic substrates
(A) Quantitation of Sti1 impact upon SDS-resistant Htt103Q-GFP or Rnq1-mRFP material as measured by SDD-AGE. (*p<0.05, **p<0.005, n=3 or more) (B) Inability of Sti1 to reorganize Htt103Q-GFP or Rnq1-mRFP to foci in a [rnq-] background. (C) Staining of Rnq1-mRFP foci with the amyloid indicator dye Thioflavin-T as well as DAPI to indicate nuclei. (D) Co-localization of Htt103-GFP and Rnq1-mRFP during Sti1 overexpression. White arrows indicate co-localization. Insets represent the same punctae indicated with white arrows in the main panel.

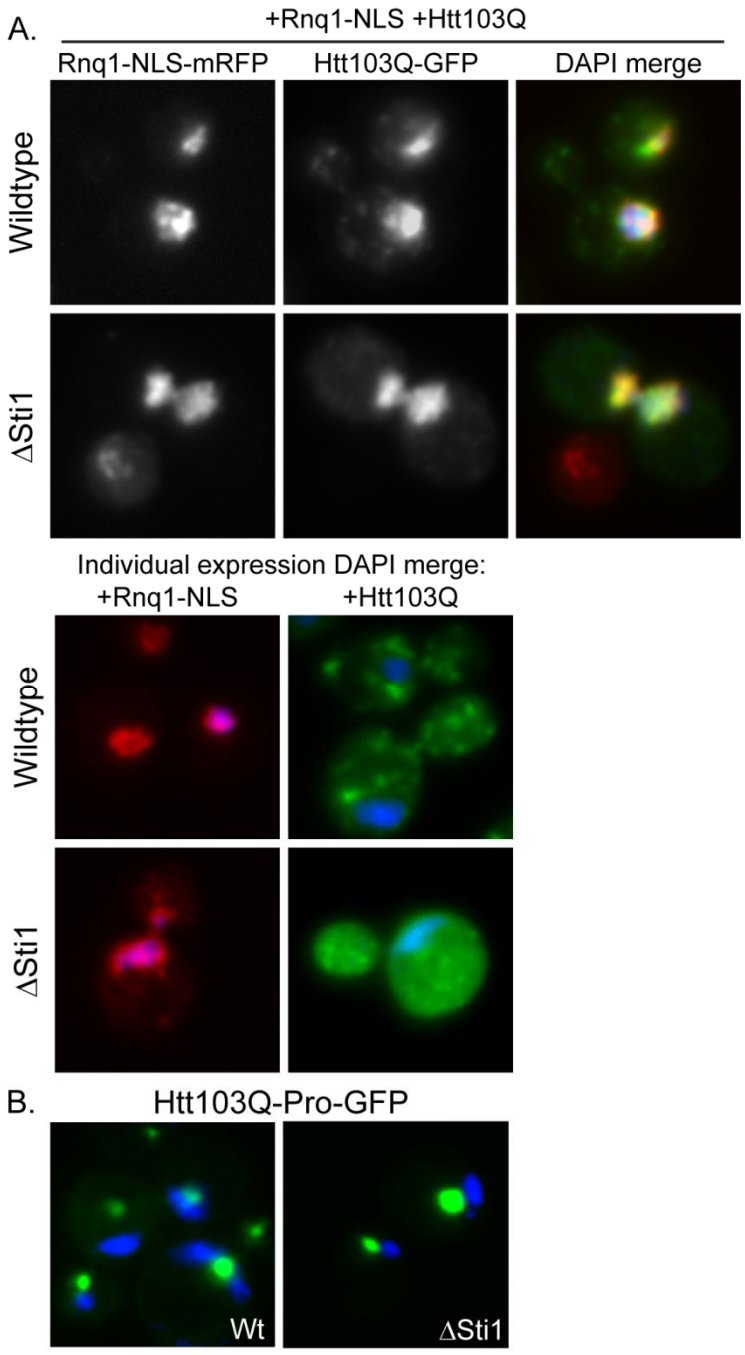

Figure 2.6 Sti1 is not required for Rnq1-NLS relocalization of Htt103Q to the nucleus

(A) Lack of Sti1 dependence for Rnq1-mRFP-NLS to target Htt103Q-GFP to the nucleus. Rnq1 was tagged with the SV40 NLS signal and expressed at low levels from the CUP1 promoter as in other Rnq1-mRFP localization studies. Samples expressed either Rnq1-mRFP-NLS, Htt103Q-GFP, or both as indicated. (B) Impact of Sti1 deletion upon foci formation of Htt103Q-GFP containing a proline rich region. Nuclei were visualized using DAPI staining.

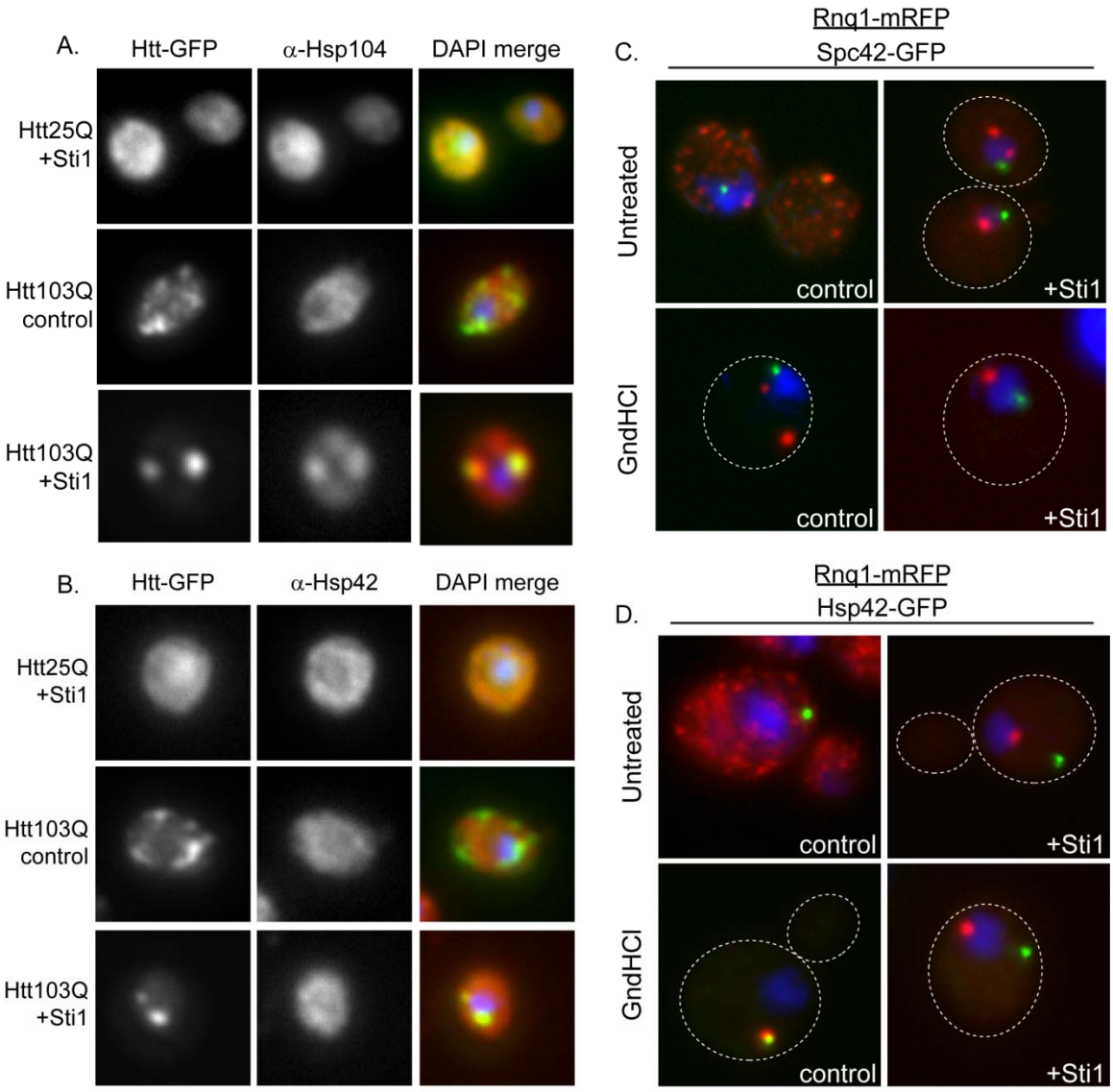

Figure 2.7 The StiF is a juxtanuclear compartment for amyloid-like proteins
(A and B) Localization of endogenous (A) Hsp104 or (B) Hsp42 as monitored by immunofluorescence using Htt103Q as a StiF marker. (C and D) Impact of Hsp104 inhibition upon Rnq1-mRFP localization at the StiF. Fluorescence microscopy was carried out in strains with (C) Spc42 or (D) Hsp42 tagged at the endogenous locus with GFP. Rnq1-mRFP was induced with 50uM CuSO4 and Hsp104 was inhibited with 3mM GndHCl for 2 h before cells were fixed. Nuclei were visualized using DAPI staining. Dotted lines indicate the outline of the cell.

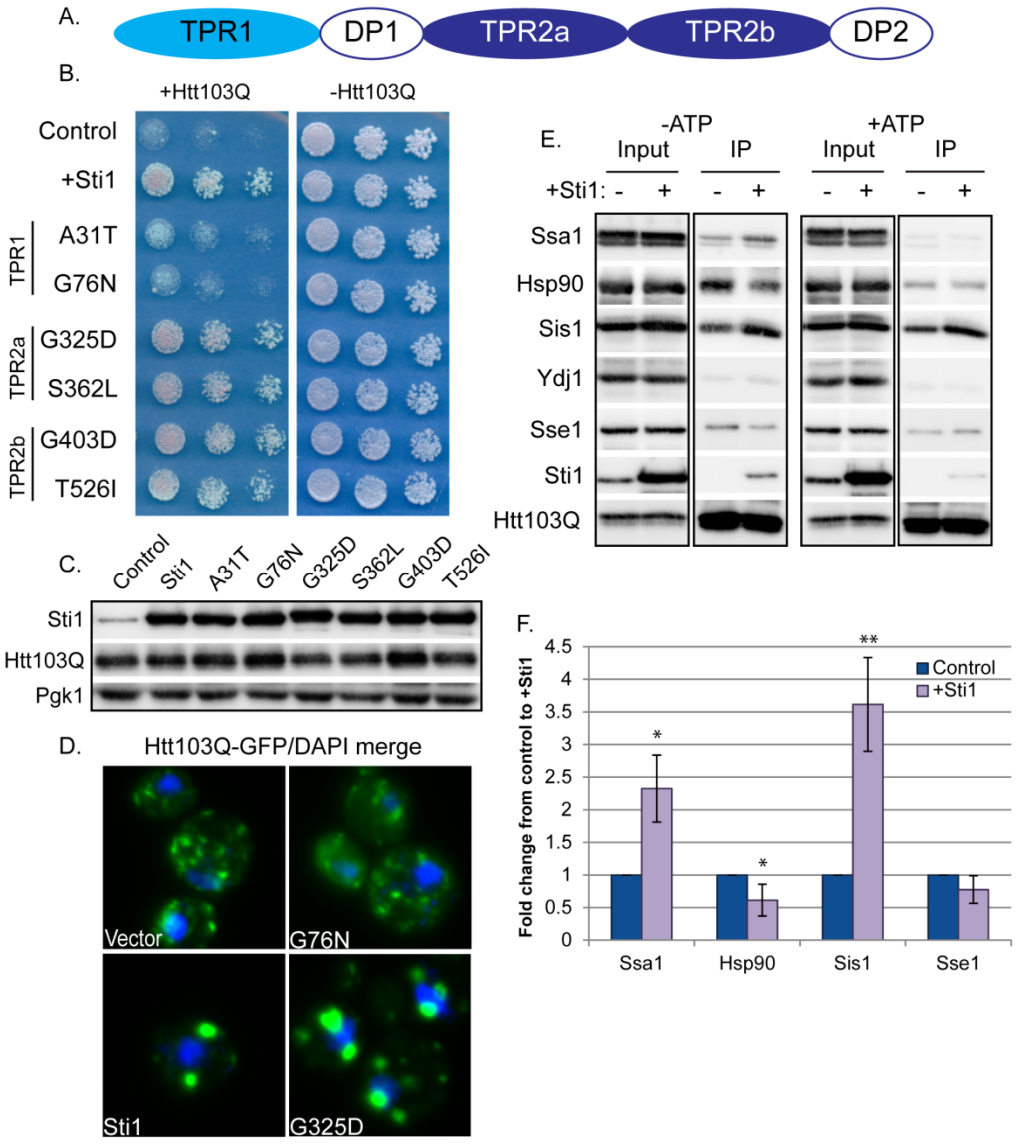

Figure 2.8 Sti1 reorganizes complexes that contain Htt103Q and Hsp70
(A) Diagram of Sti1's domain structure. (B) Impact of mutating different Sti1 TPR domains upon ability to suppress Htt103Q growth defect as monitored by cell growth assay plated in fivefold dilutions. (C) Sti1 and Htt103Q expression as monitored by Western blot analysis of strains shown in (B). (D) Impact of select Sti1 point mutations upon Sti1's ability to reorganize Htt103Q. (E) Impact of elevated Sti1 upon the multichaperone:substrate complex as monitored by co-immunoprecipitation of Htt103Q and Western blot of indicated chaperones. CoIPs were carried out in the absence or presence of ATP as indicated above each group of panels. (F) Quantitation of chaperones which co-immunoprecipitated with Htt103Q in E. (*$p<0.05$, **$p<0.005$, n=3 or more)

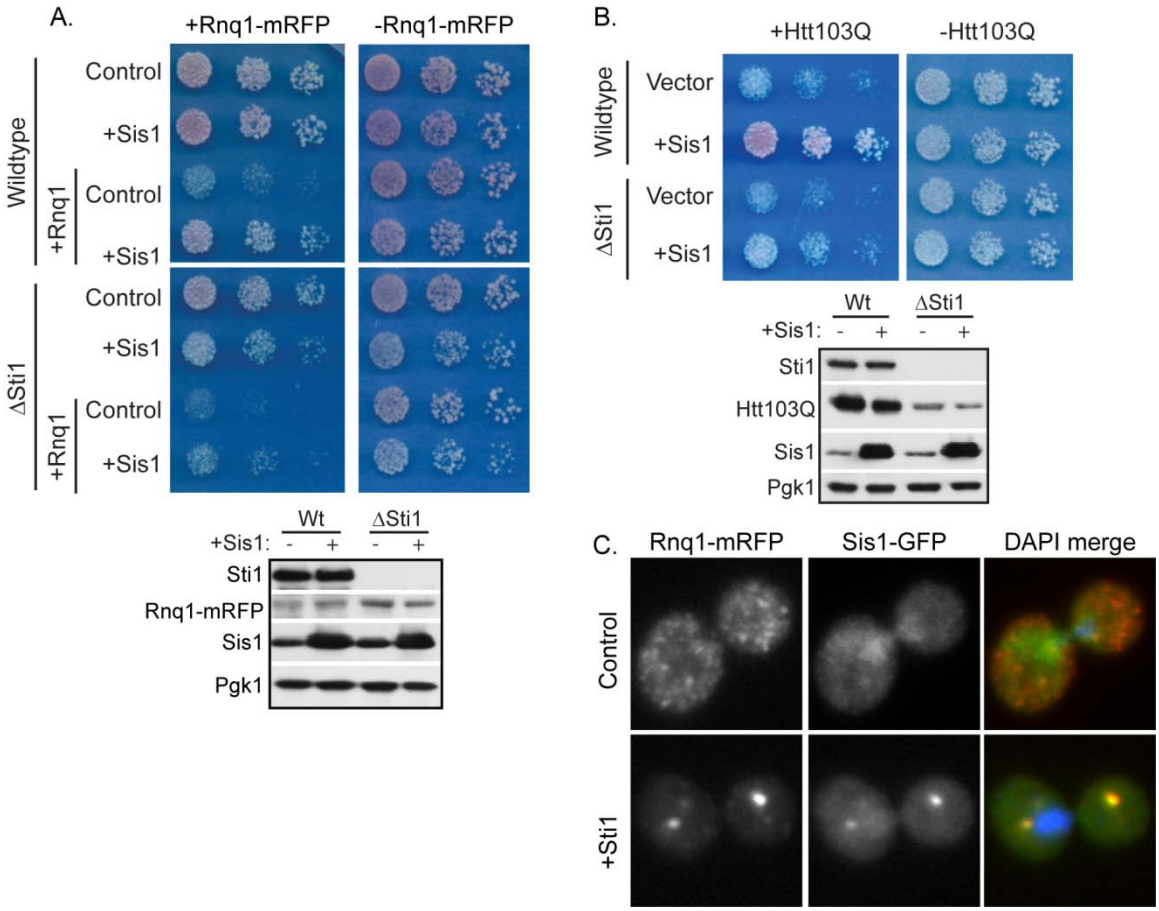

Figure 2.9 Sti1 and Sis1 cooperate to regulate Rnq1 and Htt103Q toxicity
(A and B) Inability of Sis1 to suppress growth defect of (A) Rnq1-mRFP (p423-CUP1 plasmid) or (B) Htt103Q (toxic integration strain) in a Sti1 deletion strain as monitored by cell growth assay plated in fivefold dilutions. Expression levels of Sti1, Sis1, and Htt103Q or Rnq1 were measured by Western blot analysis. (C) Impact of elevated Sti1 upon subcellular localization of Sis1 during Rnq1-mRFP expression. Experiments were carried out in a strain where Sis1 was tagged at the endogenous locus with GFP.

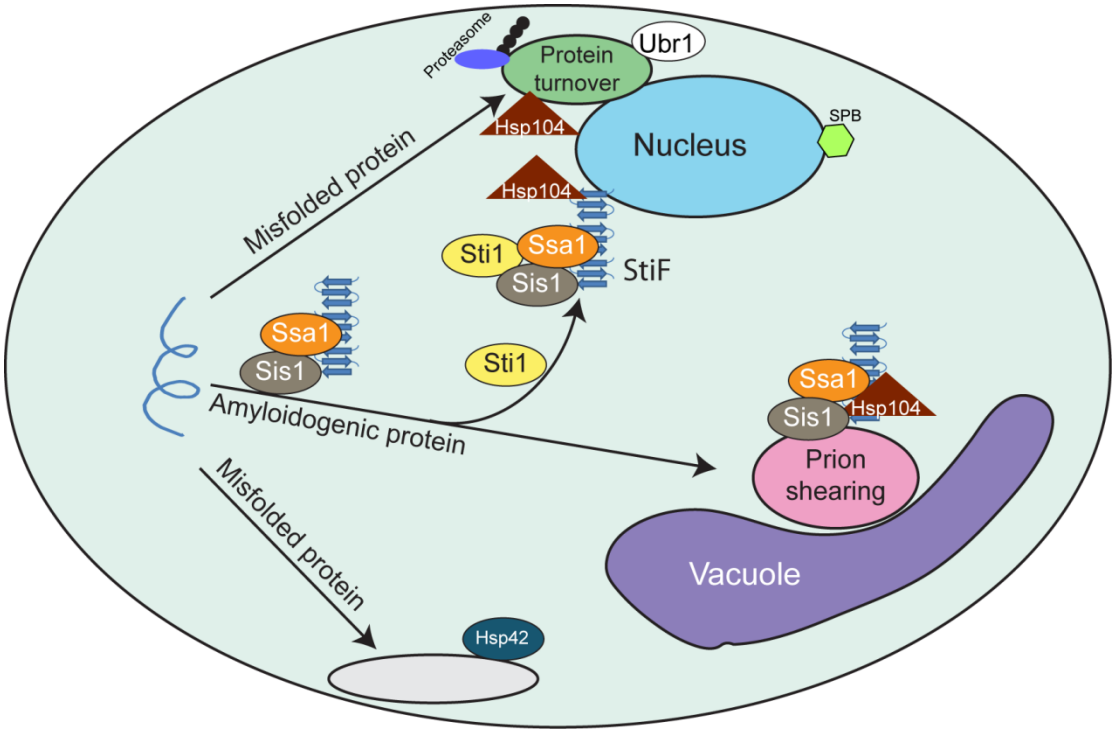

Figure 2.10 Model for StiF formation
Sti1 acts in cooperation with Ssa1 and Sis1 to redirect amyloid-like material from the IPOD prion shearing center to the StiF which is present under normal growth conditions. The StiF contains Hsp104, but not Hsp42, and is not localized at the spindle pole body (SPB).

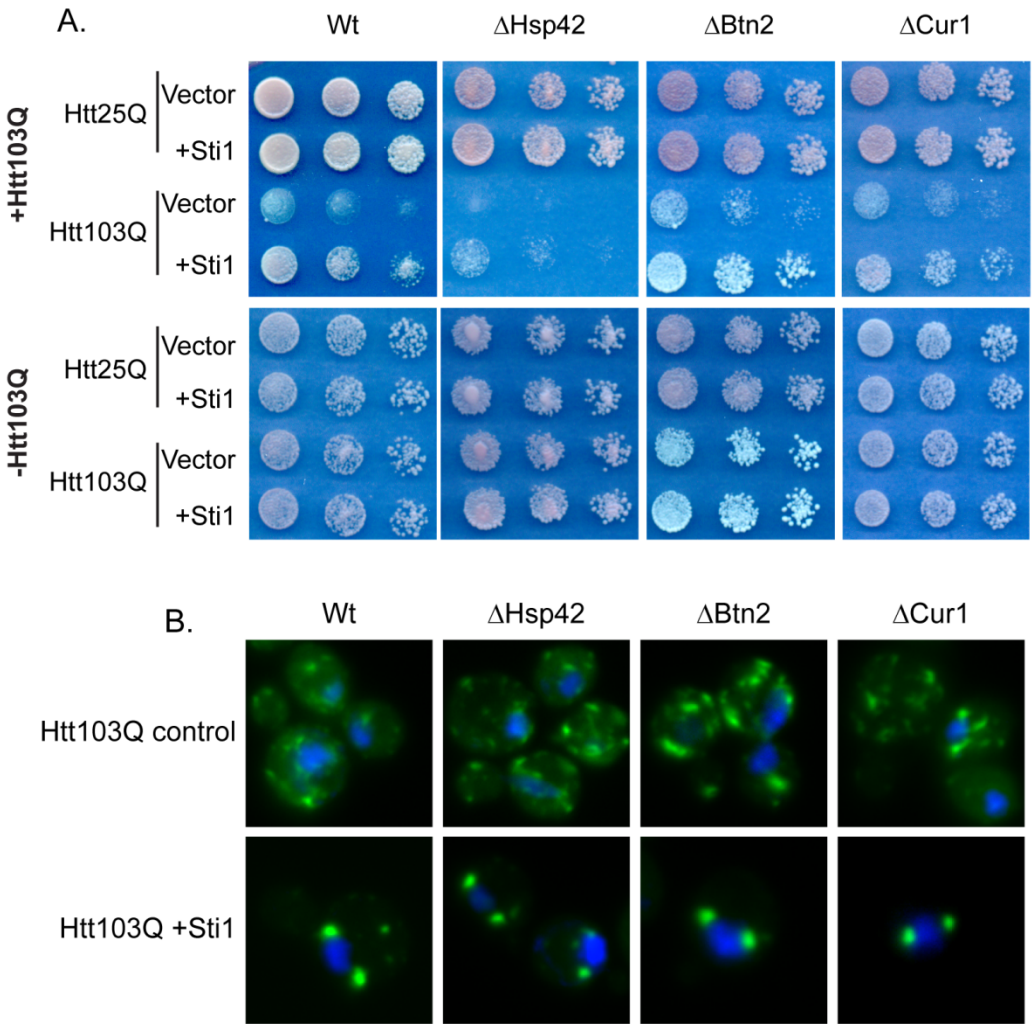

Figure 2.11 Other cellular sorting factors are not necessary for Sti1's mechanism of action

(A) Impact of deletion of indicated proteins upon Sti1's ability to suppress Htt103Q growth defect as monitored by cell growth assay plated in fivefold dilutions. (B) Impact of deletion of indicated proteins upon Sti1's ability to reorganize Htt103Q-GFP. Toxicity and fluorescence microscopy assays were carried out as in Figure 2.1.

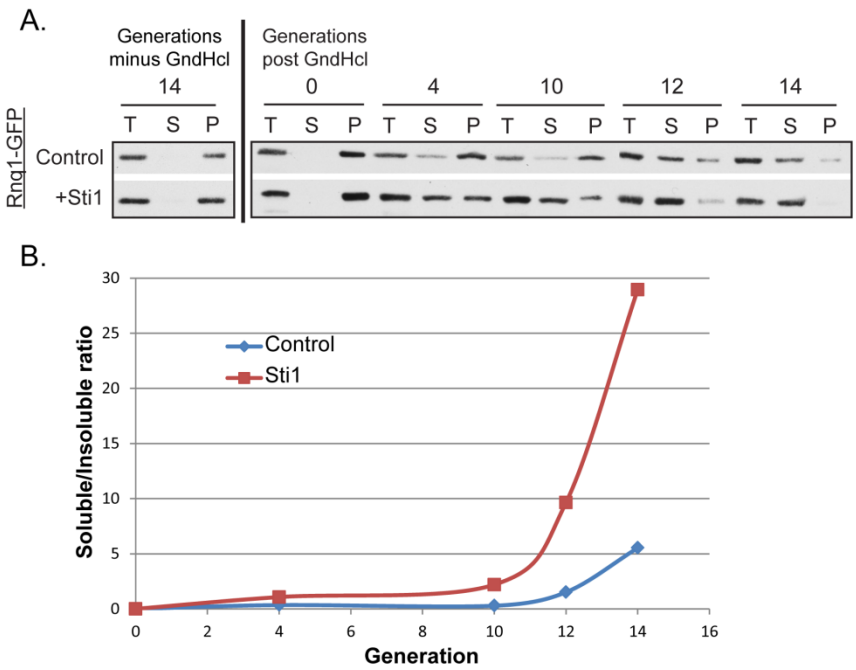

Figure 2.12 Sti1 attenuates Hsp104 shearing activity in the presence of GndHCl
(A) Curing rate of [RNQ+] is increased in the presence of GndHCl when Sti1 is overexpressed as indicated by triton solubility assay followed by Western blot. Since [RNQ+] is triton insoluble, we measured the Rnq1 triton solubility from lysates with endogenous and overexpressed Sti1 at the indicated generations post GndHCl treatment. Increased Sti1 does not completely inactivate Hsp104 and cure the cells of [RNQ+] as indicated in the left panel without GndHCl treatment. (B) Quantitation of curing rate in (A) as measured by ratio of soluble to insoluble Rnq1.

REFERENCES

1. Carrell, R.W. and D.A. Lomas, *Conformational disease.* Lancet, 1997. **350**(9071): p. 134-8.

2. Chiti, F. and C.M. Dobson, *Protein misfolding, functional amyloid, and human disease.* Annu Rev Biochem, 2006. **75**: p. 333-66.

3. Treusch, S., D.M. Cyr, and S. Lindquist, *Amyloid deposits: protection against toxic protein species?* Cell Cycle, 2009. **8**(11): p. 1668-74.

4. Haass, C. and D.J. Selkoe, *Soluble protein oligomers in neurodegeneration: lessons from the Alzheimer's amyloid beta-peptide.* Nat Rev Mol Cell Biol, 2007. **8**(2): p. 101-12.

5. Bucciantini, M., et al., *Prefibrillar amyloid protein aggregates share common features of cytotoxicity.* J Biol Chem, 2004. **279**(30): p. 31374-82.

6. Cohen, E., et al., *Opposing activities protect against age-onset proteotoxicity.* Science, 2006. **313**(5793): p. 1604-10.

7. Wolfe, K.J. and D.M. Cyr, *Amyloid in neurodegenerative diseases: friend or foe?* Semin Cell Dev Biol, 2011. **22**(5): p. 476-81.

8. Douglas, P.M., et al., *Chaperone-dependent amyloid assembly protects cells from prion toxicity.* Proc Natl Acad Sci U S A, 2008. **105**(20): p. 7206-11.

9. Muchowski, P.J. and J.L. Wacker, *Modulation of neurodegeneration by molecular chaperones.* Nat Rev Neurosci, 2005. **6**(1): p. 11-22.

10. Cyr, D.M., T. Langer, and M.G. Douglas, *DnaJ-like proteins: molecular chaperones and specific regulators of Hsp70.* Trends Biochem Sci, 1994. **19**(4): p. 176-81.

11. Tyedmers, J., A. Mogk, and B. Bukau, *Cellular strategies for controlling protein aggregation.* Nat Rev Mol Cell Biol, 2010. **11**(11): p. 777-88.

12. Cyr, D.M., J. Hohfeld, and C. Patterson, *Protein quality control: U-box-containing E3 ubiquitin ligases join the fold.* Trends Biochem Sci, 2002. **27**(7): p. 368-75.

13. Meacham, G.C., et al., *The Hsc70 co-chaperone CHIP targets immature CFTR for proteasomal degradation.* Nat Cell Biol, 2001. **3**(1): p. 100-5.

14. Langer, T., et al., *Successive action of DnaK, DnaJ and GroEL along the pathway of chaperone-mediated protein folding.* Nature, 1992. **356**(6371): p. 683-9.

15. Liberek, K., et al., *Escherichia coli DnaJ and GrpE heat shock proteins jointly stimulate ATPase activity of DnaK.* Proc Natl Acad Sci U S A, 1991. **88**(7): p. 2874-8.

16. Cyr, D.M., X. Lu, and M.G. Douglas, *Regulation of Hsp70 function by a eukaryotic DnaJ homolog.* J Biol Chem, 1992. **267**(29): p. 20927-31.

17. Scheufler, C., et al., *Structure of TPR domain-peptide complexes: critical elements in the assembly of the Hsp70-Hsp90 multichaperone machine.* Cell, 2000. **101**(2): p. 199-210.

18. Shaner, L., et al., *The yeast Hsp110 Sse1 functionally interacts with the Hsp70 chaperones Ssa and Ssb.* J Biol Chem, 2005. **280**(50): p. 41262-9.

19. Steel, G.J., et al., *Coordinated activation of Hsp70 chaperones.* Science, 2004. **303**(5654): p. 98-101.

20. Hernandez, M.P., W.P. Sullivan, and D.O. Toft, *The assembly and intermolecular properties of the hsp70-Hop-hsp90 molecular chaperone complex.* J Biol Chem, 2002. **277**(41): p. 38294-304.

21. Reidy, M. and D.C. Masison, *Sti1 regulation of Hsp70 and Hsp90 is critical for curing of Saccharomyces cerevisiae [PSI+] prions by Hsp104.* Mol Cell Biol, 2010. **30**(14): p. 3542-52.

22. Roffe, M., et al., *Prion protein interaction with stress-inducible protein 1 enhances neuronal protein synthesis via mTOR.* Proc Natl Acad Sci U S A, 2010. **107**(29): p. 13147-52.

23. Jones, G., et al., *Propagation of Saccharomyces cerevisiae [PSI+] prion is impaired by factors that regulate Hsp70 substrate binding.* Mol Cell Biol, 2004. **24**(9): p. 3928-37.

24. Chen, S., et al., *Differential interactions of p23 and the TPR-containing proteins Hop, Cyp40, FKBP52 and FKBP51 with Hsp90 mutants.* Cell Stress Chaperones, 1998. **3**(2): p. 118-29.

25. Dai, Q., et al., *CHIP activates HSF1 and confers protection against apoptosis and cellular stress.* EMBO J, 2003. **22**(20): p. 5446-58.

26. Qian, S.B., et al., *CHIP-mediated stress recovery by sequential ubiquitination of substrates and Hsp70.* Nature, 2006. **440**(7083): p. 551-5.

27. Jiang, J., et al., *CHIP is a U-box-dependent E3 ubiquitin ligase: identification of Hsc70 as a target for ubiquitylation.* J Biol Chem, 2001. **276**(46): p. 42938-44.

28. Olzscha, H., et al., *Amyloid-like aggregates sequester numerous metastable proteins with essential cellular functions.* Cell, 2011. **144**(1): p. 67-78.

29. Last, N.B., E. Rhoades, and A.D. Miranker, *Islet amyloid polypeptide demonstrates a persistent capacity to disrupt membrane integrity.* Proc Natl Acad Sci U S A, 2011. **108**(23): p. 9460-5.

30. Kaganovich, D., R. Kopito, and J. Frydman, *Misfolded proteins partition between two distinct quality control compartments.* Nature, 2008. **454**(7208): p. 1088-95.

31. Johnston, J.A., C.L. Ward, and R.R. Kopito, *Aggresomes: a cellular response to misfolded proteins.* J Cell Biol, 1998. **143**(7): p. 1883-98.

32. Specht, S., et al., *Hsp42 is required for sequestration of protein aggregates into deposition sites in Saccharomyces cerevisiae.* J Cell Biol, 2011. **195**(4): p. 617-29.

33. Weisberg, S.J., et al., *Compartmentalization of superoxide dismutase 1 (SOD1G93A) aggregates determines their toxicity.* Proc Natl Acad Sci U S A, 2012. **109**(39): p. 15811-6.

34. Summers, D.W., et al., *The Type II Hsp40 Sis1 cooperates with Hsp70 and the E3 ligase Ubr1 to promote degradation of terminally misfolded cytosolic protein.* PLoS One, 2013. **8**(1): p. e52099.

35. Shiber, A., et al., *Ubiquitin conjugation triggers misfolded protein sequestration into quality-control foci when Hsp70 chaperone levels are limiting.* Mol Biol Cell, 2013.

36. Malinovska, L., et al., *Molecular chaperones and stress-inducible protein sorting factors coordinate the spatio-temporal distribution of protein aggregates.* Mol Biol Cell, 2012.

37. Tyedmers, J., et al., *Prion induction involves an ancient system for the sequestration of aggregated proteins and heritable changes in prion fragmentation.* Proc Natl Acad Sci U S A, 2010. **107**(19): p. 8633-8.

38. Wang, Y., et al., *Abnormal proteins can form aggresome in yeast: aggresome-targeting signals and components of the machinery.* FASEB J, 2009. **23**(2): p. 451-63.

39. Douglas, P.M., et al., *Reciprocal Efficiency of RNQ1 and Polyglutamine Detoxification in the Cytosol and Nucleus.* Mol Biol Cell, 2009.

40. Summers, D.W., et al., *The type I Hsp40 Ydj1 utilizes a farnesyl moiety and zinc finger-like region to suppress prion toxicity.* J Biol Chem, 2009. **284**(6): p. 3628-39.

41. Sondheimer, N. and S. Lindquist, *Rnq1: an epigenetic modifier of protein function in yeast.* Mol Cell, 2000. **5**(1): p. 163-72.

42. Derkatch, I.L., et al., *Prions affect the appearance of other prions: the story of [PIN(+)].* Cell, 2001. **106**(2): p. 171-82.

43. Meriin, A.B., et al., *Huntington toxicity in yeast model depends on polyglutamine aggregation mediated by a prion-like protein Rnq1.* J Cell Biol, 2002. **157**(6): p. 997-1004.

44. Duennwald, M.L., et al., *Flanking sequences profoundly alter polyglutamine toxicity in yeast.* Proc Natl Acad Sci U S A, 2006. **103**(29): p. 11045-50.

45. Dehay, B. and A. Bertolotti, *Critical role of the proline-rich region in Huntingtin for aggregation and cytotoxicity in yeast.* J Biol Chem, 2006. **281**(47): p. 35608-15.

46. Nicolet, C.M. and E.A. Craig, *Isolation and characterization of STI1, a stress-inducible gene from Saccharomyces cerevisiae.* Mol Cell Biol, 1989. **9**(9): p. 3638-46.

47. Floer, M., G.O. Bryant, and M. Ptashne, *HSP90/70 chaperones are required for rapid nucleosome removal upon induction of the GAL genes of yeast.* Proc Natl Acad Sci U S A, 2008. **105**(8): p. 2975-80.

48. Prodromou, C., et al., *Regulation of Hsp90 ATPase activity by tetratricopeptide repeat (TPR)-domain co-chaperones.* EMBO J, 1999. **18**(3): p. 754-62.

49. Sondheimer, N., et al., *The role of Sis1 in the maintenance of the [RNQ+] prion.* EMBO J, 2001. **20**(10): p. 2435-42.

50. Aron, R., et al., *J-protein co-chaperone Sis1 required for generation of [RNQ+] seeds necessary for prion propagation.* EMBO J, 2007. **26**(16): p. 3794-803.

51. Tipton, K.A., K.J. Verges, and J.S. Weissman, *In vivo monitoring of the prion replication cycle reveals a critical role for Sis1 in delivering substrates to Hsp104.* Mol Cell, 2008. **32**(4): p. 584-91.

52. Kryndushkin, D.S., et al., *Increased expression of Hsp40 chaperones, transcriptional factors, and ribosomal protein Rpp0 can cure yeast prions.* J Biol Chem, 2002. **277**(26): p. 23702-8.

53. LeVine, H., 3rd, *Thioflavine T interaction with synthetic Alzheimer's disease beta-amyloid peptides: detection of amyloid aggregation in solution.* Protein Sci, 1993. **2**(3): p. 404-10.

54. Jung, G. and D.C. Masison, *Guanidine hydrochloride inhibits Hsp104 activity in vivo: a possible explanation for its effect in curing yeast prions.* Curr Microbiol, 2001. **43**(1): p. 7-10.

55. Ferreira, P.C., et al., *The elimination of the yeast [PSI+] prion by guanidine hydrochloride is the result of Hsp104 inactivation.* Mol Microbiol, 2001. **40**(6): p. 1357-69.

56. Flom, G., et al., *Definition of the minimal fragments of Sti1 required for dimerization, interaction with Hsp70 and Hsp90 and in vivo functions.* Biochem J, 2007. **404**(1): p. 159-67.

57. Song, Y. and D.C. Masison, *Independent regulation of Hsp70 and Hsp90 chaperones by Hsp70/Hsp90-organizing protein Sti1 (Hop1).* J Biol Chem, 2005. **280**(40): p. 34178-85.

58. Chernoff, Y.O., et al., *Role of the chaperone protein Hsp104 in propagation of the yeast prion-like factor [psi+].* Science, 1995. **268**(5212): p. 880-4.

59. Treusch, S. and S. Lindquist, *An intrinsically disordered yeast prion arrests the cell cycle by sequestering a spindle pole body component.* J Cell Biol, 2012. **197**(3): p. 369-79.

60. Lee, P., et al., *Sti1 and Cdc37 can stabilize Hsp90 in chaperone complexes with a protein kinase.* Mol Biol Cell, 2004. **15**(4): p. 1785-92.

61. Gamerdinger, M., et al., *BAG3 mediates chaperone-based aggresome-targeting and selective autophagy of misfolded proteins.* EMBO Rep, 2011. **12**(2): p. 149-56.

62. Muller, P., et al., *C-terminal phosphorylation of Hsp70 and Hsp90 regulates alternate binding to co-chaperones CHIP and HOP to determine cellular protein folding/degradation balances.* Oncogene, 2012.

63. Martins-de-Souza, D., et al., *Proteomic analysis identifies dysfunction in cellular transport, energy, and protein metabolism in different brain regions of atypical frontotemporal lobar degeneration.* J Proteome Res, 2012. **11**(4): p. 2533-43.

64. Hawrylycz, M.J., et al., *An anatomically comprehensive atlas of the adult human brain transcriptome.* Nature, 2012. **489**(7416): p. 391-9.

65. Lee, S., et al., *Identification of essential residues in the type II Hsp40 Sis1 that function in polypeptide binding.* J Biol Chem, 2002. **277**(24): p. 21675-82.

CHAPTER 3

Identification of polyglutamine rich proteins that alter huntingtin toxicity and aggregation

3.1 Overview

Protein conformational maladies such as Huntington Disease (HD) are characterized by accumulation of intracellular and extracellular protein inclusions. In HD, disease onset and cell death occurs after protease cleavage of the polyglutamine expanded huntingtin (Htt) protein, followed by translocation into the nucleus where an N-terminal fragment accumulates in inclusions. Interestingly, there is an inverse correlation between Htt toxicity and aggregation, suggesting that protein aggregation is a cellular coping mechanism for an otherwise toxic species. To more clearly understand cellular mechanisms for suppression of proteotoxicity, we carried out a high copy screen for suppressors of growth defects caused by nuclear polyglutamine expanded huntingtin (Htt103Q). Nuclear Htt103Q is highly toxic and less aggregation prone than its cytosolic form, so we screened for proteins that suppress toxicity while promoting aggregation of nuclear Htt103Q. We identified Nab3, Pop2, and Cbk1, which themselves contain polyQ-rich regions, as suppressors of Htt toxicity. Nab3 is an essential nuclear protein that functions in RNA processing, which appears to be inactivated by Htt103Q. Function of Pop2 and Cbk1 does not appear to be impacted by nuclear Htt103Q, as their respective

polyQ-rich domains are sufficient to suppress Htt103Q toxicity. Elevation of Pop2 and Cbk1 increases accumulation of detergent insoluble Htt103Q, and drives Htt103Q into perinuclear protein quality control centers. Pop2 and Cbk1 action is dependent upon the Hsp70 co-chaperone Sti1 which functions in packaging of amyloid-like proteins into benign aggregates. Data presented suggest that Htt103Q interacts with its polyQ domain containing neighbors with differing outcomes. Some interactions are harmful due to sequestration away from essential functions while other interactions are beneficial because they result in funneling of toxic Htt103Q species to the Hsp70-Sti1 pathway and assembly into benign aggregates.

3.2 Introduction

A variety of human disorders, termed conformational disorders (CD), result from misfolding and aggregation of different underlying proteins [1]. Intracellular and extracellular inclusions found in tissue of affected individuals contain amyloid-like proteins that are enriched in beta-sheet structure, are detergent insoluble, and bind amyloid indicator dyes [1-4]. Amyloid assembly is a regulated process which occurs through a nucleated polymerization reaction [5]. When soluble protein interacts with templated species, it gets incorporated into the growing amyloid fibril demonstrating that protein-protein interactions mediate polymerization [6-8]. Whether the amyloid-like aggregates themselves are causative or a protective cellular defense mechanism against an unknown toxic species is a topic of debate [3]. The harmful species in some CD may be small oligomeric intermediates of the templated aggregation pathway while accumulation of larger benign assemblies may either be a by-product of such a pathway or a productive defense mechanism [9-16]. Therefore, protection against proteotoxicity

in CD may involve either preventing entry of native proteins into the amyloid-like assembly pathway or, once entry has already occurred, driving formation of a benign aggregate species. In both cases, the cell would be diverting proteins away from a toxic aggregation pathway intermediate.

Huntington Disease (HD) is one of several maladies associated with expansion of a polyglutamine (polyQ) tract within a disease associated gene (HTT). Protease cleavage of the full length polyQ expanded Htt protein is necessary for HD onset and cell death [17,18]. N-terminal fragments of Htt are translocated into the nucleus where they accumulate in inclusions [19]. Both cytoplasmic and intranuclear Htt inclusions are associated with HD [19-21], but toxicity and behavioral phenotypes are more severe when Htt is targeted to the nucleus [22-24]. While a clear mechanistic understanding of nuclear versus cytosolic polyQ toxicity remains to be discovered, several factors have been implicated in this process. The relative concentration of proteostatic factors in the cytosol and nucleus are different creating a specific environment in each subcellular location. The nuclear environment may not be as well-equipped as the cytosol to handle toxic species of polyQ proteins. Disease related polyQ proteins can titrate essential nuclear proteins such as transcription factors away from normal function leading to transcriptional dysregulation and to cell death [25-28]. PolyQ proteins can also interfere with function of protein quality control components such as the ubiquitin proteasome [29-31]. Molecular chaperones help prevent polyQ toxicity by refolding, targeting protein for degradation, or promoting aggregation [3,32-34]. These examples provide evidence that protein-protein interactions have both positive and negative influences on the cell's ability to buffer expression of potentially toxic proteins [35-38].

Many of the basic principles of chaperone modulation of proteotoxicy and aggregation come from ectopic expression of disease related proteins in yeast. Yeast expressing a construct (Htt103Q) containing the first 17 amino acids from HTT exon 1 and a polyQ tract of 103 residues and lacking the proline domain recapitulates polyQ length dependent aggregation and toxicity [6,24,39]. As in mammalian systems, addition of a nuclear localization signal (NLS) caused this protein to be even more toxic [24]. In the yeast model, enhanced toxicity of Htt103Q-NLS was associated with decreased packaging into SDS-resistant aggregates [24]. Htt103Q aggregation and toxicity is dependent on the conformation of the glutamine/asparagine-rich yeast prion protein Rnq1 [6,40]. Interaction of Htt103Q and [RNQ+] prion causes templating of Htt103Q into an amyloid-like conformation [6,40]. Sti1, an Hsp70 co-chaperone, seems to be one factor that contributes to a cells capacity to buffer proteotoxicity of polyQ proteins in the cytosol. We recently characterized a role for Sti1 in promoting protective aggregation of Htt103Q. Increased SDS-resistant aggregation correlated with accumulation of Htt103Q at a perinuclear compartment, demonstrating that Sti1 functions in a pathway for packaging Htt103Q into a protective quality control compartment (Chapter 2). Targeting Htt103Q to the nucleus may remove the substrate from an environment where a toxic species would have been sequestered into a benign SDS-resistant inclusion.

In order to better understand the pathway for protective aggregation, we carried out a high copy toxicity suppressor screen utilizing Htt103Q-NLS as the substrate. The nuclear Htt103Q, which is more toxic yet more detergent soluble, allowed us to identify suppressors of proteotoxicity which also impacted Htt aggregation. We further characterized screen hits in the context of Htt103Q to better understand these aggregation

phenotypes. Although numerous other studies have screened for factors impacting polyQ toxicity or aggregation [6,35-38,41-46], our approach of utilizing the nuclear Htt103Q allowed us to identify novel components promoting protective aggregation. Strikingly, over half of the genomic fragments that suppressed toxicity included ORFs encoding polyQ containing proteins. While characterizing the Htt103Q aggregation phenotype of several of these polyQ genes, we discovered that Nab3 had little effect upon aggregation and required a functional RNA binding domain to suppress Htt103Q-NLS toxicity. Pop2 and Cbk1 promoted protective aggregation through interaction of their polyQ-rich regions with Htt103Q. Modification of Htt103Q aggregation was dependent upon Sti1, another recently described screen hit (Chapter 2). These data demonstrate that polyQ proteotoxicity can be modulated by multiple mechanisms and suggest that polyQ interactions can drive Htt103Q towards chaperone mediated protective aggregation.

3.3 Results

3.3.1 Genomic fragments from high copy screen suppress Htt103Q-NLS toxicity

In order to understand mechanisms for protective aggregation of polyQ, we screened a yeast high copy expression library for toxicity suppressors of a more toxic and more soluble Htt103Q [24]. The proteotoxic substrate utilized in the screen contains an N terminal FLAG tag, the first 17 amino acids encoded by HTT exon 1, a polyQ stretch of 103 amino acids, a C terminal GFP tag, and the SV40 nuclear localization signal (NLS), and it lacks the proline-rich region (Htt103Q-NLS). A galactose inducible form of Htt103Q-NLS was integrated into a W303α strain which causes a growth arrest that can be seen when cells are plated on solid media containing galactose. This strain was transformed with a yeast multicopy expression library [22], and visible colonies after 3

days growth on galactose were isolated. Following plasmid rescue and sequencing of all 23 plasmid dependent suppressors, it was evident that several hits contained overlapping regions of DNA suggesting that the screen reached saturation.

The screen revealed 12 fragments of DNA that alleviated Htt103Q-NLS toxicity which were designated number 1 to 12 (Table 3.1 and Figure 3.1A). Each of the hits recovered from the suppressor screen contained a portion of DNA approximately 5-10 Kb long, which included 1-7 ORFs (Table 3.1). Several of these hits (genomic fragments 5, 6, 10, and 12) decreased steady state protein levels of Htt103Q-NLS (Figure 3.1B). This was likely the reason for suppression of Htt103Q-NLS toxicity and so these fragments were excluded from further verification. Two of the hits (genomic fragments 11 and 12) contained ORFs encoding proteins involved in sugar metabolism so we also excluded these from further validation as this was likely an artifact of the promoter used to induce Htt103Q-NLS expression.

Notably, we observed that 7 of the 12 genomic fragments (GF) contained ORFs encoding a polyQ-rich region (Table 3.1). Additionally, several hits (GF 1-3, 6 and 7) increased intranuclear Htt103Q-NLS aggregation as monitored both by intensity of fluorescent foci and number of cells containing nuclear foci (Figure 3.1C). An example of control cells expressing diffuse Htt103Q-NLS, as well as an example of intranuclear foci are depicted for reference (Figure 3.1C). Since decreased SDS-resistant aggregation leads to enhanced Htt103Q toxicity of the nuclear localized construct [24], we reasoned that increased aggregation should correlate with lower toxicity as was seen in several of the screen hits. Thus, we focused our attention on further verifying individual genes from GF 1-4, and 6-8 as these altered aggregation and/or contained a polyQ ORF. Individual

genes from each of these full length screen hits were subcloned with the 5' and 3' untranslated regions into a high copy plasmid to replicate expression conditions during the screen. No single gene in GF 6-8 recapitulated toxicity suppression indicating that there was likely a combinatorial effect of several genes. We identified 4 genes, Sti1, Pop2, Cbk1, and Nab3, encoding proteins which can independently act to suppress Htt103Q-NLS toxicity when they are overexpressed. Sti1 is an Hsp70 co-chaperone that functions to suppress Htt103Q toxicity by promoting accumulation of amyloid-like material in perinuclear foci (Chapter 2). Herein, we investigated the mechanism by which elevation of the levels of Pop2, Cbk1, and Nab3 suppress toxicity of Htt103Q.

3.3.2 PolyQ-rich proteins suppress Htt103Q-NLS and Htt103Q toxicity

Pop2 and Cbk1 contain polyQ-rich regions N-terminal to the functional domain of the proteins while the Nab3 contains a polyQ-rich region located C-terminally to the functional region (Figure 3.2A). Each of these "polyQ-rich" regions contains several stretches of Q repeats of 6 or more residues (Figure 3.3A and 3.3B). While stretches in between these polyQ tracts contain some hydrophobic residues, there is little sequence similarity between the polyQ-rich regions of these 3 proteins besides the polyQ tracts themselves (Figure 3.3C). These polyQ-rich domains are predicted to have a relatively high propensity for being disordered [47] suggesting they are conformationally dynamic. Conformational switching is a characteristic of prion proteins which can be folded normally or adopt a self-propagating amyloid-like conformation. Pop2, Cbk1, and Nab3 were all hits in a bioinformatics screen for novel prion domain containing proteins [48]. The criteria for determining prion domains were based upon an algorithim that searched for sequences similar to the prion domains of the yeast prions Sup35, Ure2, and Rnq1.

Based upon the prion domain forming ranking system for the top 100 hits, Cbk1, Nab3, and Pop2 fell at positions 6, 41, and 51, respectively [48]. When expressed in yeast, the prion domains of Cbk1 and Pop2 formed SDS-resistant oligomers, while Nab3 did not [48]. Thus, Cbk1 and Pop2, but not Nab3, contain a polyQ-rich region which may have some intrinsic aggregation propensity and has similar properties to previously characterized yeast prion domains such as in the [RNQ+] prion.

Overexpression of Pop2, Cbk1, and Nab3 each partially suppressed toxicity of both Htt103Q-NLS and a similar construct lacking the NLS (Htt103Q) which aggregates in the cytosol (Figure 3.2B). Reduced toxicity was not due to altered levels of the Htt proteins (Figure 3.2B). As each of these proteins was expressed from its endogenous promoter, each protein was expressed above its own normal steady state levels to a different extent. Cbk1, having a lower relative abundance than the Pop2 and Nab3 [49], was elevated approximately 1.5 fold over endogenous protein levels. Nab3 and Pop2 were elevated approximately 2.4 and 3 fold over their endogenous forms respectively. As was seen with the full length GF for each of these suppressors, reduction in Htt103Q-NLS toxicity correlated with changes in aggregation during Pop2 and Cbk1, but not Nab3, over-expression (Figure 3.2C). Overexpression of Cbk1 and Pop2 caused cytosolic speckled Htt103Q-GFP to be condensed to one or two perinuclear foci which was even more dramatically noticeable than changes in Htt103Q-NLS aggregation.

Since Htt103Q toxicity and aggregation in yeast depends upon the templated status of the prion protein Rnq1 [6,40], we next examined whether or not these suppressors also alleviated the growth defect associated with Rnq1 overexpression. The polyQ-rich proteins specifically acted upon Htt103Q as they were unable to suppress

toxicity associated with Rnq1 overexpression (Figure 3.2D). When Rnq1 is in the [rnq-] non-prion conformation, Htt103Q is no longer toxic. Using Pop2 as a representative, we ruled out the possibility that the polyQ-rich proteins altered Rnq1 prion status because expression of the polyQ proteins did not alter the templated status of Rnq1 as evidenced by Rnq1-GFP aggregation during Pop2 overexpression (Figure 3.2E). Likewise, the polyQ-rich suppressors did not co-localize with Rnq1 aggregates (Figure 3.2E). Thus, Pop2, Cbk1, and Nab3 over-expression only modulates toxicity and aggregation of Htt103Q without any impact upon a yeast prion protein.

As Cbk1 and Pop2 alter Htt103Q aggregation and Nab3 does not, these proteins appear to fall into two different classes of polyQ-rich proteins whose elevation can suppress Htt103Q toxicity. Additionally, although the polyQ-rich proteins identified in our screen suppress polyQ expanded Htt toxicity, other polyQ-rich proteins actually enhance toxicity [50]. The toxicity enhancers described in that study also were hits ranked within the top100 in the above mentioned prion domain screen [48]. These data implicate polyQ-rich proteins as having a multifaceted role in proteotoxicity of a polyQ disease related protein. Therefore, we sought to distinguish the different mechanisms of toxicity suppression in order to better understand basic principles of how the cell buffers toxicity of polyQ expanded proteins and is impacted by neighboring molecules.

3.3.3 Functional Nab3 is required for suppression of Htt toxicity

Nab3 is an essential nuclear protein that functions in the Nrd1 complex as an RNA binding protein through its RNA recognition motif [51,52]. Htt103Q-NLS may titrate Nab3 away from its normal function, depleting the cell of an essential protein. In order to determine if this is the case, we carried out a structure/function analysis to

determine if overexpressed Nab3 required a functional domain in order to suppress Htt103Q-NLS toxicity. In these studies, we employed a strain where Nab3 expression halts when the cells are grown in the presence of doxycycline (Figure 3.4A). A mutation within the RNA recognition motif at S399, but not at the neighboring S397, inactivates Nab3 function rendering the yeast inviable if this is the sole copy of Nab3 in the cell (Figure 3.5A) [52]. The Nab3(S397A) is expressed at a lower level than Nab3(399A) yet still allows for normal growth. This observation suggests that Nab3(S399A) has not lost ability to complement Nab3 depletion due to low expression levels. Expression of a version of Nab3 lacking the C-terminal polyQ-rich region also failed to complement the deletion strain (Figure 3.5A).

Utilizing these Nab3 constructs, we examined which form of Nab3 was able to impact Htt103Q-NLS toxicity. The only forms of Nab3 that were able to suppress Htt103Q-NLS toxicity when over-expressed were functional forms that were able to complement Nab3 depletion (Figure 3.5B). Neither the Q-rich deletion nor the E399A forms of Nab3 alleviated the Htt103Q-NLS growth defect (Figure 3.5B). Since a non-functional, polyQ-rich containing Nab3 was unable to suppress toxicity, it appears that the polyQ-rich region of Nab3 is not sufficient to suppress toxicity. In monitoring subcellular localization, we found that a monomeric RFP (mRFP) tagged form of Nab3 and Htt103Q-NLS are both localized in the nucleus (Figure 3.5C). At this level of expression, the Htt103Q-NLS protein forms small punctae in approximately 30-40%% of cells expressing the construct while the remaining population exhibits a diffuse nuclear signal as described previously [24]. When Htt103Q-NLS was co-expressed with Nab3-mRFP, the nuclear Nab3-mRFP became enriched in the location where the Htt103Q-NLS

punctae formed, but the same approximate number of cells exhibited the Htt punctae (Figure 3.5C). These data suggest that, although its aggregation status does not change, Htt103Q-NLS interacts with Nab3. In support of this hypothesis, Nab3 was identified in a mass spectrometry screen which utilized SILAC labeling to quantitatively determine interaction partners of a Htt construct with a 96 residue polyQ tract [53]. If Htt103Q-NLS titrates Nab3 away from its normal and essential function, then suppression of toxicity by overexpression would occur by replacing the lost functional protein. This is a partial suppression of toxicity because Nab3 is one of numerous other proteins such as transcription factors likely to also be titrated away from their normal functions [28,54].

3.3.4 The polyQ-rich region of Cbk1 forms perinuclear foci where Htt103Q accumulates during toxicity suppression

Cbk1 and Pop2 suppress polyQ expanded Htt toxicity and impact Htt103Q aggregation. To explore this mechanism, we utilized Htt103Q because these are cytosolic proteins and are able to alter aggregation of cytosolic Htt103Q more distinctly than Htt103Q-NLS. Cbk1 is a kinase of the Ndr/Lats family and functions in the regulation of Ace2 and morphogenesis network [55]. However, this function of Cbk1 is not necessary for the protein to act as a Htt103Q toxicity suppressor because over-expression of either a kinase dead form (Cbk1(D475A)-mRFP) [55] or the N-terminal portion of Cbk1 containing the polyQ-rich region and lacking the functional domain (Cbk1(1-326)-mRFP) could still alleviate Htt103Q toxicity (Figure 3.6A). Conversely, expression of Cbk1 lacking the polyQ-rich region (Cbk1(327-756)-mRFP) was unable to alleviate Htt103Q toxicity even though the expression level of Cbk1(327-756)-mRFP was approximately equivalent to that of full length Cbk1 (Figure 3.6A).

As the N-terminus of Cbk1 was necessary and sufficient for toxicity suppression, we next asked if over-expression of this polyQ-rich region could also alter Htt103Q aggregation. These experiments were carried out in conjunction with the full length Cbk1 protein to ensure that the Cbk1 polyQ-rich domain exhibited similar behaviors. Interestingly, over-expression of both full length Cbk1 and Cbk1(1-326) localized to a perinuclear foci when expressed individually (Figure 3.6B). This was reminiscent of Rnq1 foci that form when over-expressed, however, elevation of Rnq1 causes a growth defect [13] where Cbk1 over-expression does not (Figure 3.1A). When Cbk1 or the polyQ-rich domain was expressed along with Htt103Q, the Htt103Q shifted from amorphous looking aggregates speckled throughout the cytosol, to co-localize at the perinuclear foci with Cbk1 (Figure 3.6B). These data suggest that the polyQ rich region of Cbk1 interacts with Htt103Q, which mediates cytoprotective accumulation of Htt103Q in a distinct foci.

3.3.5 A short proline-rich stretch in the Pop2 polyQ domain is required for impact upon Htt103Q toxicity and aggregation

Like Cbk1, elevation of Pop2, a subunit of the Ccr4/Not complex, alters Htt103Q aggregation and is not essential. A similar structure/function analysis (Figure 3.7A) revealed that the N-terminal polyQ-rich region of Pop2 (Pop2(1-159)) also is necessary to suppress Htt103Q toxicity (Figure 3.7B). The 12 amino acids at the C-terminus of the Pop2 polyQ domain are enriched in proline residues (Figure 3.7A). Since addition of a poly-proline region to the Htt103Q construct renders it benign [56,57], we asked whether the proline rich region at the end of Pop2(1-159) acts in similar manner. Excitingly, this indeed appears to be the case, as expression of Pop2(1-147) was unable to suppress

Htt103Q toxicity. Proline-rich residues 148-159 of Pop2 were not sufficient to alleviate toxicity without the polyQ-rich region, however, as expression of Pop2(148-443) was unable to suppress Htt103Q toxicity. In order to determine if there was a correlation between toxicity suppression and a change in Htt103Q aggregation, we monitored the aggregation pattern of Htt103Q during co-expression with Pop2. Expression of full length Pop2 or Pop2(1-159) caused Htt103Q to shift from the amorphous looking speckled punctae throughout the cytosol to distinct perinuclear foci (Figure 3.7C). Pop2(1-147) which lacked the short proline rich region, however, was unable to alter Htt103Q aggregation (Figure 3.7C). Unlike over-expressed Cbk1 which formed perinuclear foci, each of the Pop2 constructs was expressed in a diffuse pattern throughout the cell (Figure 3.7C). Upon expression of Htt103Q, however, Pop2 and Pop2(1-159) did co-localize with Htt103Q in the perinuclear foci (Figure 3.7C).

One of the features of Htt103Q aggregation, and a characteristic of amyloid-like proteins, is that it forms SDS-resistant protein oligomers. Over-expression of Cbk1 and Pop2(1-159), but not Pop2(1-147) promoted accumulation of Htt103Q into distinct perinuclear foci, so we asked if SDS-resistant oligomer formation followed the same pattern. Under expression conditions where over-expressed polyQ-rich protein suppressed Htt103Q toxicity, there was an increase in SDS-resistant Htt103Q as measured by SDD-AGE (Figure 3.7D). While Cbk1 and Pop2(1-159) impacted aggregation in this manner, expression of Pop2(1-147) again had no effect on Htt103Q. Using gel filtration chromatography, we verified that Pop2(1-159) indeed increased the pool of high molecular weight SDS-resistant Htt103Q that remained in the stacking portion of the SDS-PAGE gel (Figure 3.4B). Additionally, Htt103Q and Pop2(1-159) co-

precipitated from the high molecular weight fractions, but not the monomeric fractions providing evidence of an interaction or complex containing these proteins (Figure 3.4C).

This correlation between packaging into foci, elevated SDS-resistant aggregates, and suppression of polyQ toxicity is consistent with a mechanism involving protective aggregation. In contrast to Nab3, the polyQ-rich domains of Cbk1 and Pop2, rather than the functional domains, alter Htt103Q toxicity and this characteristic correlates with a shift in Htt103Q aggregation pattern. These data suggest that interaction of Htt103Q with certain polyQ domains is sufficient to promote protective aggregation. These results were obtained during overexpression of polyQ-rich domains, but Cbk1 and Pop2 are not extremely abundant proteins. Thus, whether or not these endogenous proteins have a role in polyQ toxicity remains unclear. These data, however, serve as an example of how polyQ-rich protein domains can buffer toxicity of polyQ expanded Htt.

3.3.6 Pop2 and Cbk1 alter Htt103Q toxicity and localization in a Sti1-dependent manner

Not only does overexpression of Pop2 and Cbk1 increase aggregation of Htt103Q, but the spatial distribution of Htt103Q is also altered. Interestingly, another hit identified in the screen, Sti1, acts with Hsp70 to promote accumulation of SDS-resistant material, including Htt103Q, in a perinuclear quality control center. Elevation of Sti1 re-directs templated Htt103Q to Sti1 induced foci where potentially toxic amyloid-like material is sequestered in a cytoprotective manner. As over-expression of Pop2 and Cbk1 appear to act in a similar way and were discovered in the same screen, these polyQ-rich proteins may fall within the same Sti1-dependent protective aggregation pathway. Thus, we tested whether or not Pop2 and Cbk1 could still function as toxicity suppressors in the

absence of Sti1. While each of these proteins suppressed Htt103Q toxicity to a similar extent in a wildtype strain, Pop2 and Cbk1 lost this ability in a ΔSti1 strain demonstrating that suppression of toxicity is Sti1 dependent (Figure 3.8A).

Endogenous Sti1 functions as an important component to buffer amyloid-like proteotoxicity because deletion of Sti1 decreases Htt103Q aggregation while enhancing toxicity, essentially interrupting the protective aggregation pathway. This change in aggregation can be visualized utilizing fluorescence microscopy (Figure 3.8B). As suppression of Htt103Q toxicity by Pop2 and Cbk1 overexpression requires Sti1, we next examined Htt103Q aggregation during Pop2 and Cbk1 overexpression in a ΔSti1 strain. Once again, Pop2 and Cbk1 activities were dependent upon the presence of Sti1 as Htt103Q was no longer redistributed into distinct foci in the ΔSti1 strain (Figure 3.8B). These data demonstrate a correlation between toxicity and aggregation, and place Pop2 and Cbk1 upstream of Sti1 in a chaperone facilitated protective aggregation pathway (Figure 3.8C).

3.4 Discussion

Here, we identified cellular coping mechanisms for the proteotoxic insult caused by expression of a polyQ expanded Htt fragment in yeast. Over-expression of Nab3, Pop2, and Cbk1 each individually suppress toxicity of both cytosolic and nuclear localized forms of Htt103Q. Each of these proteins contains a polyQ-rich domain that appears to be responsible for interactions with Htt103Q, yet the outcome of such interactions differs for the respective suppressors. Htt103Q appears to inactivate Nab3, because only fully functional Nab3 suppresses Htt toxicity. In contrast, the ectopic expression of just the polyQ-rich regions of Pop2 and Cbk1, in the absence of their

functional domains, is sufficient to suppress Htt103Q toxicity which correlates with a spatial redistribution of Htt103Q to perinuclear foci. Although Pop2 and Cbk1 appear to alter Htt103Q aggregation by different mechanisms, polyQ-domain dependent suppression of Htt toxicity was dependent upon the Hsp70 co-chaperone Sti1. Sti1 functions in spatial quality control to organize amyloid-like protein assemblies into benign perinuclear protein quality control compartments. Thus, cytotoxicity of polyQ proteins is associated with inactivation of essential proteins that contain a polyQ-rich region, but can also be buffered via interactions with polyQ-rich proteins. This leads to the partitioning of Htt103Q to an Hsp70 chaperone dependent pathway that mediates protective protein aggregation.

Nab3 is an essential nuclear protein that, when a fully functional form is overexpressed, can suppress Htt toxicity without altering Htt aggregation. Htt103Q and Nab3 co-localize in the nucleus, so Htt103Q appears to inactivate Nab3, thereby causing proteotoxicity. Inactivation of essential proteins by Htt103Q occurs with a number of transcription factors [25,26,58], and the identification of Nab3 as a target suggests the Nrd1 complex is an RNA processing machine that is negatively impacted. Other RNA binding proteins have also been identified in aggregates that contain toxic forms of Htt, so polyQ expanded Htt appears to cause proteotoxicity by inactivation of multiple targets [38,59]. We observed Nab3 and Htt103Q-NLS co-localize in nuclear punctae, thus, it appears that sequestration of Nab3 into Htt103Q-NLS aggregates can titrate Nab3 away from its essential function in the Nrd1 complex. Consistent with these data, Nab3 was also identified as a polyQ expanded Htt interacting protein in a recent mass spectrometry screen [53]. Interactions between Nab3 and Htt103Q-NLS may occur through the Q-

domain because this region is required for Nab3 to be functional. The essential importance of the Nab3 polyQ domain is illustrated by our observation that a Nab3 construct lacking this domain is unable to suppress the lethal phenotype resultant from depletion of Nab3 and also is unable to suppress Htt103Q-NLS toxicity. Since only overexpression of a functional form of Nab3 can suppress Htt103Q-NLS toxicity and there is no change in Htt103Q-NLS aggregation, restoration of functional Nab3 available to act in the Nrd1 complex is likely to be the mechanism for proteotoxicity suppression.

Approximately 1-3% of eukaryotic proteomes contain proteins with a polyQ stretch of at least 5 residues [60,61]. Some of these polyQ stretch proteins are capable of interacting with the expanded polyQ domains of disease proteins [6,27,42,43,53,62,63], and in most cases such interactions seem to have negative outcomes on protein function and cell viability [6,7,43,62,63]. In one instance, interaction between Htt103Q and cellular proteins appears to seed formation of toxic Htt103Q [13,24,40,50,64]. Over-expression of Pop2 and Cbk1 promotes the assembly of Htt103Q into benign SDS-resistant assemblies, thus, these proteins fall into a unique category of polyQ containing proteins which have a positive impact on disease related polyQ. Why there are both positive and negative outcomes of Htt interaction with polyQ protein neighbors remains unclear, yet there are several scenarios that could explain these differences. Flanking sequences of the polyQ proteins have a profound effect upon polyQ toxicity and aggregation [56,57,65]. Over-expression of the polyQ domain of Pop2 can direct Htt103Q to a perinuclear foci, but only if a short proline-rich stretch following the Pop2 polyQ region is present. Interestingly, the polyQ stretch in Htt exon 1 is followed by a poly-proline stretch, and addition of the this stretch to Htt103Q (in cis) or to Htt25Q (in

trans) serves to detoxify Htt103Q in yeast [56,57,66]. Reduced toxicity correlates with accumulation of Htt103Q at a perinuclear location which corresponds with spindle pole body markers [50,56]. Thus, elevated levels of Pop2 may serve a similar function by targeting the Htt103Q to a benign quality control center as a result of the proline-rich stretch.

In addition to flanking regions, subtle differences within the polyQ domains themselves may also impact how they affect Htt103Q toxicity. In this case, the nature of the polyQ domain may alter the strength of the interaction or the conformation of Htt103Q, which in turn would dictate the amount of templated material and available surfaces that can form aberrant interactions. For example, proline stretches not only target Htt103Q to a benign subcellular location, but also can affect Htt conformation [65,67,68]. Thus, the proline rich region of Pop2(1-159) might be stabilized in an alternate conformation as compared to Pop2(1-147) which lacks the proline rich stretch. The conformational shift may change the ability of the protein to interact with Htt103Q as Pop2(1-159) is found in perinuclear foci with Htt while Pop2(1-147) is not.

In the context of the polyQ-rich proteins presented here, what might these subtle differences in polyQ domains look like? Nab3, Cbk1, and Pop2 each contain polyQ-rich regions, but little else is similar between these proteins as seen in their alignment. Nab3 contains multiple prolines and other nonpolar residues interspersed throughout the many short polyQ stretches, while these residues mainly follow 2 polyQ tracts in Pop2. Cbk1 has two longer polyQ stretches separated by a region rich in polar residues such as glutamines, asparagines, and serines, and these are interspersed with hydrophobic residues. While overexpressed Pop2 only accumulates in perinuclear foci with Htt103Q,

overexpressed Cbk1 appears in foci there even in the absence of Htt103Q. Both Pop2 and Cbk1 were identified as aggregation prone candidate prion domain containing proteins in a bioinformatics screen, but Cbk1's composition resembled known yeast prions such as Rnq1 more than Pop2 [48]. Htt103Q only becomes toxic to yeast when Rnq1 is in its prion conformation, [RNQ+]/[PIN+], as this templates Htt103Q, allowing entry into the amyloid-like aggregation pathway [6,64]. Importantly, Rnq1 over-expression is toxic in a [RNQ+] prion background [13] while Cbk1 is not. Although Cbk1 appears to have qualities of a prion protein such as Rnq1, its sequence is distinct because Cbk1 contains several polyQ tracts, not just an enrichment in glutamines and asparagines. Thus, elevated levels of Cbk1 promote formation of protective perinuclear foci where it appears to act as a sink to sequester otherwise toxic Htt103Q. This interaction and sequestration may be based on its affinity for both itself and polyQ expanded Htt, and possibly interfering with Rnq1:Htt103Q interaction.

Cbk1 and Pop2, when over-expressed, both alter Htt103Q aggregation and toxicity albeit by different mechanisms which may be sequence, conformation, or targeting based. The outcome in both cases, however, is protective aggregation of Htt103Q and is dependent upon the Hsp70 co-chaperone Sti1. Pop2 and Cbk1 suppress toxicity by acting through a chaperone dependent spatial quality control pathway to drive accumulation of proteotoxic Htt103Q in a benign location. In related studies, we demonstrated that elevated Sti1 induces formation of perinuclear foci containing amyloid-like material such as Htt103Q (chapter 2). Elevated levels of Sti1 suppress Htt103Q toxicity while deletion of the co-chaperone exacerbates toxicity and inhibits SDS-resistant oligomer formation. These activities are facilitated by the Hsp70/Hsp40

machinery which also acts much earlier in the amyloid-like aggregation pathway to prevent entry and stimulate refolding of client proteins (Figure 3.8C). Interestingly, Pop2, Cbk1, and Sti1 were all discovered in the same screen, and Pop2 and Cbk1 over-expression are unable to promote protective aggregation in the absence of Sti1. These observations place the polyQ neighbors of Htt103Q upstream of Sti1 in a chaperone dependent facilitated aggregation pathway (Figure 3.8C). Interaction of Htt103Q with a subset of polyQ proteins may impact partitioning of a potentially toxic species towards a chaperone dependent pathway to buffer toxicity (Figure 3.8C). Increased levels of components in this spatial quality control pathway promote packaging of Htt103Q into perinuclear foci.

Altogether, there is a complex relationship between polyQ containing proteins where Htt103Q can interfere with normal function of certain polyQ proteins, and other polyQ proteins can interfere with toxicity of Htt103Q. A chaperone dependent pathway for protective aggregation regulates spatial quality control of proteotoxic polyQ proteins. Variations in the relative abundance of components within this polyQ interaction network as well as chaperones in a facilitated aggregation pathway may occur from cell type to cell type, as well as within a certain cell population over time. Further studies will better define this complex interaction network and how it impacts mechanisms for protective packaging and aggregation of polyQ disease proteins.

3.5 Methods

Strains and plasmids

Yeast strains and plasmids used in this study are listed in Supplemental tables 2 and 3. All strains harbored Rnq1 in its [RNQ^{+}] prion form unless otherwise indicated. The

generation of isogenic [*rnq*-] strains was accomplished via sequential passage of cells on plates containing 3mM guanidinium-HCl. Plasmid transformation into yeast was performed using a lithium acetate method as described previously [13]. Yeast cell culture was carried out in synthetic media containing the appropriate amino acids for selection of auxotrophic markers. The Htt25Q and Htt103Q (both with and without the NLS) integration strains were generated as described previously (MBoC Sti1 paper). The Htt construct used in these studies consisted of the first 17 amino acids of Htt exon 1 followed by 25 or 103 glutamine residues, and lacking the proline-rich region. It also contained an N-terminal FLAG tag and a C-terminal GFP tag. During microscopy and Western blot experiments, expression of Htt was induced from the galactose promoter with 2% galactose for 4 h. Cbk1-mRFP constructs and Nab3-mRFP were all expressed from a CUP1 promoter induced with 100uM $CuSO_4$ for 5 h. Each of the remaining suppressor constructs were expressed constitutively from their endogenous promoters. Rnq1-GFP was also expressed from a CUP1 promoter but no additional copper was added to the media in order to see low level overexpression.

High copy screen for toxicity suppressors

The Htt103Q-NLS integration strain was transformed with a 2μ yeast expression library [69]. Plasmids in this library carried a 5-10 Kb fragment of genomic DNA. Transformations were plated on synthetic media containing 2% galactose to induce expression of the toxic Htt103Q-NLS construct. Colonies which were able to grow under these conditions were isolated and screened using 5-FOA. This step was to ensure that isolates were not able to grow under toxic conditions due to a mutation. A plasmid rescue was carried out on each colony which exhibited plasmid dependent growth. These

plasmids underwent a sequencing reaction to determine the fragment of DNA which was able to suppress Htt103Q-NLS toxicity. Numerous gene regions (which were not just the same DNA fragment, but had overlapping DNA regions) were found multiple times suggesting the screen reached saturation. ORFS in each suppressor were subcloned into a pRS426 plasmid along with approximately 400 bp 5' and 3' UTR regions so that the protein would be expressed from its endogenous promoter to similar levels as those during the original screen.

Toxicity assays

Yeast samples were normalized to the same OD_{600}, then 5 fold serial diluted with sterile distilled water in a 96-well plate. Dilutions were plated in 10uL spots on appropriate synthetic dropout media. Most images of yeast grown on glucose were scanned at 48h and galactose at 72h. Htt103Q toxicity was assessed on plates containing 2% galactose, and in the case of Cbk1-mRFP constructs, supplemented with 500uM $CuSO_4$. Control growth plates contained 2% glucose.

Fluorescence microscopy

Fluorescence microscopy was carried out as described previously [24]. Briefly, cultures were fixed with 4% formaldehyde and 0.1M KPO_4 pH 7.4, and stored in 0.1M KPO_4 pH 7.4 with 1.2M sorbitol. Cells were then permeabilized with 0.1% Triton and stained with 0.5ug/mL DAPI. An Olympus IX81 motorized inverted fluorescence microscope paired with Metamorph software was used to collect images. Micrographs were merged and processed using ImageJ (NIH) and Photoshop (Adobe).

Nab3 depletion

The Nab3-TetR strain shuts down expression of Nab3 upon addition of doxycycline to the growth medium. This strain was transformed with the indicated plasmids, and colonies were expanded in liquid culture. At mid-log phase growth, 10 ug/mL doxycycline was added to the media. Samples were taken at the indicated timepoints starting at time of drug addition (T=0) out to 20 h post doxycycline. Samples were lysed and run on SDS-PAGE followed by Western blotting for endogenous Nab3.

Western blotting

Lysates were prepared from pellets of yeast by either mechanical disruption via mechanical disruption (for SDD-AGE, co-IP, and gel filtration) as described previously [13,24] or an alkali lysis method as described previously [70]. When using mechanical disruption, the lysis buffer used was 0.1% Triton X-100, 75mM Tris pH7.4, 150mM NaCl, 1mM EDTA, 1mM PMSF, and Sigma protease inhibitor cocktail. Standard separation techniques were used to analyze lysates via SDS-PAGE. Protein was transferred to nitrocellulose for 75-90 min at 110V, and probed using the indicated antibodies. Antibodies used in this study are listed in Supplemental Table 4.

SDD-AGE

Semi-denaturing detergent agarose gel electrophoresis (SDD-AGE) was carried out as described previously [13]. Briefly, Htt103Q was induced for 4 h in cells expressing either empty vector, or the indicated toxicity suppressor under control of their respective endogenous promoters. Samples were collected, lysed, and normalized (DC protein assay kit; Bio-Rad) and equivalent amounts of total protein were loaded on a standard SDS-PAGE gell or into a 1.4% agarose gel containing 0.1% SDS. The agarose gel was

run at 90-100V for approximately 2h, then transferred to PVDF at 12V for 15h and Western blotting was carried out.

Gel filtration chromatography and co-immunoprecipitation

Cell lysates were prepared via mechanical disruption using the lysis buffer listed above. A 500uL loop was loaded with lysates at a concentration of 7 mg/mL total protein which was then injected through a sephacryl S-200 gel filtration column (GE Healthcare) at a rate of 0.25 mL/min. Fractions of 1 mL were collected and run on a 10% SDS-PAGE gel, followed by standard Western blotting. For co-IP from column fractions, a 400uL aliquot or the indicated fractions were incubated with anti-GFP (to IP the Htt103Q) followed by incubation with a 50/50 Protein G bead slurry. After the beads were washed with lysis buffer, they were resuspended in sample buffer and boiled for 10 min prior to loading on a 10% SDS-PAGE gel, followed by Western blotting. Pop2(1-159)-mRFP was detected using polyclonal anti-RFP antibody and Htt103Q was detected using polyclonal anti-YFP (C. Beckers).

3.7 Tables and Figures

Table 3.1 Genomic fragements that suppress Htt103Q-NLS toxicity

Gen. fragment #	gene	biological process	polyQ rich	Null
1	STI1	protein folding, Hsp90	No	viable
	CIN5	RNA pol II transcription factor activity	No	viable
2	POP2	deadenylation, CCR4/NOT complex	Yes	viable
	BRE5	Ubiquitin protease cofactor, deubiquitination	No	viable
3	CBK1	Ser/Thr protein kinase	Yes	viable
	YGP1	Response to nutrient/stress	No	viable
	ASI2	ubiquitin-dependent protein catabolic process	No	viable
	PGA1	mannosyltransferase activity	No	inviable
4	GUP2	glycerol transport	No	viable
	COA2	Cytochrome oxidase assembly factor	No	viable
	NAB3	pol II regulation	Yes	inviable
5	ZDS2	transcriptional silencing	No	viable
	YML108W	unknown	No	viable
	PML39	mRNA export from nucleus	No	viable
	URA5	pyrimidine biosynthesis	No	viable
	SEC65	protein targeting to ER	No	inviable
	MDM1	mito. Inheritance, nuc migration	No	viable
	NUP188	import and export from nucleus	Yes	viable
6	SCD5	actin cytoskelton organization	Yes	inviable
	PDR10	ABC transporter	No	viable
7	SUL2	sulfate transport	No	viable
	NYV1	vesicle fusion	No	viable
	GIS3	unknown	No	viable
	IOC2	chromatin remodeling	Yes	viable
8	BUD22	bud site selection	No	viable
	ERG5	ergosterol biosynthetic process	No	viable
	SOK2	pseudohyphal growth, transcription factor	Yes	viable
	SPO20	ascospore-type prospore formation	No	viable
9	YHR122w	unknown, required for chromatid cohesion	No	inviable
	EPT1	phosphatidylethanolamine synthesis	No	viable
	NDT80	Transcription factor	No	viable
	YHR126c	unknown	No	viable
	YHR127w	mitotic spindle elongation	No	viable
	FUR1	pyrimidine salvage	No	viable
	ARP1	nuclear migration	No	viable
10	SEC3	transport, vesicle fusion	No	inviable
	NTF2	protein import into nucleus	No	inviable
	YER010C	unknown	No	viable
	TIR1	response to stress	No	viable
11	SOK1	cAMP mediated signaling	No	viable
	TRP1	tryptophan biosynthesis	No	viable
	GAL3	galactose metabolism	No	viable
	SNQ2	ABC transporter, response to drug	No	viable
12	MIG1	transcription factor, glucose repression	No	viable

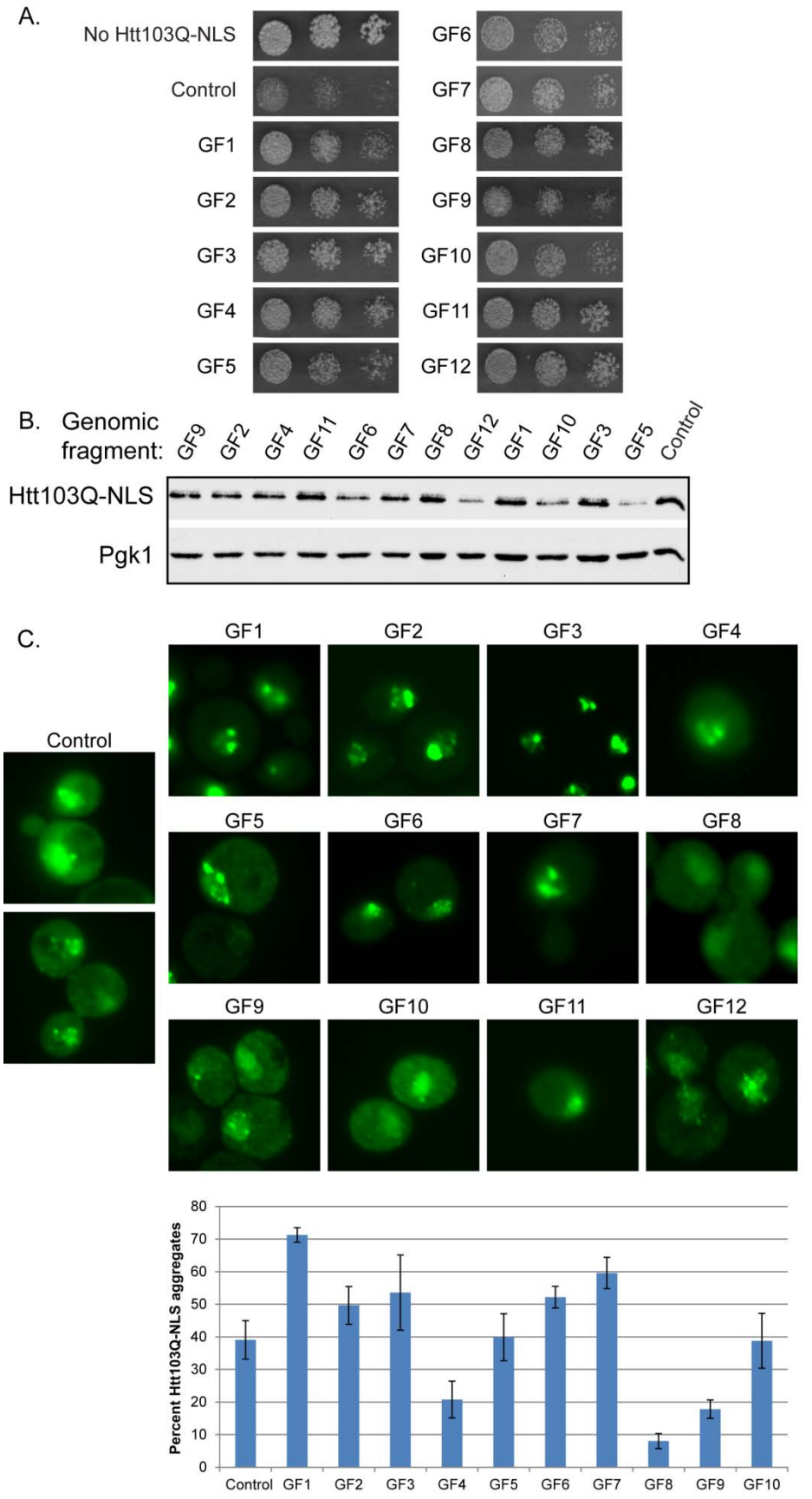
A.
No Htt103Q-NLS
Control
GF1
GF2
GF3
GF4
GF5
GF6
GF7
GF8
GF9
GF10
GF11
GF12
B.
Genomic fragment:
GF9
GF2
GF4
GF11
GF6
GF7
GF8
GF12
GF1
GF10
GF3
GF5
Control
Htt103Q-NLS
Pgk1
C.
Control
GF1
GF2
GF3
GF4
GF5
GF6
GF7
GF8
GF9
GF10
GF11
GF12
Percent Htt103Q-NLS aggregates
0
10
20
30
40
50
60
70
80
Control
GF1
GF2
GF3
GF4
GF5
GF6
GF7
GF8
GF9
GF10

Figure 3.1. Genomic fragments from high copy screen suppress Htt103Q-NLS toxicity

(A) Genomic fragments (GF) 1 through 12 suppress Htt103Q-NLS toxicity as monitored by growth assay plated in 5-fold dilutions on galactose containing media.(B) Impact of GF1-12 upon Htt103Q-NLS expression levels as monitored by Western blot. (C) Impact of GF1-12 upon aggregation of Htt103Q-NLS as monitored by fluorescence microscopy. Bar graph indicates percent of cells with Htt103Q-NLS found in intranuclear foci. Each bar indicates the average ± standard deviation of at least 100 cells counted in at least 3 different experiments. Cultures for Western blotting and microscopy were obtained by inducing Htt103Q-NLS with 2% galactose for 4-5 h.

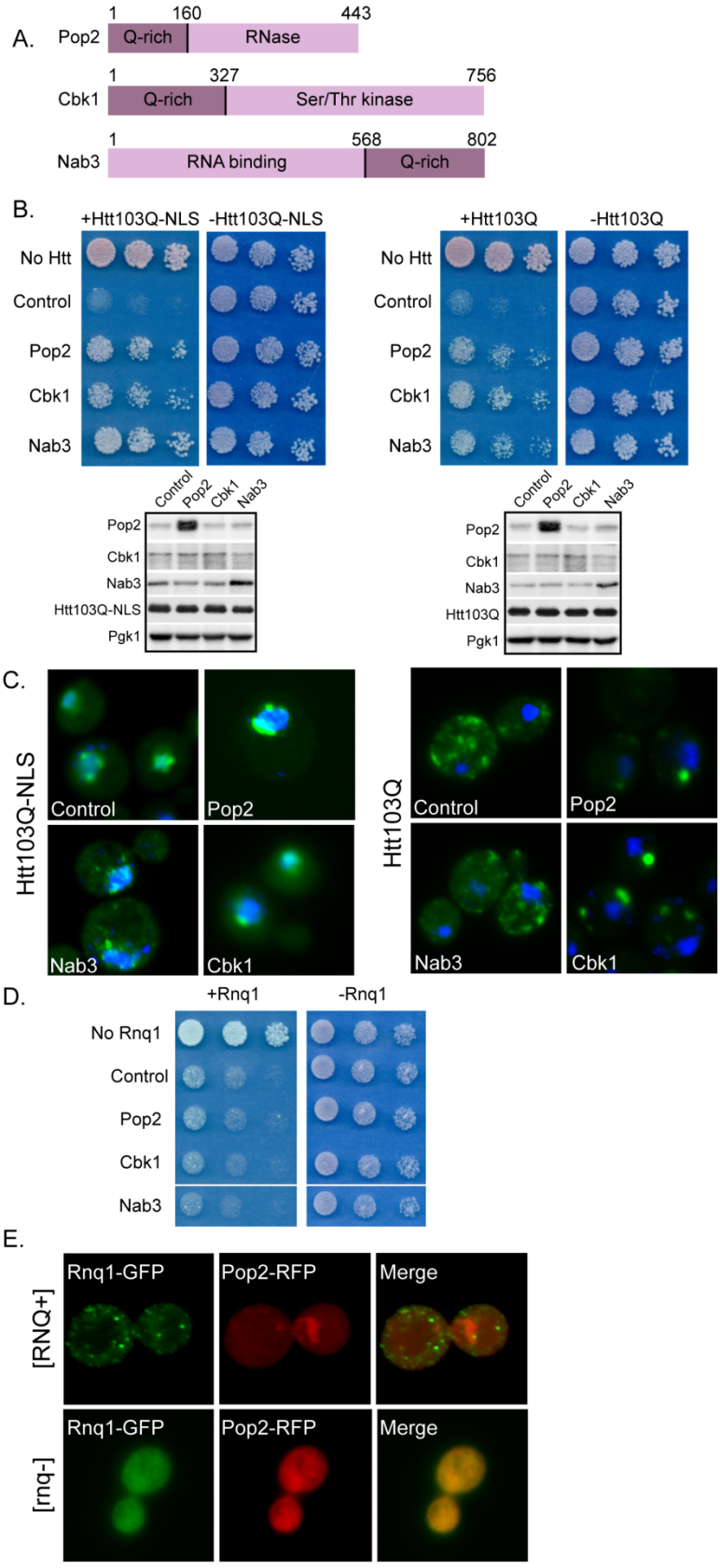
A.
Pop2
1
160
443
Q-rich
RNase
Cbk1
1
327
756
Q-rich
Ser/Thr kinase
Nab3
1
568
802
RNA binding
Q-rich
B.
+Htt103Q-NLS
-Htt103Q-NLS
+Htt103Q
-Htt103Q
No Htt
Control
Pop2
Cbk1
Nab3
Control
Pop2
Cbk1
Nab3
Pop2
Cbk1
Nab3
Htt103Q-NLS
Pgk1
Htt103Q
C.
Htt103Q-NLS
Htt103Q
Control
Pop2
Nab3
Cbk1
D.
+Rnq1
-Rnq1
No Rnq1
Control
Pop2
Cbk1
Nab3
E.
[RNQ+]
[rnq-]
Rnq1-GFP
Pop2-RFP
Merge

Figure 2. PolyQ-rich proteins suppress Htt103Q-NLS and Htt103Q toxicity
(A) Diagram of polyQ-rich screen hits. Numbers represent amino acids. N- or C-terminal poly Q-rich regions and functional domains are indicated. Further information is shown in supplemental Figure 1. (B) Pop2, Cbk1, and Nab3 suppress growth defect associated with Htt103Q-NLS and Htt103Q. Growth assays were plated in 5-fold dilutions on glucose (-Htt) or galactose (+Htt). Western blot indicates Htt expression levels at 4 h galactose induction with indicated proteins co-expressed. (C) Pop2 and Cbk1 but not Nab3 alter Htt103Q-NLS and Htt103Q aggregation as monitored by fluorescence microscopy. Nuclei were visualized with DAPI staining. (D) Toxicity associated with Rnq1 over-expression is unaffected by screen hits. Growth assays were plated in 5-fold dilutions on glucose (-Rnq1) or galactose (+Rnq1). Endogenous Rnq1 is present in a [RNQ+] prion state in this experiment. (E) Pop2 does not alter Rnq1 localization or prion status. [RNQ+] prion status was monitored via aggregation of Rnq1-GFP expressed from Cup1 promoter at basal levels of copper in media. Pop2, Cbk1, and Nab3 were expressed from high copy plasmids under control of their endogenous promoters in each experiment.

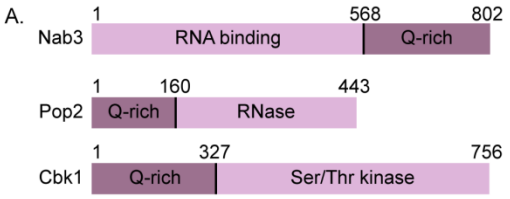

B. Nab3(aa568-802)

QQNIYGAPPLPVPNGPAVGPPPQTNYYQGYSMPPPQQQQQQPYGNYGMPPP
SHDQGYGSQPPIPMNQSYGRYQTSIPPPPPQQQIPQGYGRYQAGPPPQPPS
QTPMDQQQLLSAIQNLPPNVVSNLLSMAQQQQQQPHAQQQLVGLIQSMQGQ
APQQQQQQLGGYSSMNSSSPPPMSTNYNGQNISAKPSAPPMSHQPPPPQQQ
QQQQQQQQQQQQQPAGNNVQSLLDSLAKLQK

Pop2(aa1-159)

MQSMNVQPRVLAVGGEQFFSQRQASEQHQQQNMGPQVYSPKVNRARMFPQG
MPVNTINGSVNQEMNNAYLLKQKNEPLLTQQQQQQQQQQQPFNIGTPVSVA
SLPPGLNVLQQQQQQQQQQQQQQQGVGLNRPLASQLPKHLTNQSMPPIFLP
PPNYLF

Cbk1(aa1-326)

MYNSSTNHHEGAPTSGHGYYMSQQQDQQHQQQQQYANEMNPYQQIPRPPAA
GFSSNYMKEQGSHQSLQEHLQRETGNLGSGFTDVPALNYPATPPPHNNYAA
SNQMINTPPPSMGGLYRHNNNSQSMVQNGNGSGNAQLPQLSPGQYSIESEY
NQNLNGSSSSSPFHQPQTLRSNGSYSSGLRSVKSFQRLQQEQENVQVQQQL
SQAQQQNSRQQQQQLQYQQQQQQQQQQQHMQIQQQQQQQQQQQQSQSPVQS
GFNNGTISNYMYFERRPDLLTKGTQDKAAAVKLKIENFYQSSVKYAIERNE
RRVELETELTSHNWSEERKS

C.

```
Nab3(568-802)-------------------------------------QQNIYGAPP--------------
Pop2(1-159)  -------------------------------------MQSMNVQPRVL-----------
Cbk1(1-326)  MYNSSTNHHEGAPTSGHGYYMSQQQDQQHQQQQQYANEMNPYQQIPRPPAAGFSSNYMKE
                                                    :     *

Nab3(568-802)------------------------LPVPNGPAVGPPPQTNYYQGYSMPPPQQQQQQPYGN
Pop2(1-159)  ------------------------------------------------------------
Cbk1(1-326)  QGSHQSLQEHLQRETGNLGSGFTDVPALNYPA-TPPPHNNYAASNQM-------------

Nab3(568-802)YGMPPPSHDQGYGSQPP--IPMNQSYGRYQTSIPPPP-PQQQIPQGYGRYQAGPPPQPPS
Pop2(1-159)  ------AVGGEQFF--------SQRQASEQHQQQNMGPQVYSPKVNRAR-----------
Cbk1(1-326)  INTPPPSMGGLYRHNNNSQSMVQNGNGSGNAQLPQLSPGQYSIESEYNQNLNGSSSSS--
                   :               .:  .  : .         .      :

Nab3(568-802)QTPMDQQQLLSAIQNLPPNVVSNLLSM-----AQQQQQQPHAQQQLVGLIQSMQGQAPQQ
Pop2(1-159)  --MF--PQGMPV-NTINGSVNQEMNNA---YLLKQKNEPLLTQQQ---------QQQQQ
Cbk1(1-326)  --PFHQPQTLR----SNGSYSSGLRSVKSFQRLQQEQENVQVQQQLSQ----AQQQNSRQ
                :   * :        .  . : .       :*:::   .***          *  :*

Nab3(568-802)QQQQLGGYSSMNSSSPPPMSTNYNGQNISAKPSAPPMSHQPPPPQQQQQQQQQQQQQQQQQ
Pop2(1-159)  QQQPFN---------------IGTP-VS-------VASLPPGLNVLQQQQQQQQQQQQQ
Cbk1(1-326)  QQQQLQ---------------YQQQ-QQ-------QQQQQQHMQIQQ-QQQQQQQQQ--
             *** :                      .              :  * *********

Nab3(568-802)PAGNNVQSLLDS-LAKLQK-------------------------------------------
Pop2(1-159)  QQGVGLNRPLASQLPKHLTNQSMP--PIFLPPPNYLF-----------------------
Cbk1(1-326)  ----QSQSPVQSGF----NNGTISNYMYFERRPDLLTKGTQDKAAAVKLKIENFYQSSVK
                   :  : * :    .
                                                  Nonpolar
Nab3(568-802)---------------------------          Polar
Pop2(1-159)  ---------------------------          Acidic
Cbk1(1-326)  YAIERNERRVELETELTSHNWSEERKS          Basic
```

Figure 3.3 PolyQ-rich protein domain details

(A) Diagram of polyQ-rich proteins. Numbers indicate amino acid residues. (B) Sequences of polyQ-rich regions in Nab3, Pop2, and Cbk1. (C) ClustalW2 alignment of sequences from (B). Color legend is indicated.

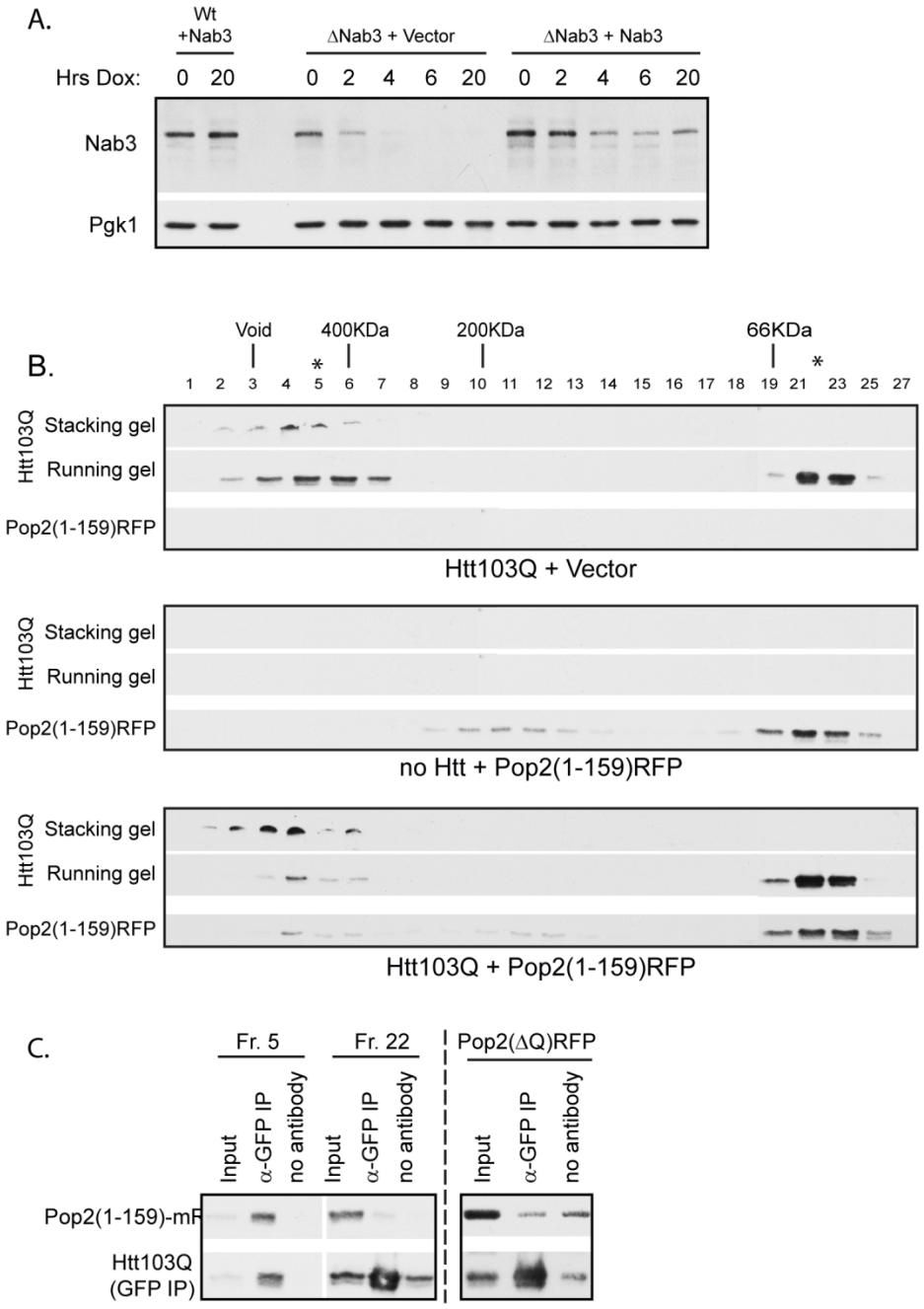

Figure 3.4 Nab3 is depleted by doxycycline and the polyQ-rich region of Pop2 promotes Htt103Q aggregation

(A) Doxycycline treatment inhibits expression of Nab3 as monitored by Western blot. (B-D) Impact of Pop2(Q) upon Htt103Q aggregation as monitored by size exclusion chromatography. Samples were prepared as indicated in the methods from cultures expressing (B) Htt103Q alone, (C) Pop2(Q) alone, or (D) both Htt103Q and Pop2(Q). (E) Interaction of Pop2(Q) with high molecular weight Htt103Q material as monitored by co-IP. Htt103Q was precipitated from column fractions indicated.

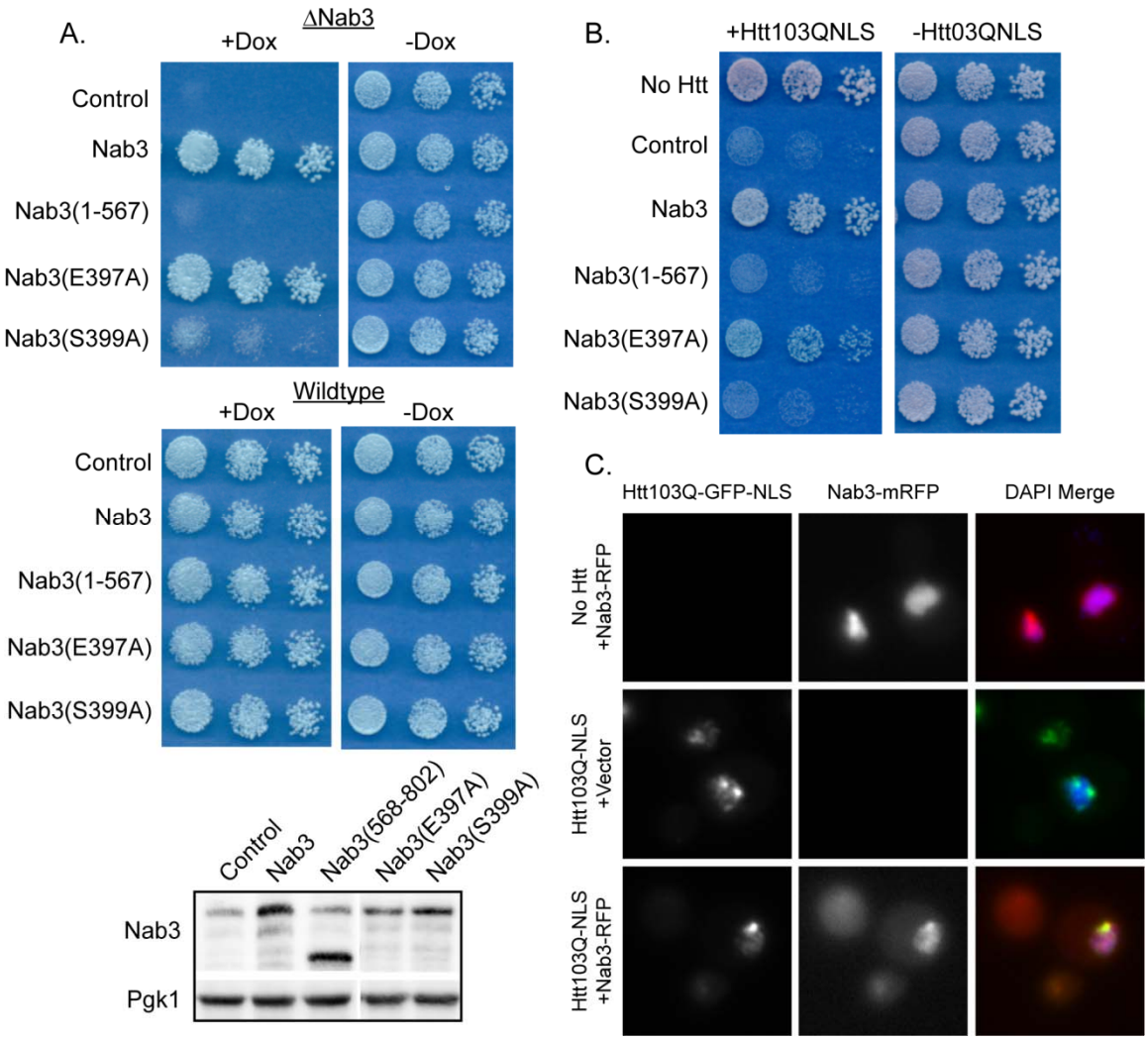

Figure 3.5 Overexpression of Nab3 must be functional for Htt103Q-NLS toxicity suppression

(A) Nab3 requires both the polyQ-rich region and a functional RNA recognition motif to complement Nab3 deletion. Growth assays were plated in 5-fold dilutions on glucose plates in the presence or absence of 10ug/mL doxycycline which inhibits Nab3 expression. Western blots indicate expression levels of Nab3 constructs each of which are under control of the endogenous Nab3 promoter. (B) Over-expression of non-functional Nab3 does not suppress Htt103Q-NLS toxicity as monitored by growth assays plated in 5-fold dilutions. (C) Nab3-mRFP co-localizes with Htt103Q-NLS in the nucleus and in intranuclear foci as monitored by fluorescence microscopy. Nuclei were visualized with DAPI staining. Nab3(1-567) lacks the C-terminal polyQ rich region of the protein.

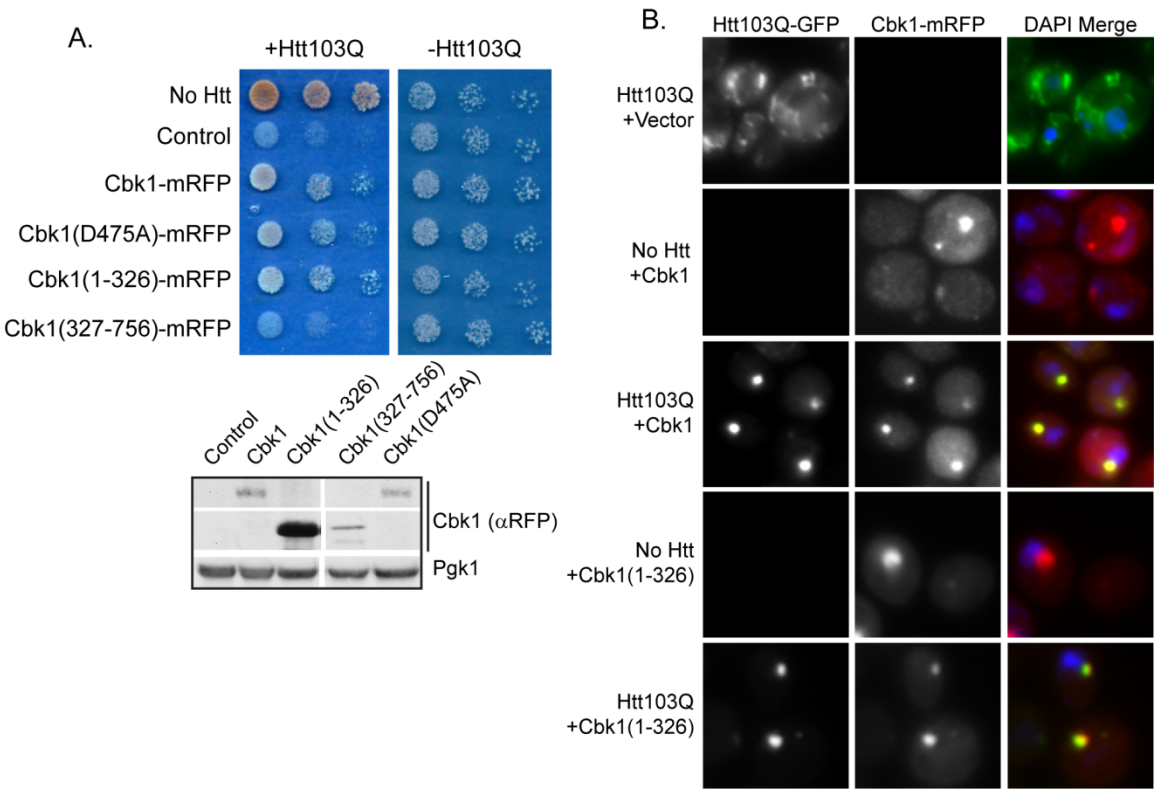

Figure 3.6 The polyQ-rich region of Cbk1 alters Htt103Q toxicity and aggregation
(A) Impact of indicated Cbk1 truncations or mutations upon Htt103Q toxicity as monitored via growth assays plated in 5-fold dilutions. Cbk1(1-326) is the polyQ-rich region of the protein, and Cbk1(327-756) lacks this region. (B) Cbk1-mRFP and Cbk1(1-327)-mRFP co-localize with Htt103Q in distinct foci. Cbk1 constructs were expressed from a copper inducible promoter induced with 100uM $CuSO_4$ for 5 h total and Htt103Q was induced with 2% galactose for 4 h total. Nuclei were visualized with DAPI staining.

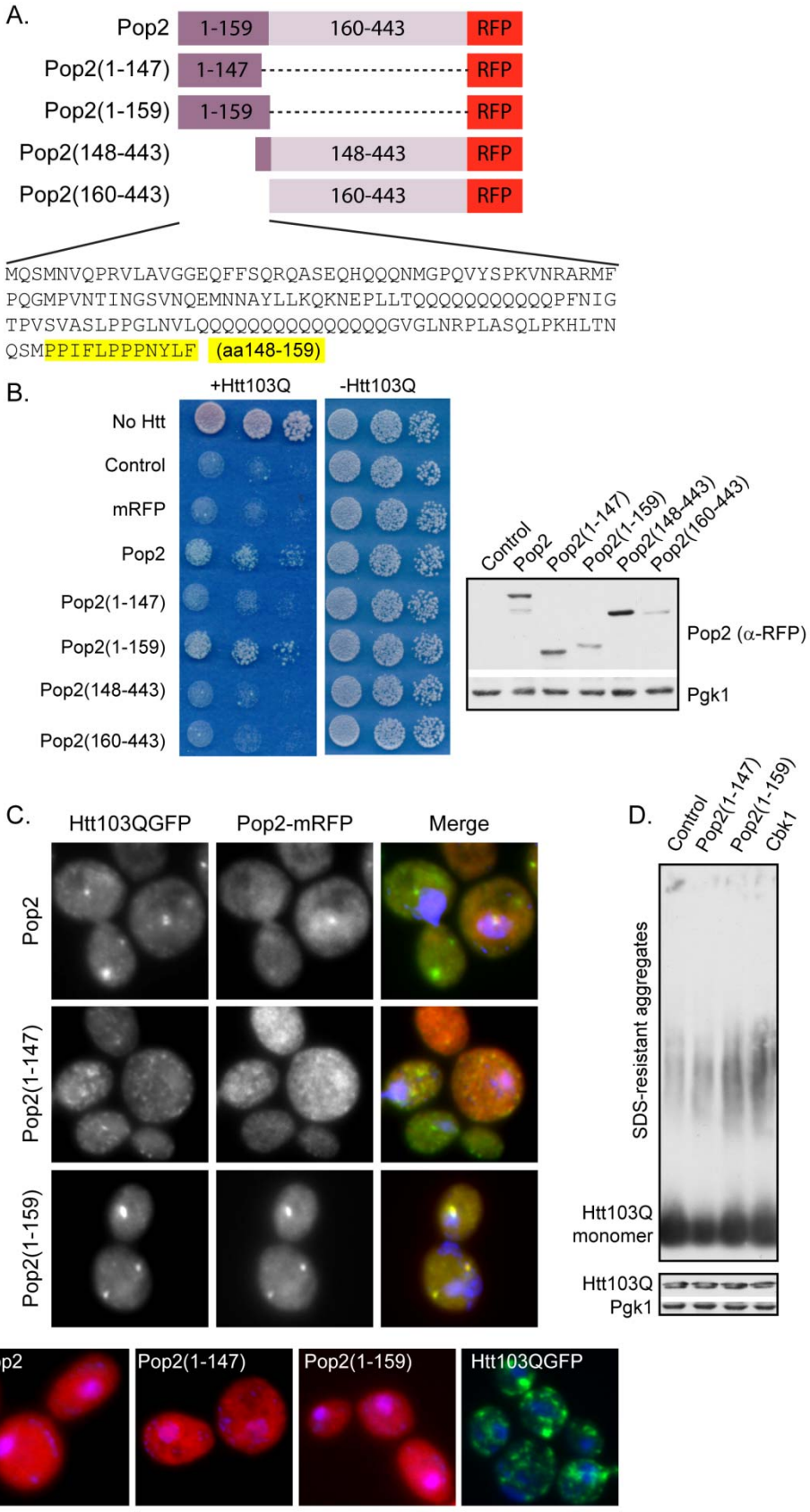
A.
Pop2
1-159
160-443
RFP
Pop2(1-147)
1-147
Pop2(1-159)
Pop2(148-443)
148-443
Pop2(160-443)
MQSMNVQPRVLAVGGEQFFSQRQASEQHQQQNMGPQVYSPKVNRARMF
PQGMPVNTINGSVNQEMNNAYLLKQKNEPLLTQQQQQQQQQQQQPFNIG
TPVSVASLPPGLNVLQQQQQQQQQQQQQQQQGVGLNRPLASQLPKHLTN
QSMPPIFLPPPNYLF (aa148-159)
B.
+Htt103Q
-Htt103Q
No Htt
Control
mRFP
Pop2
Pop2(1-147)
Pop2(1-159)
Pop2(148-443)
Pop2(160-443)
Control
Pop2
Pop2(1-147)
Pop2(1-159)
Pop2(148-443)
Pop2(160-443)
Pop2 (α-RFP)
Pgk1
C.
Htt103QGFP
Pop2-mRFP
Merge
Pop2
Pop2(1-147)
Pop2(1-159)
D.
Control
Pop2(1-147)
Pop2(1-159)
Cbk1
SDS-resistant aggregates
Htt103Q monomer
Htt103Q
Pgk1
Pop2
Pop2(1-147)
Pop2(1-159)
Htt103QGFP

Figure 3.7 A short proline-rich stretch in the Pop2 polyQ domain is required for impact upon Htt103Q toxicity and aggregation
(A) A diagram illustrating the constructs utilized in these experiments and the sequence of the polyQ domain. The proline-rich region of the Pop2 polyQ domain is highlighted. Numbers indicate amino acid residues. (B) Only full length Pop2 and Pop2(1-159) suppress Htt103Q toxicity. Expression of Pop2 constructs was monitored by Western blot detection using an anti-RFP antibody. (C) Pop2 lacking the proline-rich region is unable to alter Htt103Q aggregation as monitored by fluorescence microscopy. Nuclei were visualized with DAPI staining. (D) Pop2(1-159) and Cbk1 increase SDS-resistant Htt103Q aggregation as monitored by SDD-AGE and Western blot analysis. Pop2 and Cbk1 were expressed from high copy plasmids under control of their endogenous promoters. Htt103Q was induced with 2% galactose for 4 h.

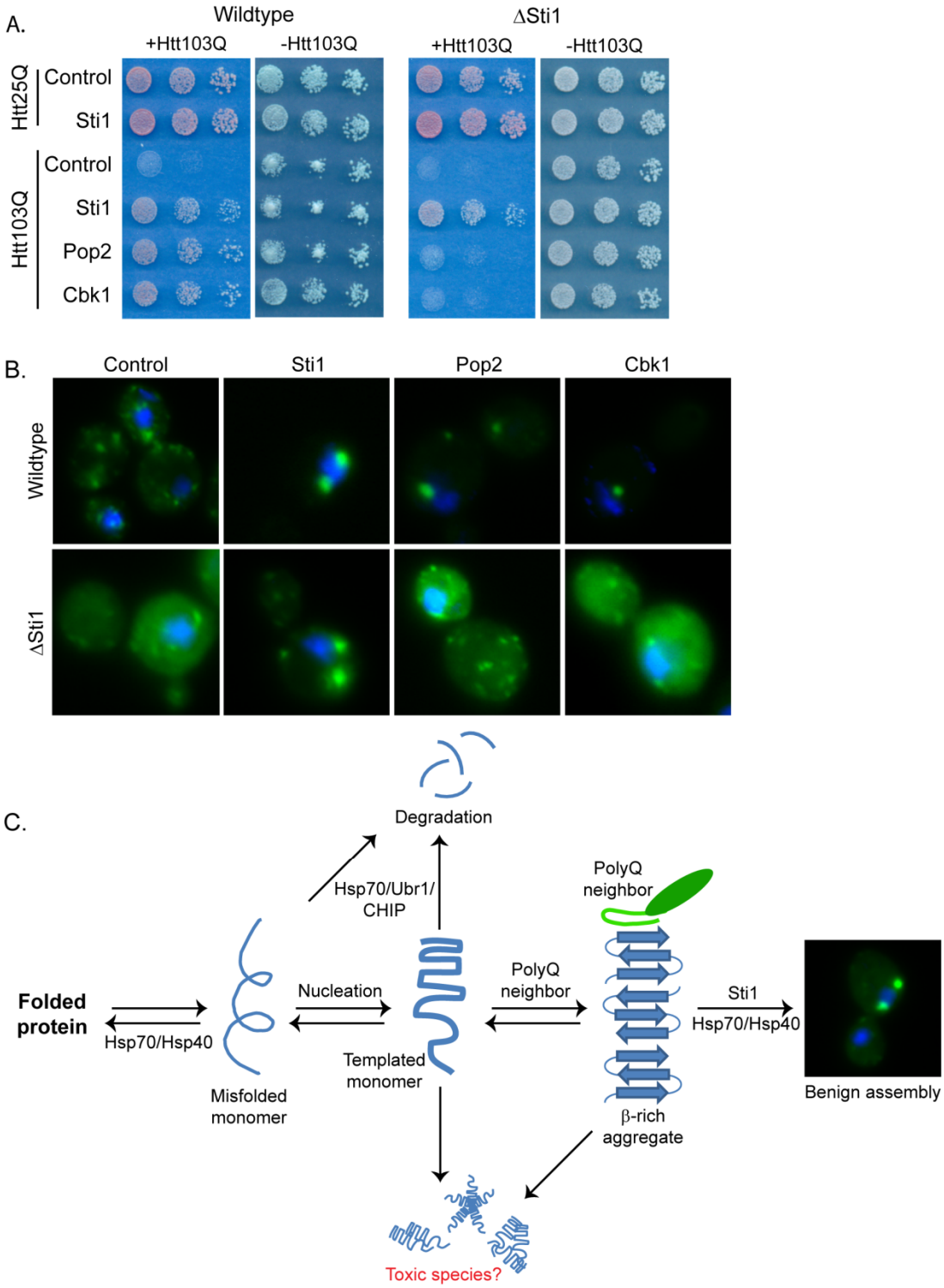

Figure 3.8 Cbk1 and Pop2 act in a Sti1-dependent manner
(A) Impact of Sti1 deletion upon Pop2 and Cbk1 ability to suppress Htt103Q toxicity. Growth assays were plated in 5-fold dilutions on glucose (-Htt) or galactose (+Htt). (B) Impact of Sti1 deletion upon Pop2 and Cbk1 ability to alter Htt103Q aggregation. (C) Model for Htt103Q benign aggregate assembly.

REFERENCES

1. Carrell, R.W. and D.A. Lomas, *Conformational disease.* Lancet, 1997. **350**(9071): p. 134-8.

2. Chiti, F. and C.M. Dobson, *Protein misfolding, functional amyloid, and human disease.* Annu Rev Biochem, 2006. **75**: p. 333-66.

3. Treusch, S., D.M. Cyr, and S. Lindquist, *Amyloid deposits: protection against toxic protein species?* Cell Cycle, 2009. **8**(11): p. 1668-74.

4. Haass, C. and D.J. Selkoe, *Soluble protein oligomers in neurodegeneration: lessons from the Alzheimer's amyloid beta-peptide.* Nat Rev Mol Cell Biol, 2007. **8**(2): p. 101-12.

5. Jarrett, J.T. and P.T. Lansbury, Jr., *Seeding "one-dimensional crystallization" of amyloid: a pathogenic mechanism in Alzheimer's disease and scrapie?* Cell, 1993. **73**(6): p. 1055-8.

6. Meriin, A.B., et al., *Huntington toxicity in yeast model depends on polyglutamine aggregation mediated by a prion-like protein Rnq1.* J Cell Biol, 2002. **157**(6): p. 997-1004.

7. Busch, A., et al., *Mutant huntingtin promotes the fibrillogenesis of wild-type huntingtin: a potential mechanism for loss of huntingtin function in Huntington's disease.* J Biol Chem, 2003. **278**(42): p. 41452-61.

8. Scherzinger, E., et al., *Self-assembly of polyglutamine-containing huntingtin fragments into amyloid-like fibrils: implications for Huntington's disease pathology.* Proc Natl Acad Sci U S A, 1999. **96**(8): p. 4604-9.

9. Nagai, Y., et al., *A toxic monomeric conformer of the polyglutamine protein.* Nat Struct Mol Biol, 2007. **14**(4): p. 332-40.

10. Saudou, F., et al., *Huntingtin acts in the nucleus to induce apoptosis but death does not correlate with the formation of intranuclear inclusions.* Cell, 1998. **95**(1): p. 55-66.

11. Arrasate, M., et al., *Inclusion body formation reduces levels of mutant huntingtin and the risk of neuronal death.* Nature, 2004. **431**(7010): p. 805-10.

12. Klein, W.L., W.B. Stine, Jr., and D.B. Teplow, *Small assemblies of unmodified amyloid beta-protein are the proximate neurotoxin in Alzheimer's disease.* Neurobiol Aging, 2004. **25**(5): p. 569-80.

13. Douglas, P.M., et al., *Chaperone-dependent amyloid assembly protects cells from prion toxicity.* Proc Natl Acad Sci U S A, 2008. **105**(20): p. 7206-11.

14. Behrends, C., et al., *Chaperonin TRiC promotes the assembly of polyQ expansion proteins into nontoxic oligomers.* Mol Cell, 2006. **23**(6): p. 887-97.

15. Slow, E.J., et al., *Absence of behavioral abnormalities and neurodegeneration in vivo despite widespread neuronal huntingtin inclusions.* Proc Natl Acad Sci U S A, 2005. **102**(32): p. 11402-7.

16. Kuemmerle, S., et al., *Huntington aggregates may not predict neuronal death in Huntington's disease.* Ann Neurol, 1999. **46**(6): p. 842-9.

17. Wellington, C.L., et al., *Caspase cleavage of mutant huntingtin precedes neurodegeneration in Huntington's disease.* J Neurosci, 2002. **22**(18): p. 7862-72.

18. Wellington, C.L., et al., *Inhibiting caspase cleavage of huntingtin reduces toxicity and aggregate formation in neuronal and nonneuronal cells.* J Biol Chem, 2000. **275**(26): p. 19831-8.

19. DiFiglia, M., et al., *Aggregation of huntingtin in neuronal intranuclear inclusions and dystrophic neurites in brain.* Science, 1997. **277**(5334): p. 1990-3.

20. Bennett, E.J., et al., *Global impairment of the ubiquitin-proteasome system by nuclear or cytoplasmic protein aggregates precedes inclusion body formation.* Mol Cell, 2005. **17**(3): p. 351-65.

21. Davies, S.W., et al., *Formation of neuronal intranuclear inclusions underlies the neurological dysfunction in mice transgenic for the HD mutation.* Cell, 1997. **90**(3): p. 537-48.

22. Peters, M.F., et al., *Nuclear targeting of mutant Huntingtin increases toxicity.* Mol Cell Neurosci, 1999. **14**(2): p. 121-8.

23. Benn, C.L., et al., *Contribution of nuclear and extranuclear polyQ to neurological phenotypes in mouse models of Huntington's disease.* Hum Mol Genet, 2005. **14**(20): p. 3065-78.

24. Douglas, P.M., et al., *Reciprocal Efficiency of RNQ1 and Polyglutamine Detoxification in the Cytosol and Nucleus.* Mol Biol Cell, 2009.

25. Dunah, A.W., et al., *Sp1 and TAFII130 transcriptional activity disrupted in early Huntington's disease.* Science, 2002. **296**(5576): p. 2238-43.

26. McCampbell, A., et al., *CREB-binding protein sequestration by expanded polyglutamine.* Hum Mol Genet, 2000. **9**(14): p. 2197-202.

27. Olzscha, H., et al., *Amyloid-like aggregates sequester numerous metastable proteins with essential cellular functions.* Cell, 2011. **144**(1): p. 67-78.

28. Schaffar, G., et al., *Cellular toxicity of polyglutamine expansion proteins: mechanism of transcription factor deactivation.* Mol Cell, 2004. **15**(1): p. 95-105.

29. Bennett, E.J., et al., *Global changes to the ubiquitin system in Huntington's disease.* Nature, 2007. **448**(7154): p. 704-8.

30. Bence, N.F., R.M. Sampat, and R.R. Kopito, *Impairment of the ubiquitin-proteasome system by protein aggregation.* Science, 2001. **292**(5521): p. 1552-5.

31. Duennwald, M.L. and S. Lindquist, *Impaired ERAD and ER stress are early and specific events in polyglutamine toxicity.* Genes Dev, 2008. **22**(23): p. 3308-19.

32. Muchowski, P.J. and J.L. Wacker, *Modulation of neurodegeneration by molecular chaperones.* Nat Rev Neurosci, 2005. **6**(1): p. 11-22.

33. Sakahira, H., et al., *Molecular chaperones as modulators of polyglutamine protein aggregation and toxicity.* Proc Natl Acad Sci U S A, 2002. **99 Suppl 4**: p. 16412-8.

34. Kim, S., et al., *Polyglutamine protein aggregates are dynamic.* Nat Cell Biol, 2002. **4**(10): p. 826-31.

35. Giorgini, F., et al., *A genomic screen in yeast implicates kynurenine 3-monooxygenase as a therapeutic target for Huntington disease.* Nat Genet, 2005. **37**(5): p. 526-31.

36. Nollen, E.A., et al., *Genome-wide RNA interference screen identifies previously undescribed regulators of polyglutamine aggregation.* Proc Natl Acad Sci U S A, 2004. **101**(17): p. 6403-8.

37. Willingham, S., et al., *Yeast genes that enhance the toxicity of a mutant huntingtin fragment or alpha-synuclein.* Science, 2003. **302**(5651): p. 1769-72.

38. Fernandez-Funez, P., et al., *Identification of genes that modify ataxin-1-induced neurodegeneration.* Nature, 2000. **408**(6808): p. 101-6.

39. Krobitsch, S. and S. Lindquist, *Aggregation of huntingtin in yeast varies with the length of the polyglutamine expansion and the expression of chaperone proteins.* Proc Natl Acad Sci U S A, 2000. **97**(4): p. 1589-94.

40. Sondheimer, N. and S. Lindquist, *Rnq1: an epigenetic modifier of protein function in yeast.* Mol Cell, 2000. **5**(1): p. 163-72.

41. Lessing, D. and N.M. Bonini, *Polyglutamine genes interact to modulate the severity and progression of neurodegeneration in Drosophila.* PLoS Biol, 2008. **6**(2): p. e29.

42. Kaltenbach, L.S., et al., *Huntingtin interacting proteins are genetic modifiers of neurodegeneration.* PLoS Genet, 2007. **3**(5): p. e82.

43. Goehler, H., et al., *A protein interaction network links GIT1, an enhancer of huntingtin aggregation, to Huntington's disease.* Mol Cell, 2004. **15**(6): p. 853-65.

44. Doumanis, J., et al., *RNAi screening in Drosophila cells identifies new modifiers of mutant huntingtin aggregation.* PLoS One, 2009. **4**(9): p. e7275.

45. Doi, H., et al., *Identification of ubiquitin-interacting proteins in purified polyglutamine aggregates.* FEBS Lett, 2004. **571**(1-3): p. 171-6.

46. Bilen, J. and N.M. Bonini, *Genome-wide screen for modifiers of ataxin-3 neurodegeneration in Drosophila.* PLoS Genet, 2007. **3**(10): p. 1950-64.

47. Linding, R., et al., *Protein disorder prediction: implications for structural proteomics.* Structure, 2003. **11**(11): p. 1453-9.

48. Alberti, S., et al., *A systematic survey identifies prions and illuminates sequence features of prionogenic proteins.* Cell, 2009. **137**(1): p. 146-58.

49. Ghaemmaghami, S., et al., *Global analysis of protein expression in yeast.* Nature, 2003. **425**(6959): p. 737-41.

50. Duennwald, M.L., et al., *A network of protein interactions determines polyglutamine toxicity.* Proc Natl Acad Sci U S A, 2006. **103**(29): p. 11051-6.

51. Wilson, S.M., et al., *Characterization of nuclear polyadenylated RNA-binding proteins in Saccharomyces cerevisiae.* J Cell Biol, 1994. **127**(5): p. 1173-84.

52. Hobor, F., et al., *Recognition of transcription termination signal by the nuclear polyadenylated RNA-binding (NAB) 3 protein.* J Biol Chem, 2011. **286**(5): p. 3645-57.

53. Park, S.H., et al., *PolyQ Proteins Interfere with Nuclear Degradation of Cytosolic Proteins by Sequestering the Sis1p Chaperone.* Cell, 2013. **154**(1): p. 134-45.

54. Treusch, S. and S. Lindquist, *An intrinsically disordered yeast prion arrests the cell cycle by sequestering a spindle pole body component.* J Cell Biol, 2012. **197**(3): p. 369-79.

55. Weiss, E.L., et al., *The Saccharomyces cerevisiae Mob2p-Cbk1p kinase complex promotes polarized growth and acts with the mitotic exit network to facilitate daughter cell-specific localization of Ace2p transcription factor.* J Cell Biol, 2002. **158**(5): p. 885-900.

56. Wang, Y., et al., *Abnormal proteins can form aggresome in yeast: aggresome-targeting signals and components of the machinery.* FASEB J, 2009. **23**(2): p. 451-63.

57. Duennwald, M.L., et al., *Flanking sequences profoundly alter polyglutamine toxicity in yeast.* Proc Natl Acad Sci U S A, 2006. **103**(29): p. 11045-50.

58. Nucifora, F.C., Jr., et al., *Interference by huntingtin and atrophin-1 with cbp-mediated transcription leading to cellular toxicity.* Science, 2001. **291**(5512): p. 2423-8.

59. Doi, H., et al., *RNA-binding protein TLS is a major nuclear aggregate-interacting protein in huntingtin exon 1 with expanded polyglutamine-expressing cells.* J Biol Chem, 2008. **283**(10): p. 6489-500.

60. Robertson, A.L., et al., *PolyQ: a database describing the sequence and domain context of polyglutamine repeats in proteins.* Nucleic Acids Res, 2011. **39**(Database issue): p. D272-6.

61. Karlin, S., et al., *Amino acid runs in eukaryotic proteomes and disease associations.* Proc Natl Acad Sci U S A, 2002. **99**(1): p. 333-8.

62. Waelter, S., et al., *Accumulation of mutant huntingtin fragments in aggresome-like inclusion bodies as a result of insufficient protein degradation.* Mol Biol Cell, 2001. **12**(5): p. 1393-407.

63. Furukawa, Y., et al., *Cross-seeding fibrillation of Q/N-rich proteins offers new pathomechanism of polyglutamine diseases.* J Neurosci, 2009. **29**(16): p. 5153-62.

64. Derkatch, I.L., et al., *Prions affect the appearance of other prions: the story of [PIN(+)].* Cell, 2001. **106**(2): p. 171-82.

65. Lakhani, V.V., F. Ding, and N.V. Dokholyan, *Polyglutamine induced misfolding of huntingtin exon1 is modulated by the flanking sequences.* PLoS Comput Biol, 2010. **6**(4): p. e1000772.

66. Dehay, B. and A. Bertolotti, *Critical role of the proline-rich region in Huntingtin for aggregation and cytotoxicity in yeast.* J Biol Chem, 2006. **281**(47): p. 35608-15.

67. Bhattacharyya, A., et al., *Oligoproline effects on polyglutamine conformation and aggregation.* J Mol Biol, 2006. **355**(3): p. 524-35.

68. Darnell, G.D., et al., *Mechanism of cis-inhibition of polyQ fibrillation by polyP: PPII oligomers and the hydrophobic effect.* Biophys J, 2009. **97**(8): p. 2295-305.

69. Carlson, M. and D. Botstein, *Two differentially regulated mRNAs with different 5' ends encode secreted with intracellular forms of yeast invertase.* Cell, 1982. **28**(1): p. 145-54.

70. Summers, D.W., et al., *The Type II Hsp40 Sis1 cooperates with Hsp70 and the E3 ligase Ubr1 to promote degradation of terminally misfolded cytosolic protein.* PLoS One, 2013. **8**(1): p. e52099.